

40. OLIGOCENE TO MIDDLE MIocene RADIOLARIAN STRATIGRAPHY OF SOUTHERN HIGH LATITUDES FROM LEG 113, SITES 689 AND 690, MAUD RISE¹

Andrea Abelmann²

ABSTRACT

At Sites 689 and 690, drilled during ODP (Ocean Drilling Program) Leg 113 on the Maud Rise (southeast Weddell Sea), moderately to well preserved radiolarian assemblages were obtained from continuously recovered upper Oligocene and Neogene sequences. Based on radiolarian investigations, a biostratigraphic zonation for a time interval covering the late Oligocene to the middle Miocene is proposed. The radiolarian zonation comprises 10 zones. Five zones are new, and five zones previously defined by Chen (1975) were modified. The zones and the ranges of the nominate species are directly calibrated with a geomagnetic polarity record. This is the first attempt at a direct correlation of late Oligocene to middle Miocene radiolarian zones with the geomagnetic time scale.

Six hiatuses were delineated in the studied upper Oligocene to middle Miocene sections. One major hiatus, spanning ca. 6 m.y., is between the upper Oligocene and the lower Miocene sequences. Another important hiatus separates the lower and middle Miocene sediments.

As a base for the biostratigraphic investigations, a detailed taxonomic study of the recovered radiolarian taxa is achieved. Three new radiolarian species that occur in upper Oligocene and lower Miocene sediments are described (*Cycladophora antiqua*, *Cyrtocapsella robusta*, and *Velicuculus altus*).

INTRODUCTION

Radiolarians are one of the useful microfossil groups in Antarctic sediments for stratigraphic, paleoceanographic, and evolutionary studies.

Previous biostratigraphic investigations of Radiolaria have been done on piston cores recovered on cruises of *Eltanin*, *Islas Orcadas*, *Vema*, and on drilled cores from DSDP Legs 28, 29, 35, and 36 (Hays and Opdyke, 1967; Chen, 1975; Petrushevskaya, 1975; Weaver, 1973, 1976, 1983). The first radiolarian zonation for Antarctic sediments has been established by Hays and Opdyke (1967) for the Pliocene and Pleistocene time interval using piston cores recovered in the Pacific sector of the Antarctic Ocean. On the basis of rotary drilled material from DSDP Leg 28 (Indian and Pacific sector) Chen (1975) developed a detailed zonation for the Miocene that was accepted by many subsequent workers. An independent zonation was established by Petrushevskaya (1975) on DSDP Leg 29 material (Pacific sector) for the Neogene and Paleogene. Weaver (1976, 1983) used the radiolarian zonation of Hays and Opdyke (1967) and Chen (1975) for age assignment of Subantarctic and Antarctic sediments of DSDP Legs 35 and 36 (Bellingshausen Sea, Falkland Plateau) and modified some parts of the zonations. Although the Pliocene and Pleistocene radiolarian zonation for Antarctic sediments is already correlated to the geomagnetic time scale (Hays and Opdyke, 1967; Keany, 1979; Weaver, 1983), the Antarctic Miocene and Paleogene zonation has not yet been calibrated to this time scale because no geomagnetic measurements were available for the studied DSDP cores.

Leg 113 Sites 689 and 690 were drilled on Maud Rise, a topographic elevation in the southeastern Weddell Sea (Fig. 1). Sites 689 and 690 were the first in the Antarctic where the hydraulic piston coring technique was used, and at both sites Neogene and upper Paleocene sediment sequences were recovered almost

continuously and undisturbed. Of the four holes drilled at Site 689 and the three holes of Site 690, Holes 689B and 690B were studied in detail, and an integrated bio- and magnetostratigraphy was established (see Gersonde et al., this volume).

The present study focused on the upper Oligocene to middle Miocene time interval of Holes 689B and 690B for the establishment of a biostratigraphic radiolarian zonation that is correlated to the geomagnetic time scale (Spieß, this volume) and to the diatom zonation (Gersonde and Burckle, this volume).

The studied sediment sequences are characterized by well-preserved radiolarian assemblages in the middle Miocene and the upper portion of the recovered lower Miocene, whereas the lower portion of the lower Miocene and the upper Oligocene sequences bear moderately to poorly preserved radiolarians. The middle Miocene to Recent radiolarians are described by Lazarus (this volume).

METHODS

Samples were taken aboard *JOIDES Resolution* during Leg 113 and in the ODP core repository at Lamont. Micropaleontological and paleomagnetic samples were taken nearly at the same core depths. Generally, four samples per core were investigated in Hole 689B from Sections 113-689B-9H-6 to 113-689B-5H-5. In Hole 690B one sample per core was studied from Sections 113-690B-7H-1 to 113-690B-5H-2. The samples were washed through a 40-μm sieve, and randomly distributed slides were prepared according to the methods described by Abelmann (1989) and Abelmann et al. (in prep.). Light microscopical investigations were made with a Leitz Orthoplan photomicroscope with apochromatic optics. Species identification was done routinely at 160× or 250×. Five semiquantitative abundance categories for estimation of radiolarian numbers were defined as: abundant (A) = > 50% of total assemblage; common (C) = 15%-50%; few (F) = 3%-15%; rare (R) = 1%-3%; trace (T) = < 1%. The preservation of the radiolarian assemblages is classed as poor (P), moderate (M), and good (G), according to degree of dissolution and breakage of the radiolarian shells. For designation of paleomagnetic events, a modified nomenclature proposed by Spieß (this volume) was used, which follows the scheme proposed by Tauxe et al. (1984, Fig. 2). This nomencla-

¹ Barker, P. F., Kennett, J. P., et al., 1990. Proc. ODP, Sci. Results, 113: College Station, TX (Ocean Drilling Program).

² Alfred-Wegener Institute for Polar and Marine Research, Bremerhaven, Columbusstraße, Federal Republic of Germany.

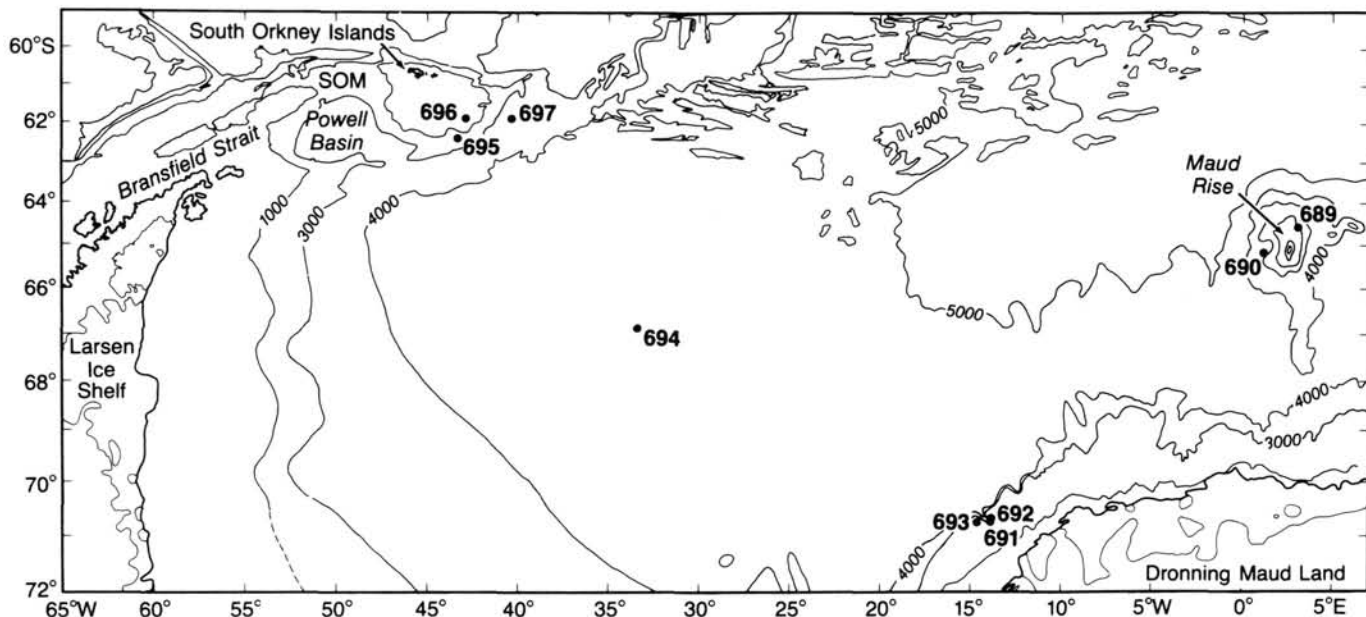


Figure 1. Location of Leg 113 sites in the Weddell Sea. Contours in meters; SOM = South Orkney microcontinent.

ture was also used in the initial reports volume of ODP Leg 113 (Barker, Kennett, et al., 1988). The absolute age assignment is according to the geomagnetic polarity time scale of Berggren et al. (1985).

DEFINITION OF RADIOLARIAN ZONES

Ten radiolarian zones are proposed for the upper Oligocene to middle Miocene time interval (Table 1, Fig. 2). Five new zones are described and five zones previously defined by Chen (1975) are modified. Most names of the biostratigraphic marker species described by Chen (1975) are not valid and represent synonyms of species described by Petrushevskaya (1975). Petrushevskaya's species have priority according to the International Rules of Zoological Nomenclature, because her paper published in the DSDP Leg 29 volume (January 1975) was delivered before Chen's publications in DSDP Leg 28 volume (July 1975) and in *Micropaleontology* (October 1974) (Van Couvering, J. A., pers. comm., 1989; see also Lazarus, this volume). In this paper the

systematic position of some biostratigraphically useful species is revised and new combinations are proposed (*Cyrtocapsella longithorax*, *Dendrospris rhodospyrodes*, *Lychnocanoma conica*).

Based on the study of densely spaced sample sets and independent magnetostratigraphic age interpretation, the definition of zonal boundaries and the age range of Chen's (1975) zones used in this paper are revised. Two of Chen's zones, the *Spongomelissa dilli* Zone and the *Calocyclus disparidens* Zone, which range in the early Miocene and the middle Miocene, respectively, could not be identified in the sequences recovered in Holes 689B and 690B. The attempt to correlate the zones and the age range of biostratigraphically useful species defined by Chen (1975) to biostratigraphic results of the present study is difficult and for some time intervals (e.g., middle Miocene) apparently not possible. The reasons for this can be summarized as follows:

1. The sediment sequences recovered at DSDP Sites 265, 266, 267, 268, and 269 used by Chen for the establishment of his zo-

Table 1. Upper Oligocene to middle Miocene Antarctic radiolarian zonation, zonal definitions and age ranges.

Radiolarian zones	Age (Ma)	Base	Top	Other important datums
<i>Antarctissa deflandrei</i> Zone (Chen, 1975 emend.)	12.4–11.7	LAD <i>Dendrospris megalcephalis</i>	FAD <i>Cycladophora spongothorax</i>	Base: FAD <i>Cornutella clathrata</i> High numbers of <i>A. deflandrei</i>
<i>Dendrospris megalcephalis</i> Zone (new)	12.55–12.4	FAD <i>Dendrospris megalcephalis</i>	LAD <i>Dendrospris megalcephalis</i>	Top: FAD <i>Cornutella clathrata</i>
<i>Actinomma golownini</i> Zone (Chen, 1975 emend.)	13.1–12.55	FAD <i>Actinomma golownini</i>	FAD <i>Dendrospris megalcephalis</i>	
<i>Cycladophora humerus</i> Zone (new)	14.2–13.1	FAD <i>Cycladophora humerus</i>	FAD <i>Actinomma golownini</i>	Base: FAD <i>Lychnocanoma</i> sp. B Near base: FAD <i>Antarctissa deflandrei</i>
<i>Eucyrtidium punctatum</i> Zone (Chen, 1975 emend.)	(17.6–15.6?)–14.2	FAD <i>Eucyrtidium punctatum</i>	FAD <i>Cycladophora humerus</i>	Top: FAD <i>Lychnocanoma</i> sp. B Near top: FAD <i>Antarctissa deflandrei</i>
<i>Cycladophora golli regipileus</i> Zone (Chen, 1975 emend.)	18.4–(17.6–15.6?)	FAD <i>Cycladophora golli regipileus</i>	FAD <i>Eucyrtidium punctatum</i>	Base: FAD <i>Stauroxiphos communis</i> FAD <i>Gondwanaria deflandrei</i>
<i>Cyrtocapsella longithorax</i> Zone (new)	(19.4–19.1)–18.4	FAD <i>Cyrtocapsella longithorax</i>	FAD <i>Cycladophora golli regipileus</i>	Base: FAD <i>Dendrospris stabilis</i> Top: FAD <i>Stauroxiphos communis</i>
<i>Cycladophora antiqua</i> Zone (new)	ca. 19.9–(19.4–19.1)	FAD <i>Cycladophora antiqua</i>	FAD <i>Cyrtocapsella longithorax</i>	Base: FAD <i>Velicucillus altus</i> LAD <i>Stylosphaera radiososa</i> LAD <i>Lychnocanoma conica</i>
<i>Stylosphaera radiososa</i> Zone (new)	27.2?–ca. 19.9	FAD <i>Stylosphaera radiososa</i>	FAD <i>Cycladophora antiqua</i>	Lower portion: <i>Lithomelissa robusta</i> Top: LAD <i>Stylosphaera radiososa</i> LAD <i>Lychnocanoma conica</i>
<i>Cyrtocapsella robusta</i> (new)	27.7?–27.2?	FAD <i>Cyrtocapsella robusta</i>	FAD <i>Stylosphaera radiososa</i>	

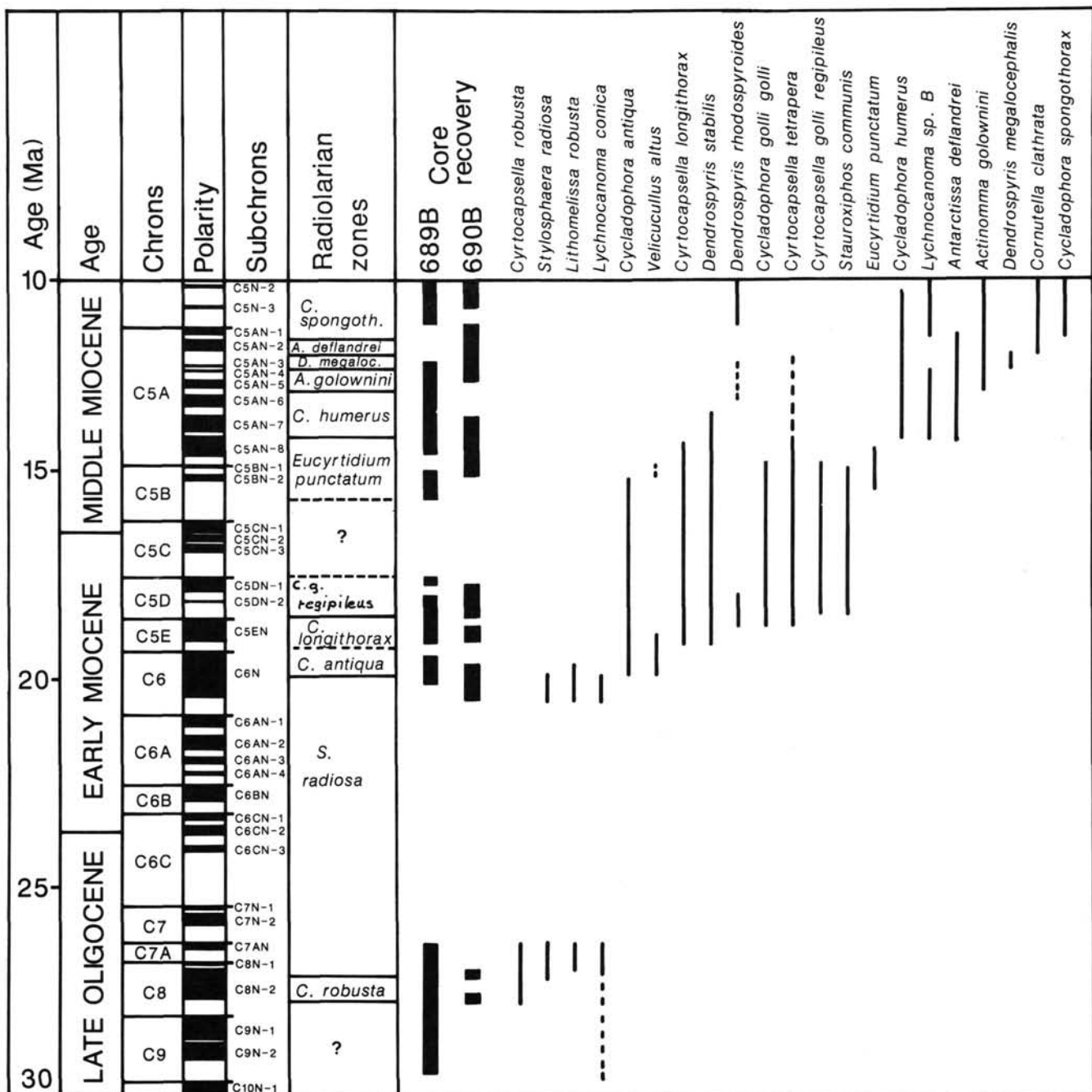


Figure 2. Proposed radiolarian zonation for upper Oligocene to middle Miocene Antarctic sediments and ranges of stratigraphic marker species. Stratigraphic intervals recovered at Holes 689B and 690B are correlated to the standard paleomagnetic time scale.

nation are disturbed by a number of disconformities. However, these disconformities were not delineated or discussed and thus were not considered by Chen when ranges of biostratigraphic marker species and zones were defined.

2. A number of biostratigraphically useful radiolarian species used in the present study were not reported by Chen (1975).

3. Differences in species definition concepts lead possibly to significant differences in stratigraphic ranges.

As far as possible the zones proposed in the present paper are defined by the FAD (first appearance datum) of radiolarian species. By the use of first appearance datums problems related

to reworking of older species into younger sediments can be avoided. Reworking is a common phenomenon in Antarctic sediments caused by bottom water activity. However, additionally, some zonal boundaries are also defined by the LAD (last appearance datum) of radiolarian species.

The age assignment of the zonal boundaries and of ranges of selected radiolarian species is based on an integrated stratigraphic interpretation of the studied sections of Holes 689B and 690B (Fig. 2). The geomagnetic polarity record established by Spieß (this volume) was interpreted based on the magnetic polarity pattern and the occurrence pattern of radiolarian species, also considering diatom biostratigraphic results of Gersonde and

Burk (this volume). The combined stratigraphic interpretation was tested on coherency by comparison of the results obtained at both studied holes. It was then used for the establishment of age-depth diagrams of Holes 689B and 690B (Figs. 3, 4; Tables 2, 3).

Problematic stratigraphic intervals are around the middle middle Miocene and below the early middle Miocene. The stratigraphic interpretation of the lower Miocene sediments, separated from upper Oligocene and middle Miocene sequences by a hiatus in Holes 689B and 690B, is still tentative. For age assignment of the established radiolarian zonation and interpretation of the magnetostratigraphy in the early Miocene, preliminary results of Leg 120 Holes 747A, 748B, and 751A were employed in this study (Abelmann, in press).

To estimate the ages of the zonal boundaries, the sub-bottom depths were first determined for all paleomagnetic polarity boundaries and zonal boundaries. The sub-bottom depths of radiolarian zonal boundaries were calculated as the midpoint between studied samples bracketing the zonal boundaries. Zonal boundary ages were then calculated by assuming constant

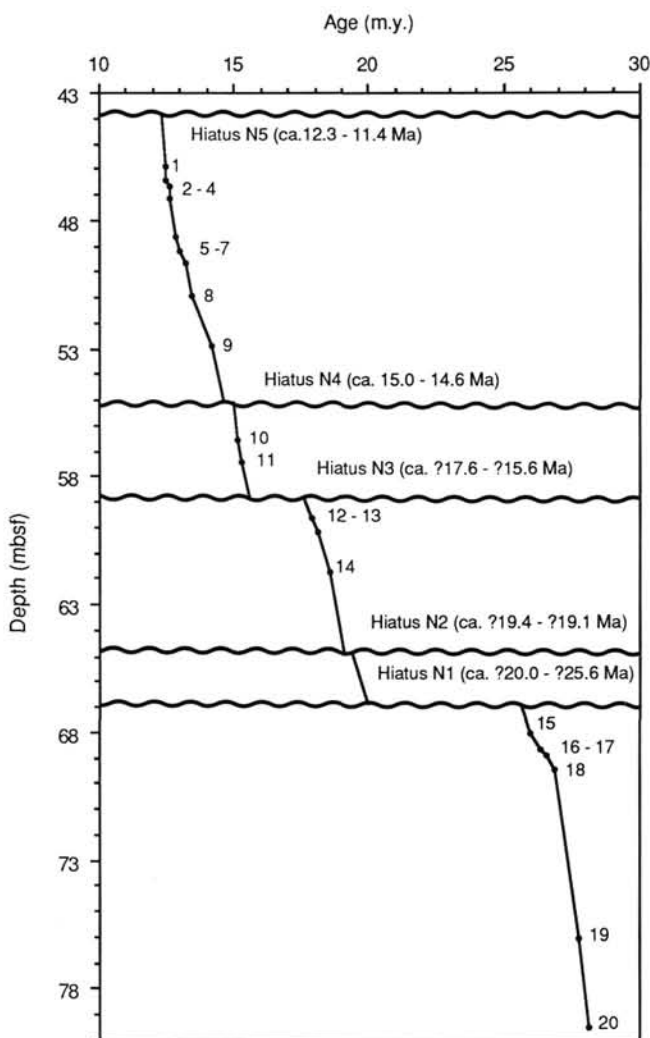


Figure 3. Age-depth diagram for the upper Oligocene to middle Miocene time interval of Hole 689B. For definition of stratigraphic datum points compare Table 2.

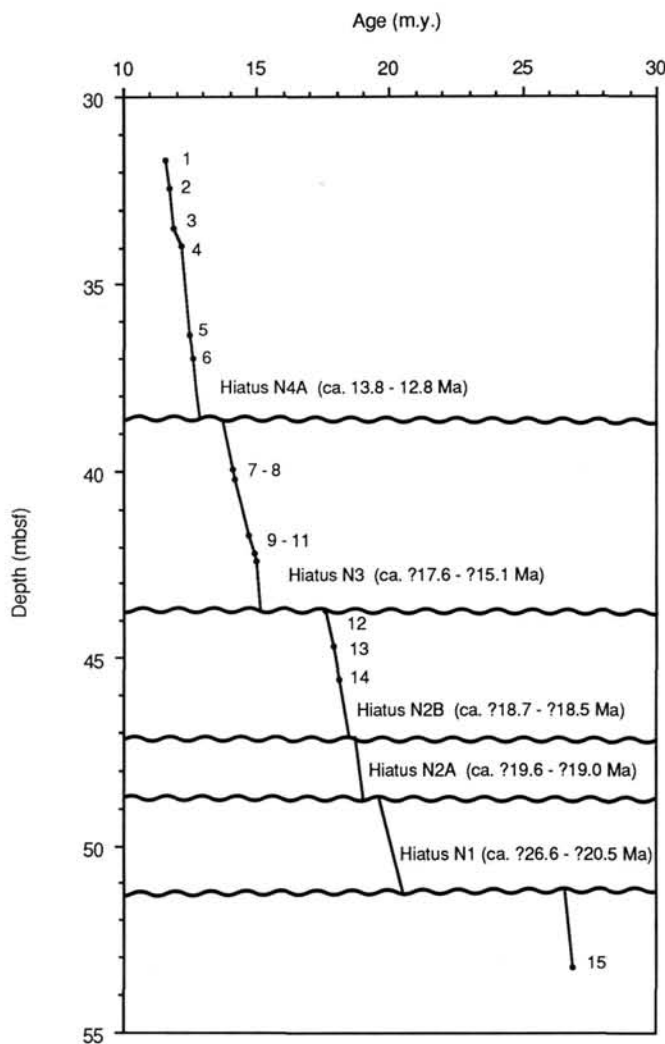


Figure 4. Age-depth diagram for the upper Oligocene to middle Miocene time interval of Hole 690B. For definition of stratigraphic datum points compare Table 3.

sediment accumulation rates between adjacent chron or sub-chron boundaries. The age determinations of hiatuses were done in the same way.

Antarctissa deflandrei Zone (12.4–11.7 Ma)

Author. Chen (1975) as *Antarctissa conradae* Zone, modified herein.
Top. First appearance of *Cycladophora spongorthorax*.

Base. Last appearance of *Dendrospryris megalcephala*.

Paleomagnetic correlation. The top of the zone lies at the top of Subchron CSAN-2, the base between CSAN-3 and CSAN-2.

Remarks. The zone is characterized by high numbers of *Antarctissa deflandrei*. Chen (1975) used the nominate species of the zone (for comments on nomenclatural changes of the nominate species see Taxonomy in this chapter) for the definition of the zonal base. However, the accurate delineation of the FAD of *A. deflandrei* (= *A. conradae*) is not easy. *A. deflandrei* probably evolves from *A. robusta*, and a gradual transition between these taxa can be observed. This transition was concluded near the base of the *Cycladophora humerus* Zone, placed at ca. 14.2 Ma. To avoid stratigraphic problems resulting from incorrect species determination the definition of the zonal base was changed. Another datum marking the base of the *A. deflandrei* Zone is probably the FAD of *Cornutella clathrata*.

Table 2. Definition and depth (mbsf) of stratigraphic datum points, and age range and depth of hiatuses in upper Oligocene to middle Miocene sediments of Hole 689B used to construct age/depth diagram in Figure 3.

Datum points and hiatuses	Age (Ma)	Depth (mbsf)	Definition
Hiatus N5	ca. 12.3–11.4	43.80	
1	12.46	45.93	Top C5AN-3
2	12.49	46.41	Base C5AN-3
3	12.58	46.68	Top C5AN-4
4	12.63	47.18	Base C5AN-4
5	12.83	48.63	Top C5AN-5
6	13.01	49.18	Base C5AN-5
7	13.20	49.68	Top C5AN-6
8	13.42	50.91	Base C5AN-6
9	14.20	52.85	Top C5AN-8
Hiatus N4	ca. 15.0–14.6	55.10	
10	15.13	56.53	Top C5BN-2
11	15.27	57.40	Base C5BN-2
Hiatus N3	ca. ?17.6–?15.6	58.80	
12	17.90	59.64	Base C5DN-1
13	18.13	60.20	Mid C5CDN-2
14	18.56	61.76	Top C5EN
Hiatus N2	ca. ?19.4–?19.1	64.76	
Hiatus N1	ca. ?20.0–?25.6	66.86	
15	25.97	68.00	Base C7N-2
16	26.38	68.61	Top C7AN
17	26.56	68.88	Base C7AN
18	26.86	69.38	Top C8N-1
19	27.74	75.98	Base C8N-2
20	28.15	79.46	Top C9N-1/2

Table 3. Definition and depth (mbsf) of stratigraphic datum points, and age range and depth of hiatuses in upper Oligocene to middle Miocene sediments of Hole 690B used to construct age/depth diagram in Figure 4.

Datum points and hiatuses	Age (Ma)	Depth (mbsf)	Definition
1	11.55	31.72	Top C5AN-1
2	11.73	32.45	Base C5AN-1
3	11.86	33.47	Top C5AN-2
4	12.12	33.95	Base C5AN-2
5	12.46	36.35	Top C5AN-3
6	12.60	37.00	Base C5AN-3
Hiatus N4A	ca. 13.8–12.8	38.50	
7	14.08	39.95	Base C5AN-7
8	14.20	40.20	Top C5AN-7
9	14.27	40.70	Base C5AN-8
10	14.66	41.68	Top C5BN-1
11	14.87	42.16	Base C5BN-1
Hiatus N3	ca. ?17.6–?15.1	43.80	
12	17.57	43.70	Top C5DN-1
13	17.90	44.68	Base C5DN-1
14	18.14	45.55	Mid C5DN-1
Hiatus N2B	ca. ?18.7–?18.5	47.10	
Hiatus N2A	ca. ?19.6–?19.0	48.70	
Hiatus N1	ca. ?26.6–?20.5	51.20	
15	26.86	53.25	Top C8

Dendrospyrus megalcephalus Zone (12.55–12.4 Ma)

Author. Abelmann, herein.

Top. Last appearance of *Dendrospyrus megalcephalus*.

Base. First appearance of *Dendrospyrus megalcephalus*.

Paleomagnetic correlation. Top of the zone is placed between Subchrons C5AN-2 and C5AN-3, the base between C5AN-3 and C5AN-4.

Remarks. The *D. megalcephalus* Zone spans a short time interval of about 200 k.y. The stratigraphic range of *D. megalcephalus* determined in the present study differs from that reported by Chen (1975). Chen reported a synchronous occurrence of the FAD of *D. megalcephalus* and the FAD of *Actinomma golownini* (= *A. tanyacantha*), based on results of DSDP Site 266. At Holes 689B and 690B the FAD of *D. megal-*

cephalis occurs distinctly later than the FAD of *A. golownini* and can be placed at around 12.5 Ma. In Hole 751A of ODP Leg 120 *D. megalcephalis* occurs above a middle Miocene disconformity at around 12 Ma (preliminary results of Abelmann, in press).

Actinomma golownini Zone (13.1–12.55 Ma)

Author. Chen (1975), as *Actinomma tanyacantha* Zone, modified herein.

Top. First appearance of *Dendrospyrus megalcephalus*.

Base. First appearance of *Actinomma golownini*.

Paleomagnetic correlation. The top of the zone is placed between the Subchrons C5AN-3 and C5AN-4, the base between C5AN-5 and C5AN-6.

Remarks. Chen's zone, originally described as *Actinomma tanyacantha* Zone, is modified at its top. (For comments on nomenclatural changes of the nominate species see Taxonomy in this chapter.)

Cycladophora humerus Zone (14.2–13.1 Ma)

Author. Abelmann, herein.

Top. First appearance of *Actinomma golownini*.

Base. First appearance of *Cycladophora humerus*.

Paleomagnetic correlation. The top of the zone is placed between the Subchrons C5AN-5 and C5AN-6, the base at the top of C5AN-8.

Remarks. An additional important stratigraphic mark at the base of this zone is the FAD of *Lychnocanoma* sp. B. Near the zonal base the probable evolutionary transition from *Antarctissa robusta* to *A. deflandrei* is completed.

Eucyrtidium punctatum Zone (14.2–17.6/15.6 Ma)

Author. Chen (1975), modified herein.

Top. First appearance of *Cycladophora humerus*.

Base. First appearance of *Eucyrtidium punctatum*.

Paleomagnetic correlation. The top of the zone is placed at the top of Subchron C5AN-8, the base occurs somewhere between the base of CSBN-2 and the top of CDN-1.

Remarks. The biostratigraphic marker species *Spongomyelissa dilli*, which defined the top of the *E. punctatum* Zone in Chen's report, is not encountered in the studied sediment sections. Therefore the top of the *E. punctatum* Zone is redefined herein. The base of this zone cannot be determined exactly because the lower portion of this zone is omitted at both investigated holes by a disconformity. This disconformity (Hiatus N3) probably spans a time interval from 17.6 to 15.6 Ma according to integrated bio- and geomagnetostratigraphic results (Figs. 3, 4; Tables 2, 3).

Cycladophora golli regipileus Zone (18.4–17.6/15.6 Ma)

Author. Chen (1975), modified herein.

Top. First appearance of *Eucyrtidium punctatum*.

Base. First appearance of *Cycladophora golli regipileus*.

Paleomagnetic correlation. The top of the zone is placed somewhere between the reversed interval below C5BN-2 and the top of C5DN-1 (Hiatus N3), the base near the top of C5EN.

Remarks. Additional important stratigraphic markers at the base of this zone are the FAD of *Gondwanaria deflandrei* and *Stauropiphox communis*. Considering the integrated bio- and geomagnetostratigraphic results, the zone can be placed in the late early Miocene, later than the age assignment of Chen, who correlated this zone to the early early Miocene.

Cyrtocapsella longithorax Zone (19.4/19.1–18.4 Ma)

Author. Abelmann, herein.

Top. First appearance of *Cycladophora golli regipileus*.

Base. First appearance of *Cyrtocapsella longithorax*.

Paleomagnetic correlation. The top of the zone is placed below the top of C5EN, the base between C5EN and CN-6.

Remarks. The base of this zone cannot be determined exactly because the lower portion of this zone is omitted at both investigated holes by a disconformity (Hiatus N2). According to integrated bio- and geomagnetostratigraphic results, the zonal base is placed between the time interval 19.4–19.1 Ma approximately (Figs. 3, 4; Tables 2, 3). An additional important stratigraphic marker at the zonal base is the "FAD's" of *Dendrospyrus stabilis*, *Tripilidium clavipes*, and *Lithomelissa cf. ehrenbergi*, which might also be caused by the hiatus (Figs. 5, 6).

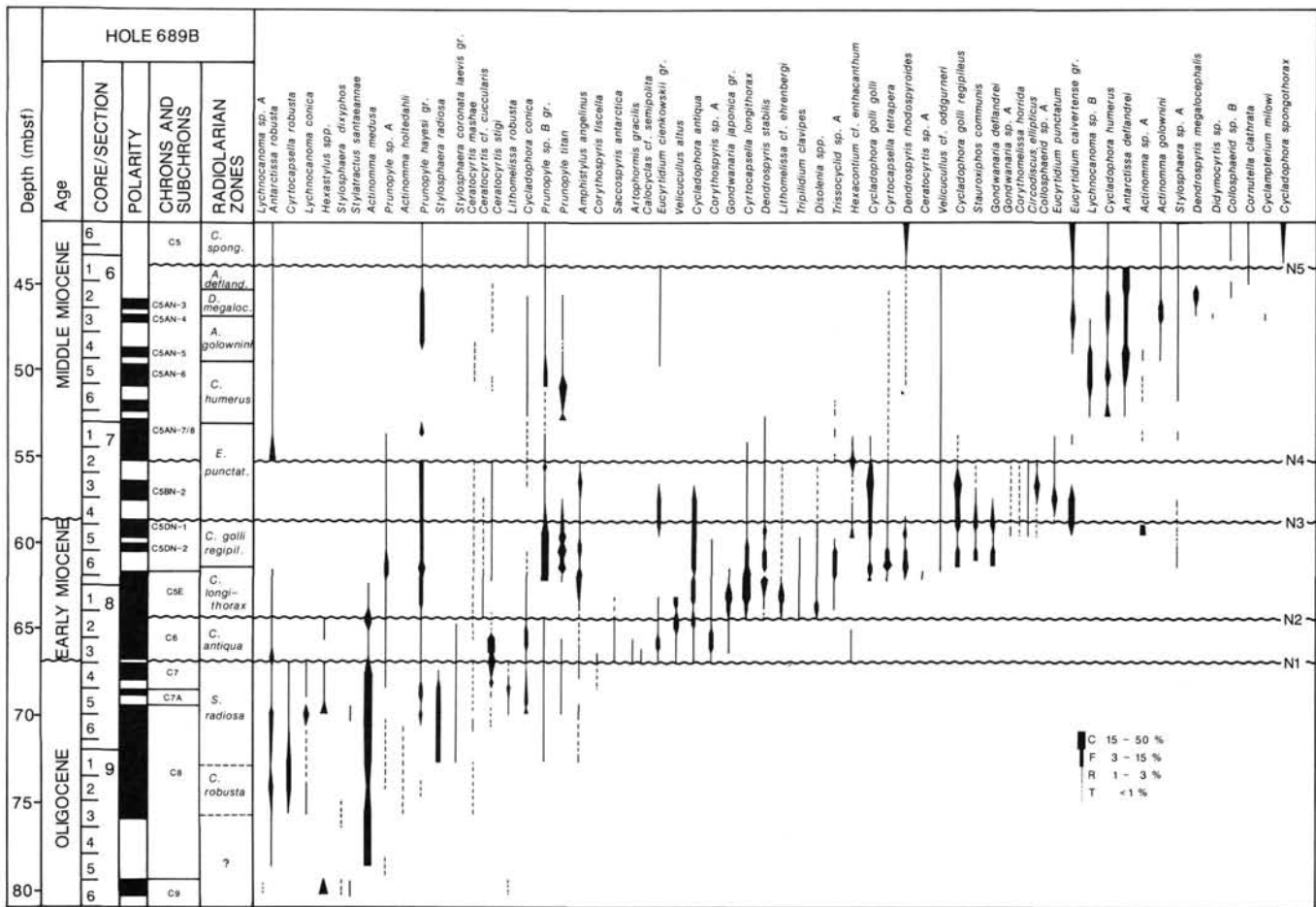


Figure 5. Ranges of selected radiolarian species and radiolarian zonation for upper Oligocene to middle Miocene Antarctic sediments in Hole 689B, correlated to the geomagnostratigraphy established by Spieß (this volume).

Cycladophora antiqua Zone (ca. 19.9–19.4/19.1 Ma)

Author. Abelmann, herein.

Top. First appearance of *Cyrtocapsella longithorax*.
Base. First appearance of *Cycladophora antiqua*.

Paleomagnetic correlation. The top of the zone is placed between C5EN and C6N, the base in the middle portion of C6N.

Remarks. Additional important stratigraphic markers at the zonal base are the FAD of *Velicuculus altus* and the LAD's of *Stylosphaera radiososa* and *Lychnocanoma conica*. The appearances of these radiolarian species at the base of the zonal boundary might also be caused by the occurrence of a hiatus, which is not yet delineated.

Stylosphaera radiososa Zone (?27.2–ca. 19.9 Ma)

Author. Abelmann, herein.

Top. First appearance of *Cycladophora antiqua*.
Base. First appearance of *Stylosphaera radiososa*.

Paleomagnetic correlation. The top of the zone is placed in the middle portion of C6N, the base in the middle part of C8N.

Remarks. The range of this zone cannot be determined exactly because a large portion of the zone is omitted at both investigated holes by a disconformity (Hiatus N1), which separates upper Oligocene from lower Miocene sediments (Fig. 2). According to integrated bio- and geomagnostratigraphic results, the hiatus probably spans a time interval of approximately 6 m.y. (Figs. 3, 4; Tables 2, 3). An additional important stratigraphic marker species of the zone is the occurrence of *Lithomelissa robusta* that appears for the first time in the lower portion of the zone, near the top of Subchron C9N.

Cyrtocapsella robusta Zone (?27.7–?27.2 Ma)

Author. Abelmann, herein.

Top. First appearance of *Stylosphaera radiososa*.
Base. First appearance of *Cyrtocapsella robusta*.

Paleomagnetic correlation. The top of the zone is placed in the middle portion of C8N, the base near the base of C8N.

Remarks. An accurate age determination of this zone is not possible because radiolarians are not well documented in this interval. Strontium isotope data established by Stott et al. (this volume) at Hole 689B indicate a younger age of 20.6 to 25.3 Ma for Section 113-689-8H-4 to 9H-5 than the age determination based on the paleomagnetic record (Spieß, this volume), which shows an age of 28.1 Ma for the base (C9N) of this interval.

RADIOLARIANS AT EACH SITE

Site 689

Site 689 is situated near the crest of Maud Rise ($64^{\circ}31.01'S$, $3^{\circ}06.03'E$) at a water depth of 2080 m (Fig. 1). Of the four holes drilled at Site 689, radiolarians were investigated from the late Oligocene (Section 113-689B-9H-6) to the end of the middle Miocene (Section 113-689B-5H-6) of Hole 689B. The ranges and the abundance pattern of the recovered radiolarians are shown in Table 4 and Figure 5. The radiolarian preservation is generally good in the middle Miocene and in the upper portion of the early Miocene and is moderate to poor in the lower por-

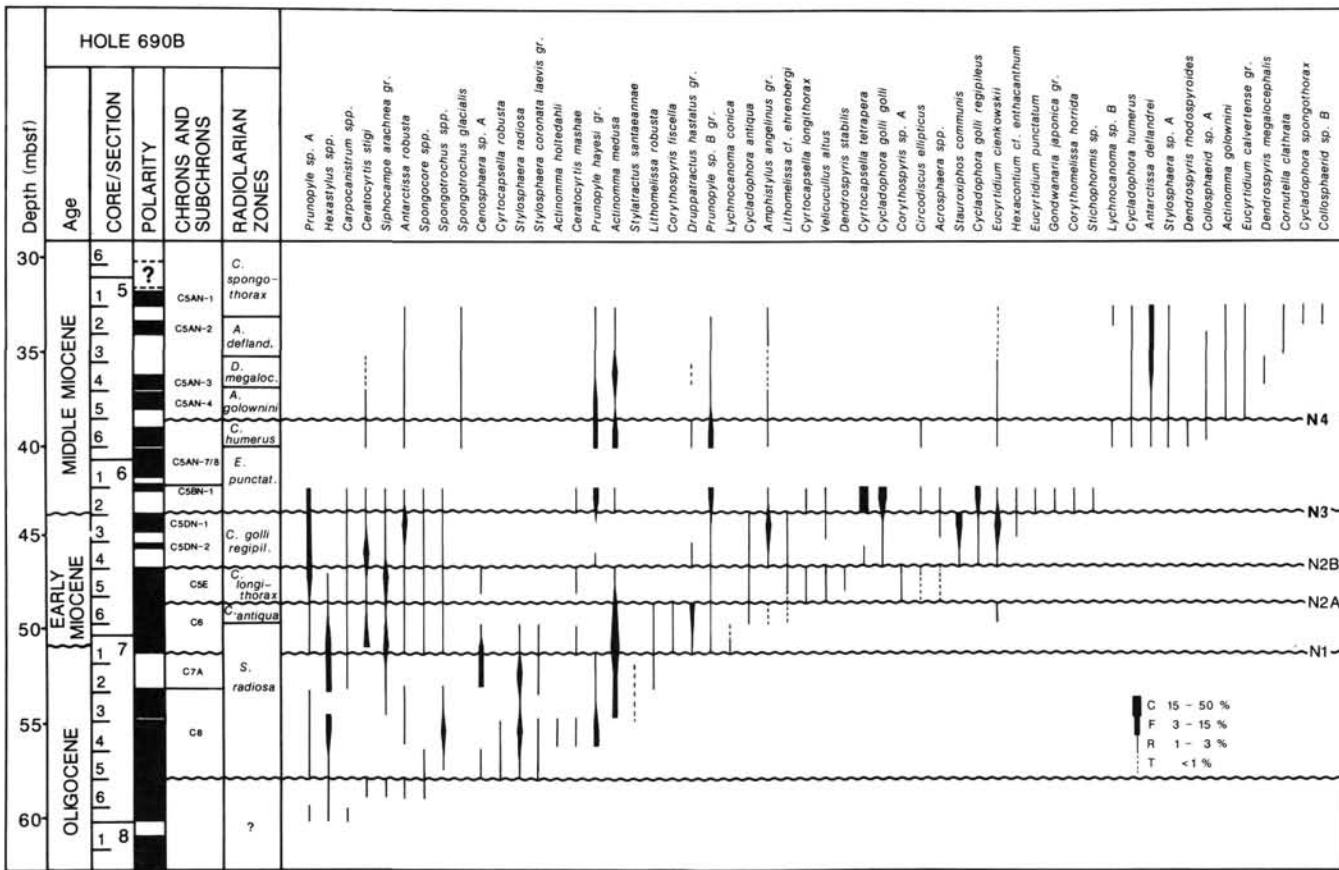


Figure 6. Ranges of selected radiolarian species and radiolarian zonation for upper Oligocene to middle Miocene Antarctic sediments in Hole 690B, correlated to the geomagnostratigraphy established by Spieß (this volume).

tion of the early Miocene and in the late Oligocene. Low radiolarian numbers occur in the late Oligocene, in the lower portion of the early Miocene, and in an interval in the middle Miocene (Samples 113-689B-7H-1, 9-11 cm, to 6H-6, 70-72 cm) where they are diluted by the mass occurrence of the diatom species *Actinocyclus ingens* (Table 4). In the upper portion of the early Miocene and in the Miocene except for the interval in the middle Miocene, radiolarian numbers are generally high. High radiolarian species diversities are observed in the upper portion of lower Miocene and in middle Miocene sediments, low species diversities in the lower portion of lower Miocene sediments. The lowest species diversity occurs in upper Oligocene sediments below Hiatus N1.

The stratigraphically oldest radiolarian assemblage investigated in this study is in Section 113-689B-9H-6 and is late Oligocene in age. An accurate age determination of the upper Oligocene is not yet possible. Strontium isotope data indicate an age of 20.6 to 25.3 Ma for Section 113-689B-8H-4 to 9H-5 (Stott et al., this volume). The paleomagnetic record was interpreted to represent an older age of 28.1 Ma (C9N) for the base of this interval (Spieß, this volume).

Five hiatuses (N1-N5) were delineated in the studied sediment sequences (Table 2, Fig. 3). Age determination of the hiatuses was made in combination with the diatom stratigraphy (Gersonde and Burckle, this volume) and magnetostratigraphy (Spieß, this volume). The oldest hiatus (N1), which separates lower Miocene from upper Oligocene sediments, occurs at 67 mbsf between Samples 113-689B-8H-3, 144-146 cm, and 8H-4, 120-122 cm, spanning an age of approximately 20.0-26.3 Ma.

Hiatus N2 occurs at 64.7 mbsf, between Samples 113-689B-8H-2, 86-88 cm, and 8H-2, 57-59 cm, from ~19.1 to 19.4 Ma. In comparison to Hole 690B the lower part of the *Cycladophora antiqua* Zone and the upper part of the *Stylosphaera radiosa* Zone are missing in Hole 689B. Thus, it can be concluded that the lower part of Chron C6 is absent in Hole 689B. Hiatus N3 is at 58.8 mbsf, between Samples 113-689B-7H-4, 148-150 cm, and 7H-3, 145-147 cm. In Hole 751A (Leg 120) the *Cyrtocapsella golli regipileus* Zone occurs in Chron C5D and the first appearance of *Eucyrtidium punctatum* at the top of C5D (preliminary results; Abelmann, in press). For that reason Hiatus N3 can be placed at the top of Subchron C5DN-1, spanning approximately 15.6-17.6 Ma, which omits Chron C5C. Hiatus N4 is at 55.1 mbsf, between Samples 113-689B-7H-2, 65-67 cm, and 7H-2, 115-116 cm, spanning approximately 14.6-15.0 Ma. This hiatus is defined by the occurrence of *Stauroxiphos communis* in the *E. punctatum* Zone in Hole 689B, and its absence in the *E. punctatum* Zone in Hole 690B, as well as by the occurrence, in Hole 690B, of *Stichophormis* sp., which does not occur in Hole 689B. Considering the geomagnetic polarity pattern, the absence of Subchron C5BN-1 in Hole 689B and Subchron C5BN-2 in Hole 690B is supposed (Figs. 5, 6). According to the diatom biostratigraphic results of Gersonde and Burckle (this volume), the youngest hiatus (N5) of the investigated sediment sequence can be placed at 43.8 mbsf between Samples 113-689B-6H-1, 70-72 cm, and 6H-1, 26-28 cm, spanning approximately 11.4-12.3 Ma.

The lowermost three sections of Core 113-689B-9H-3 (Sections 113-689B-9H-6 to 113-689B-9H-3) are not zoned because

Table 4. Radiolarians in Hole 689B, abundance and preservation.

Zones	unzoned			<i>C. robusta</i>		<i>Stylosphaera radiosa</i>								<i>Cycladophora antiqua</i>						<i>Cyrtocapsella longithorax</i>						
Core section	9H-6	9H-5	9H-4	9H-3	9H-2	9H-1	8H-6	8H-5	8H-4				8H-3			8H-2			8H-1							
Interval	71-73	71-73	71-73	71-73	71-73	71-73	145-147	120-122	86-88	55-57	144-146	119-121	86-88	144-146	120-122	86-88	56-58	149-151	120-122	86-88	57-59	144-146	120-122			
Abundance	T	T	R	R	R	F	R	R	R	F	C	C		F	C	F	F	C	F	R	F	F	F			
Preservation	P	P	P	P	M	M	G	G	G	G	G	G	G	G	G	G	G	M	G	G	G	G	G			
Spumellaria				C T R	F-C T	C T	T	F-C		R	R	R	R	R	R	R		R	R	R	T-R					
<i>Hexastylus</i> spp. <i>Stylosphaera dixiphos</i> <i>Stylaractus santaeanneae</i> <i>Actinomma medusa</i> <i>Prunopyle</i> sp. A								R	C	C	C	F-C	C	R	C	R	R	R	R	R	F-C	R	T	T		
<i>Larcopyle büttschlii</i> <i>Actinomma holtedahli</i> <i>Tholoniid</i> sp. B <i>Prunopyle hayesi</i> group <i>Stylosphaera radiosa</i>				T	R	T	T	R	T	R	R	T-R	T-R	R	R	R	R	R	R	R	T	R-F	R-F			
<i>Stylosphaera coronata laevis</i> gr. <i>Prunopyle</i> sp. B gr. <i>Amphistylus angelinus</i> <i>Actinomma</i> sp. A <i>Actinomma</i> sp. B								R	R-F	R-F	R	R-F	R-F	R-F	R	R	R	R	R	R	R	T	R	R		
<i>Prunopyle titan</i> <i>Prunopyle</i> sp. C <i>Prunopyle tetrapila</i> <i>Spongopyle osculosa</i> <i>Spongotorchus</i> spp.				R		R		R	R	R	R	R	R	R	R	R	R	R	R	R	R	T	T	T		
<i>Spongocore</i> spp. <i>Cenosphaera</i> sp. A <i>Hexaconitium</i> spp. <i>Lithelius nautiloides</i> gr. <i>Druppatractus hastatus</i> gr.						R		R	R	R	R	R-F	R	R	R	R	R	R	R	R	R	R	T-R	R		
<i>Hexaconitium</i> cf. <i>enthacanthum</i> <i>Spongotorchus glacialis</i> <i>Stylaractus neptunus</i> <i>Disolenia</i> spp. <i>Prunopyle</i> group D						R		R	R	R	R	R	R	R	R	R	R	R	R	R	R	R	R	R		
<i>Lithocarpium polyacantha</i> gr. <i>Stylosphaera</i> sp. A <i>Stauropiphos communis</i> <i>Stylodictya validispina</i> <i>Tholoniid</i> sp. B																R		R	R	R	R	F	R-F	F		
<i>Actinomma</i> sp. A <i>Spongodiscus craticulatus</i> <i>Circodiscus ellipticus</i> <i>Collosphaerid</i> sp. A <i>Heliodiscus</i> sp. A																						R				
<i>Actinomma golownini</i> <i>Tetrapyle octacantha</i> <i>Didymocystis</i> spp. <i>Collosphaerid</i> sp. B																						R				

Nassellaria	T	R	R T-R	F R-F	R F	F R	F R-F	R R	R-F R	R R	R R	R R	T-R R	F T	R-F T	R R	R R	R R	
<i>Lychnocanoma</i> sp. A																			
<i>Antarctissa robusta</i>																			
<i>Cyrtocapsella robusta</i>																			
<i>Lychnocanoma conica</i>																			
<i>Siphocampe arachnea</i> group																			
<i>Carpocanarium papillosum</i>			T T	R R	R R	R R	T T	R R	T R	T R	T R	T R	F-C T	R F	F-C F-C	F-C F-C	T T	T T	
<i>Ceratocyrtis mashae</i>																			
<i>Ceratocyrtis stigi</i>																			
<i>Lithomelissa robusta</i>																			
<i>Lithomelissa tricornis</i>	T																		
<i>Cyrtopera laguncula</i>							T T	T T	T T	T T	T T	T T	T T	T R	T R	T T	T T	T T	
<i>Artrostrobis annulatus</i>																			
<i>Cyrtocapsella cornuta</i>																			
<i>Cornutella profunda</i>																			
<i>Dictyophimus gracilipes</i>																			
<i>Cycladophora conica</i>																			
<i>Peripyramis circumtexa</i>																			
<i>Lithomelissa</i> sp. A																			
<i>Carpocanistrum</i> spp.																			
<i>Corythospyris fiscella</i>																			
<i>Saccospyris antarctica</i>																			
<i>Artophysmis gracilis</i>																			
<i>Calocycles</i> cf. <i>semipolita</i>																			
<i>Dictyophimus</i> cf. <i>platycephalus</i>																			
<i>Corythospyris</i> sp. A																			
<i>Velicucillus altus</i>																			
<i>Cycladophora antiqua</i>																			
<i>Cyrtocapsella longithorax</i>																			
<i>Eucyrtidium ciénkowskii</i> gr.																			
<i>Ceratocyrtis</i> cf. <i>cucullaris</i>																			
<i>Gondwanaria japonica</i> gr.																			
<i>Lithomelissa</i> cf. <i>ehrenbergi</i>																			
<i>Dendrospyris stabilis</i>																			
<i>Cyrtocapsella cornuta</i>																			
<i>Triplidium clavipes</i>																			
<i>Trissocyliid</i> sp. A																			
<i>Ceratocyrtis</i> sp. A																			
<i>Cycladophora golli golli</i>																			
<i>Cyrtocapsella tetraptera</i>																			
<i>Cyrtocapsella japonica</i>																			
<i>Vellecucillus</i> cf. <i>oddgurneri</i>																			
<i>Dendrospyris rhodospyroides</i>																			
<i>Gondwanaria deflandrei</i>																			
<i>Cycladophora golli regipileus</i>																			
<i>Gondwanaria</i> sp. A																			
<i>Corythomelissa horrida</i>																			
<i>Eucyrtidium punctatum</i>																			
<i>Eucyrtidium calvertense</i> gr.																			
<i>Lychnocanoma</i> sp. B																			
<i>Cycladophora humerus</i>																			
<i>Antarctissa deflandrei</i>																			
<i>Cyclampterium milowi</i>																			
<i>Dendrospyris megalcephalis</i>																			
<i>Phormostichoartus corbula</i>																			
<i>Cornutella clathrata</i>																			
<i>Cycladophora spongothorax</i>																			

Table 4 (continued).

Zones	Cyrtocapsella longithorax				Cycladophora golli regipileus						Eucyrtidium punctatum												
Core section	7H-7		7H-6		7H-5				7H-4		7H-3		7H-3		7H-2		7H-2		7H-1				
Interval	88-90	56-58	21-23	145-147	117-119	89-91	60-62	143-145	120-122	86-88	55-57	148-150	145-147	56-58	107-109	70-72	65-67	9-11	120-122	88-90	70-72	57-59	32-34
Abundance	F	F	F	F	C	C	C	F	F	F	C	C	A	A	C	A	F	B	T	R	F	F	R
Preservation	G	G	G	G	G	G	G	G	G	M	G	G	G	G	G	G	G	G	G	G	G	G	C
Spu mellaria																							
<i>Hexastylus</i> spp. <i>Stylosphaera dixiphos</i> <i>Stylatractus santeannae</i> <i>Actinomma medusa</i> <i>Prunopyle</i> sp. A	R		T-R		T-R		R-F		F		R		R		R-F		F		R		R		R
<i>Larcopyle büttschlii</i> <i>Actinomma holtedahli</i> <i>Tholoniid</i> sp. B <i>Prunopyle hayesi</i> group <i>Stylosphaera radiosia</i>	R-F		F		F-C		R-F		T		R-F		T		F		T		R-F		R		T
<i>Stylosphaera coronata laevis</i> gr. <i>Prunopyle</i> sp. B gr. <i>Amphistylus angelinus</i> <i>Actinomma</i> sp. A <i>Actinomma</i> sp. B	R-F		F		F-C		F		C		F		F		F		F		R-F		F		T F
<i>Prunopyle titan</i> <i>Prunopyle</i> sp. C <i>Prunopyle tetrapila</i> <i>Spongopyle osculosa</i> <i>Spongotrochus</i> spp.	R		F-C		C		R-F		R		F-C		R-F		F-C		R		T		R		R
<i>Spongocore</i> spp. <i>Cenosphaera</i> sp. A <i>Hexacontium</i> spp. <i>Lithelius nautiloides</i> gr. <i>Druppatractus hastatus</i> gr.	R		R		R		R		T		T		T		T-R		T		R		T		R
<i>Hexacanthium</i> cf. <i>enthaecanthum</i> <i>Spongotrochus</i> <i>glacialis</i> <i>Stylatractus</i> <i>neptunus</i> <i>Disolenia</i> spp. <i>Prunopyle</i> group D	T-R		R		R		R		T-R		R		T-R		R		T		T-R		F-C		F
<i>Lithocarpium polyacantha</i> gr. <i>Stylosphaera</i> sp. A <i>Stauropihos communis</i> <i>Stylocidictya validispina</i> <i>Tholoniid</i> sp. B	R-F		R-T		R-T		R-F		R		R-F		R		T		T		R-F		R-F		R
<i>Actinomma</i> sp. A <i>Spongodiscus craticulatus</i> <i>Circodiscus ellipticus</i> <i>Collosphaerid</i> sp. A <i>Heliodiscus</i> sp. A															R-F		R-F		R-F		R-F		R
<i>Actinomma golownini</i> <i>Tetrapyle octacantha</i> <i>Didymocystis</i> spp. <i>Collosphaerid</i> sp. B															T-R		T		R-F		R-F		R

Nassellaria	R R R-F R-F R R R R R T		F R-F R
<i>Lynchocanoma</i> sp. A <i>Antarctissa robusta</i> <i>Cyrtocapsella robusta</i> <i>Lynchocanoma conica</i> <i>Siphocampe arachnea</i> group	R T T R T R-F R R R-F R-F R-F R-F R-F R T R T T T T T T T T T T T T T T	T T	T T T T T T T T T T T R T T T T
<i>Carpocanarium papillosum</i> <i>Ceratocyrtis mashae</i> <i>Ceratocyrtis stigi</i> <i>Lithomelissa robusta</i> <i>Lithomelissa tricornis</i>	R T T T T R-F R R R-F R-F R-F R-F R-F T T R T T T T T T T T T T T T T T	T R T T T T T T T T T R T T T T	T T T T T T T T T R T T
<i>Cyrtopera laguncula</i> <i>Artrostrobus annulatus</i> <i>Cyrtocapsella cornuta</i> <i>Cornutella profunda</i> <i>Dictyophimus gracilipes</i>	T T T T T T T T R T T T T T T R R R R T R F R F R-F R-F R-F R	T T T T T T T T T T T R T T T T	T T T T T T R T T R T T
<i>Cycladophora conica</i> <i>Peripyramis circumtexa</i> <i>Lithomelissa</i> sp. A <i>Carpocanistrum</i> spp. <i>Corythospyris fiscella</i>	R R-F R R R T T R R R R R-F R-F R-F R-F R R R R R R R R	T T R R T T T T R F R-F R R-F R-F R T R T R T T T R T R T T	T T T R T T T T T R T-R
<i>Saccospirys antarctica</i> <i>Artorphormis gracilis</i> <i>Calocycles</i> cf. <i>semipolita</i> <i>Dictyophimus</i> cf. <i>platycephalus</i> <i>Corythospyris</i> sp. A	T T R T R T R T R R T R T R T-R R T	T T T T T T R T R R T T R T R R T R T R R	T T T T
<i>Velicucillus altus</i> <i>Cycladophora antiqua</i> <i>Cyrtocapsella longithorax</i> <i>Eucyrtidium cienkowskii</i> gr. <i>Ceratocyrtis</i> cf. <i>cucullaris</i>	R-F F F R R-F F-C F-C C C F-C T T R F-C R T T-R R T	F F F R-F T-R F R-F F R-F T-R F R R R R T F R R T T T	R-F T R R T-R R T T T T T T T T T T T T T T T
<i>Gondwanaria japonica</i> gr. <i>Lithomelissa</i> cf. <i>ehrenbergi</i> <i>Dendrospyris stabilis</i> <i>Cyrtocapsella cornuta</i> <i>Triplidium clavipes</i>	F-C F-C T-R R T F-C F-C T-R R T R R C T R T T T R T R R T-R R	F R-F R-F T R T F R R R R T F R R T T T F R R T T T	T T T T T T T T T T T T T T T T T T T T
<i>Trissocyclid</i> sp. A <i>Ceratocyrtis</i> sp. A <i>Cycladophora golli golli</i> <i>Cyrtocapsella tetrapera</i> <i>Cyrtocapsella japonica</i>	R R R R R R T R F-C R-F T T F-C T T T	F F F R R F R R R R F R-F F T T F R R T R F R R T T	T R R T T
<i>Vellucullus</i> cf. <i>oddgurneri</i> <i>Dendrospyris rhodospyroides</i> <i>Gondwanaria deflandrei</i> <i>Cycladophora golli regipileus</i> <i>Gondwanaria</i> sp. A	R R-F T	R R R R R ?F R-F R-F R R T T T T T R-F F F R R T-R F F R R	R R R R R R-F F-C F R-F R T T T-R T-R T R-F T T R R R-F T R R T
<i>Corythomelissa horrida</i> <i>Eucyrtidium punctatum</i> <i>Eucyrtidium calvertense</i> gr. <i>Lynchocanoma</i> sp. B <i>Cycladophora humerus</i>		T T R F	T R T R-F R T R R R-F R R T T R R
<i>Antarctissa deflandrei</i> <i>Cyclampterium milowi</i> <i>Dendrospyris megalcephalis</i> <i>Phormostichoartus corbula</i> <i>Cornutella clathrata</i>			
<i>Cycladophora spongothorax</i>			

Table 4 (continued).

Zones	Cycladophora humerus												Actinomma golownini			Dendrospriris megalcephalis			Antarctissa deflandrei		C. spong-thorax												
Core section	6H-7		6H-6		6H-5								6H-4		6H-3		6H-2			6H-1		5H-6											
Interval	32-34	10-12	144-146	117-119	84-86	70-72	144-146	116-118	89-91	70-72	54-56	31-33	108-110	56-58	143-145	91-93	58-60	83-85	70-72	32-34	143-145	84-86	144-146										
Abundance	R	R	R	R	R	T	C	C	F	C	F	R	F	C	C	C	C	C	C	C	F												
Preservation	G	G	G	G	G	G	G	G	M	G	G	G	M	M	G	G	G	G	G	G	G												
Spumellaria																																	
<i>Hexastylus</i> spp.																																	
<i>Stylosphaera dixiphos</i>																																	
<i>Stylaractus santaeannae</i>																																	
<i>Actinomma medusa</i>																																	
<i>Prunopyle</i> sp. A																																	
<i>Larcopyle bletschlii</i>	R	R R R												T	R R		R		R														
<i>Actinomma holtedahlii</i>																																	
<i>Tholoniid</i> sp. B																R-F F			R R		R R												
<i>Prunopyle hayesi</i> group																																	
<i>Stylosphaera radiosa</i>																																	
<i>Stylosphaera coronata laevis</i> gr.													F F		R R																		
<i>Prunopyle</i> sp. B gr.																																	
<i>Amphistylus angelinus</i>																																	
<i>Actinomma</i> sp. A																																	
<i>Actinomma</i> sp. B	R	T		C C										T	R R		R R		R R														
<i>Prunopyle titan</i>	C	F		C R												R R																	
<i>Prunopyle</i> sp. C																R					R												
<i>Prunopyle tetrapila</i>																																	
<i>Spongopyle osculosa</i>																																	
<i>Spongotrochus</i> spp.																																	
<i>Spongocore</i> spp.	T	T		T										T T	T																		
<i>Cenosphaera</i> sp. A	R	R		R R										R T-R	F-C		R																
<i>Hexacodium</i> spp.																																	
<i>Lithelius nautiloides</i> gr.																																	
<i>Druppatractus hastatus</i> gr.																																	
<i>Hexacodium cf. enthacanthum</i>																					R												
<i>Spongotrochus glacialis</i>																																	
<i>Stylaractus neptunus</i>																																	
<i>Disolenia</i> spp.																																	
<i>Prunopyle</i> group D																T-R		R R		R R		R R											
<i>Lithocarpium polyacanthum</i>																T-R		R R		T-R		R R											
<i>Stylosphaera</i> sp. A																																	
<i>Stauropiophos communis</i>	T	T-R		R R										T						T-R		R R											
<i>Stylodictya validispina</i>																																	
<i>Tholoniid</i> sp. B																																	
<i>Actinomma</i> sp. A																R R		R															
<i>Spongodiscus craticulatus</i>																R-F		R															
<i>Circodiscus ellipticus</i>																T T		R R					R										
<i>Collosphaerid</i> sp. A																R		R R					R										
<i>Heliodiscus</i> sp. A																T		R-F R					R R										
<i>Actinomma golownini</i>																R T		R-F R					R R										
<i>Tetrapyle octacantha</i>																R		R					R R										
<i>Didymocystis</i> spp.																T		R					R R										
<i>Collosphaerid</i> sp. B																T		R					R R										

Nassellaria							
<i>Lynchocanoma</i> sp. A <i>Antarcissa robusta</i> <i>Cyrtocapsella robusta</i> <i>Lynchocanoma conica</i> <i>Siphocampe arachnea</i> group	R T	R R	R R	R R	R R	F-C R	R R R
<i>Carpocanarium papillosum</i> <i>Ceratocyrtis mashae</i> <i>Ceratocyrtis stigi</i> <i>Lithomelissa robusta</i> <i>Lithomelissa tricornis</i>		T T			T		
<i>Cyrtopera laguncula</i> <i>Arrostrobus annulatus</i> <i>Cyrtocapsella cornuta</i> <i>Cornutella profunda</i> <i>Dicyophimus gracilipes</i>	R R-F	R R	T R	R R	T R	R R	R R R
<i>Cycladophora conica</i> <i>Peripyramis circumtexa</i> <i>Lithomelissa</i> sp. A <i>Carpocanistrum</i> spp. <i>Corythospyris fiscella</i>	R R	R R	R R	R R	R R R	R R	R R
<i>Saccospyris antarctica</i> <i>Artophormis gracilis</i> <i>Calocyclas</i> cf. <i>semipolita</i> <i>Dicyophimus</i> cf. <i>platycephalus</i> <i>Corythospyris</i> sp. A	R	T			T T		
<i>Velicucillus altus</i> <i>Cycladophora antiqua</i> <i>Cyrtocapsella longithorax</i> <i>Eucyrtidium cienkowskii</i> gr. <i>Ceratocyrtis</i> cf. <i>cucullaris</i>			T		T T	R R	R R
<i>Gondwanaria japonica</i> gr. <i>Lithomelissa</i> cf. <i>ehrenbergi</i> <i>Dendrospyris stabilis</i> <i>Cyrtocapsella cornuta</i> <i>Triplidium clavipes</i>	T-R	T T					
<i>Trissocyld</i> sp. A <i>Ceratocyrtis</i> sp. A <i>Cycladophora golli golli</i> <i>Cyrtocapsella tetrapera</i> <i>Cyrtocapsella japonica</i>		R T T	T T	T T	T		
<i>Vellucillus</i> cf. <i>oddgurneri</i> <i>Dendrospyris rhodospyroides</i> <i>Gondwanaria deflandrei</i> <i>Cycladophora golli regipileus</i> <i>Gondwanaria</i> sp. A	R T	R T	R T	R R	T T	R R	F
<i>Corythomelissa horrida</i> <i>Eucyrtidium punctatum</i> <i>Eucyrtidium calvertense</i> gr. <i>Lynchocanoma</i> sp. B <i>Cycladophora humerus</i>	R F	R R	R-F R	R-F R-F	R F R	R-F R F F	R R R R
<i>Antarcissa deflandrei</i> <i>Cyclampterium milowi</i> <i>Dendrospyris megalcephalis</i> <i>Phormostichoartus corbula</i> <i>Cornutella clathrata</i>	T	R R	R F	F-C F	F R	F-C F-C	R R R R
<i>Cycladophora spongotorax</i>							F

of low abundance and poor preservation of radiolarians. The assemblage recovered in this interval consists of *Antarctissa robusta*, *Hexastylus* spp., *Lychnocanoma* sp. A, *Stylosphaera dixyphos*, *Stylatractus santeannae*, and *Actinomma medusa*. The first appearance of *Cyrtocapsella robusta*, which marks the base of the *C. robusta* Zone, occurs at 76 mbsf between Samples 113-689B-9H-3, 71–73 cm, and 113-689B-9H-4, 71–73 cm. At this level are also the first occurrences of *Actinomma holtedahli* and *Ceratocyrtis mashae*. Taxa included in the *Prunopyle hayesi* group occur in the upper part of this interval. The first appearance of *Stylosphaera radios*a is placed at 72.6 mbsf between Samples 113-689B-9H-1, 71–73 cm, and 113-689B-9H-2, 71–73 cm. Below Hiatus N1 (Samples 113-689B-8H-3, 144–146 cm, to 8H-4, 120–122 cm), at 67.0 mbsf, *Stylosphaera radios*a, *Lychnocanoma conica*, *Lithomelissa robusta*, and *Corythospyris fiscella* occur for the last time. Above Hiatus N1, *Cycladophora antiqua*, *Velicucullus altus*, and *Eucyrtidium cienkowskii* group occur for the first time. At the same level the first occurrences of *Artophormis gracilis* and *Calocyclus cf. semipolita* are noted. *Artophormis gracilis* and *Calocyclus cf. semipolita* occur only in the short interval between Hiatus N1 and Sample 113-689B-8H-3, 120–122 cm. The first occurrence of *Cyrtocapsella longithorax* is above Hiatus N2, between Samples 113-689B-8H-2, 86–88 cm, and 113-689B-8H-2, 57–59 cm. At the same level also fall the first occurrences of *Dendrosprysis stabilis*, *Trissocyclid* sp. A, *Lithomelissa cf. ehrenbergi*, *Gondwanaria japonica*, *Triplidium clavipes*, and *Disolenia* spp. Within the *C. longithorax* Zone the first occurrences of *Cycladophora golli golli*, *Cyrtocapsella tetrapera*, and *Dendrosprysis rhodospyroides* were encountered between Samples 113-689B-7H-7, 21–23 cm, and 113-689B-8H-1, 56–58 cm. The FAD of the nominate species of the *Cycladophora golli regipileus* Zone together with the first appearance of *Stauroxiphos communis* and *Gondwanaria deflandrei* is noted between Samples 113-689B-7H-6, 89–91 cm, and 113-689B-7H-6, 117–119 cm. The first occurrence of *Eucyrtidium punctatum* is between Samples 113-689B-7H-4, 148–150 cm, and 113-689B-7H-3, 145–147 cm, an interval marked by a hiatus (N3). Thus, the FAD of *E. punctatum* cannot be defined accurately. The first appearances of *Cycladophora humerus*, *Lychnocanoma* sp. B, and *Antarctissa deflandrei* are placed between Samples 113-689B-6H-7, 32–34 cm, and 113-689B-7H-1, 32–34 cm, and the first appearance of *Actinomma golownini* between Samples 113-689B-6H-4, 108–110 cm, and 113-689B-6H-5, 31–33 cm. The first appearance of *Dendrosprysis megalcephalis* occurs between Samples 113-689B-6H-3, 58–60 cm, and 113-689B-6H-3, 70–72 cm, and its last appearance between Samples 113-689B-6H-2, 70–72 cm, and 113-689B-6H-2, 32–34 cm, together with the first appearance of *Cornutella clathrata*. *Cycladophora spongorthorax* has its first appearance together with *Collosphaerid* sp. B between Samples 113-689B-6H-1, 26–28 cm, and 113-689B-5H-6, 144–146 cm.

Site 690

Site 690 is located on the southeastern flank of Maud Rise ($65^{\circ}9.63'S$, $1^{\circ}12.30'E$), 116 km southwest from Site 689, at a water depth of 2914 m (Fig. 1). Of the three holes drilled at this site, only Hole 690B was studied. A sediment interval between Sections 113-690B-7H-7 and 113-690B-5H-2, which represents upper Oligocene to middle Miocene sediments, was investigated. Ranges and abundance patterns of radiolarians in the studied sections are shown in Table 5 and Figure 6. The preservation of the radiolarians is similar to that in Hole 689B, good in the upper portion of lower Miocene and in middle Miocene sediments and moderate to poor in the lower portion of lower Miocene and upper Oligocene sediments. Low radiolarian numbers occur in the late Oligocene, in the lower portion of the early Miocene, and in a time interval in the middle Miocene (Samples

113-690B-6H-1, 49–51 cm, to 113-690B-5H-6, 49–51 cm), where, as in Hole 689B, the radiolarians are diluted by the mass occurrence of the diatom species *Actinocyclus ingens*. In the upper portion of the early Miocene and in the middle Miocene (except the interval with the mass occurrence of the diatom species *A. ingens*) the abundance of radiolarians is generally high. The species diversity of radiolarians is low in the late Oligocene, higher in the Miocene.

Six hiatuses were delineated (Table 3, Fig. 4). The lowermost hiatus is in the late Oligocene between Samples 113-690B-7H-5, 49–51 cm, and 113-690B-7H-6, 49–51 cm. At this time the detailed range of this hiatus cannot yet be determined. Another hiatus (N4) is situated at 51.2 mbsf, between Samples 113-690B-7H-2, 114–115 cm, and 113-690B-7H-1, 49–51 cm, and separates upper Oligocene from lower Miocene sediments. This hiatus spans approximately 27.0–20.5 Ma. Hiatus N2A is at 48.7 mbsf between Samples 113-690B-6H-6, 49–51 cm, and 113-690B-6H-6, 27–28 cm, spanning approximately 19.6–19.0 Ma. This hiatus separates the lower portion of the *Cycladophora antiqua* Zone, characterized by the occurrences of *Corythospyris fiscella* and *Lithomelissa robusta*, from the *Cyrtocapsella longithorax* Zone. *Velicucullus altus*, which occurs in the *C. antiqua* Zone of Hole 689B, is not found in the *C. antiqua* Zone of Hole 690B. On the other side *C. fiscella* and *L. robusta*, which are distinctive for the lower part of the *C. antiqua* Zone of Hole 689B, do not occur in the *C. antiqua* Zone of Hole 690B. Therefore it can be suggested that the hiatus omits the upper part of the *Cycladophora antiqua* Zone, which is recovered in Hole 689B. Hiatus N2B is noted at 47.1 mbsf between Samples 113-690B-6H-4, 114–115 cm, and 113-690B-5H-5, 49–51 cm, from ~18.7 to 18.5 Ma. Hiatus N2B occurs at the boundary between the *Cyrtocapsella longithorax* and *Cycladophora golli regipileus* Zones. The hiatus is delineated by the lack of *Cycladophora golli golli* and *Cyrtocapsella tetrapera* in the *Cyrtocapsella longithorax* Zone of Hole 690B and their occurrence in the *C. longithorax* Zone of Hole 689B. Both species occur the first time together with *Cycladophora golli regipileus* and *Stauroxiphos communis* above Hiatus N2B. Hiatus N3 is placed at 43.8 mbsf between Samples 113-690B-6H-3, 49–51 cm, and 113-690B-6H-2, 114–115 cm. Hiatus N3 separates the *C. golli regipileus* and *Eucyrtidium punctatum* Zone, marked by a sharp transition from biogenic calcareous sediments (below N3) and biogenic siliceous sediments (above N3) (Barker, Kennett, et al., 1988). As in Hole 689B, the range of this hiatus cannot yet be defined accurately. According to preliminary results of Site 751 (Leg 120), the *C. golli regipileus* Zone ranges in Chron C5D, and the first appearance of *E. punctatum* can be placed at the top of C5D in Site 751 (Leg 120). Thus, it can be suggested that Hiatus N3 omits Chron C5C. At the base of the *E. punctatum* Zone in Hole 690B occurs the radiolarian species *Stichophormis* sp., which was also found in Site 751 (Leg 120) in the lower *E. punctatum* Zone and which is missing in Hole 689B. In Hole 689B *Stauroxiphos communis* ranges into the *E. punctatum* Zone, and the last appearance of *Cycladophora antiqua* is also situated in the lower portion of the *E. punctatum* Zone. The lack of these radiolarian species in the *E. punctatum* zone of Hole 690B indicates that the lower part of the *E. punctatum* Zone with the paleomagnetic Subchron C5BN-2 is missing while Subchron CBN-1 is recovered. In contrast to Hole 690B, the upper portion of the *E. punctatum* Zone (C5BN-1) is not recovered in Hole 689B, but the lower portion with subchron C5BN-2 is present (Figs. 5, 6). The estimated range of N3 spans ~17.6–15.1 Ma. Hiatus N4A marks the boundary between the *Cycladophora humerus* and *Actinomma golownini* Zone, at 38.4 mbsf between Samples 113-690B-5H-6, 28–29 cm, and 113-690B-5H-5, 114–115 cm, spanning ~13.8–12.8 Ma. The radiolarian species *Lychnocanoma* sp. B occurs with few to common abundances

Table 5. Radiolarians in Hole 690B, abundance and preservation.

Zones	unzoned	<i>Stylosphaera radiosa</i>						<i>C. antiqua</i>	<i>C. longithorax</i>	<i>C. g. regipileus</i>	<i>E. punctatum</i>	<i>C. humerus</i>	<i>A. golownini</i>	<i>D. megalcephal.</i>	<i>A. deflandrei</i>	<i>C. spongotorax</i>	
Core section	7H-7 7H-6	7H-5	7H-4	7H-3	7H-2	7H-1	6H-6	6H-5	6H-4	6H-3	6H-2	6H-1	5H-6	5H-5	5H-4	5H-3	5H-2
Interval	49-51	49-51	49-51	49-51	49-51	49-51	49-51	49-51	49-51	49-51	49-52	49-51	49-51	49-51	49-51	49-51	49-51
Abundance	R R	R-F	F F	R-F	F-C	F	F-C	F	C	C-A	R	F-C	F	F-C	F-C	F	
Preservation	P P	P M	M M	P M	P	P	P	M M	M-G	G	M-P	M-P	M	M-G	M-G	M-G	
Spumellaria																	
<i>Prunopyle</i> sp. A	R R	R R	R R	R R	R R	R R	R R	F R	F R	F R	F R	R R	R R	T R	R	R	
<i>Hexastylus</i> spp.																	
<i>Spongocore</i> spp.																	
<i>Larcopyle butschlii</i>																	
<i>Spongotrochus</i> spp.																	
<i>Spongotrochus glacialis</i>																	
<i>Prunopyle tetrapila</i>																	
<i>Canospaera</i> sp. A																	
<i>Lithocarpium polyacantha</i> gr.																	
<i>Stylosphaera coronata laevis</i> gr.																	
<i>Stylosphaera radiosa</i>																	
<i>Actinomma holtedahli</i>																	
<i>Prunopyle hayesi</i>																	
<i>Actinomma</i> sp. C																	
<i>Stylosphaera santaeannae</i>																	
<i>Tholoniid</i> sp. A								R									
<i>Tholoniid</i> sp. B									R								
<i>Lithelius nautiloides</i> gr.										R							
<i>Druppatractus hastatus</i> gr.											R						
<i>Prunopyle</i> sp. B gr.												R	R	R	R	R	
<i>Stylactractus neptunus</i>																	
<i>Circodiscus ellipticus</i>																	
<i>Acrosphaera</i> spp.																	
<i>Stauropiphos communis</i>																	
<i>Prunopyle</i> sp. C																	
<i>Hexacontium cf. enthaanthum</i>																	
<i>Heliодiscus</i> sp.																	
<i>Stylosphaera</i> sp. A																	
<i>Spongopyle osculosa</i>																	
<i>Collosphaerid</i> sp. A																	
<i>Actinomma golownini</i>																	
<i>Collosphaerid</i> sp. B																	
Nassellaria																	
<i>Carpocanarium papillosum</i>	R R	R R	R R	R R	R R	R R	R R	R R	R R	R R	R R	R R	R R	R R	R R	R R	
<i>Ceratocyrtis stigi</i>																	
<i>Siphocampe arachnea</i> gr.																	
<i>Antarctissa robusta</i>																	
<i>Cyrtocapsella robusta</i>																	
<i>Ceratocyrtis mashae</i>																	
<i>Cycladophora conica</i>																	
<i>Lithomelissa robusta</i>																	
<i>Corythospyris fiscella</i>																	
<i>Lychnocanoma conica</i>																	
<i>Cycladophora antiqua</i>																	
<i>Cyrtocapsella tetraptera</i>																	
<i>Lithomelissa ehrenbergi</i>																	
<i>Cyrtocapsella longithorax</i>																	
<i>Velicucullus altus</i>																	
<i>Eucyrtidium cienkowskii</i> gr.																	
<i>Corythospyris</i> sp. A																	
<i>Dendrosypyris stabilis</i>																	
<i>Cycladophora golli regipileus</i>																	
<i>Eucyrtidium punctatum</i>																	
<i>Gondwanaria japonica</i> gr.																	
<i>Corythomelissa horrida</i>																	
<i>Stichophormis</i> sp.																	
<i>Lychnocanoma</i> sp. B																	
<i>Cycladophora humerus</i>																	
<i>Antarctissa deflandrei</i>																	
<i>Eucyrtidium calvertense</i> gr.																	
<i>Dendrosypyris megalcephalis</i>																	
<i>Cornutella clathrata</i>																	
<i>Cycladophora spongotorax</i>																	

in the *Cycladophora humerus* and *Actinomma golownini* Zone of Hole 689B. However, in Hole 690B *Lychnocanoma* sp. B is only found in low numbers in the *C. humerus* Zone and is lacking in the *A. golownini* Zone. Considering the geomagnetic polarity pattern established by Spieß (this volume), it can be concluded that Hiatus N4 omits Subchrons C5AN-6 and C5AN-5.

The late Oligocene is not zoned because of the low abundance and poor preservation of radiolarians in the lowermost interval of Core 113-689B-7H between Samples 7H-7, 49–51 cm, and 113-689B-7H-6, 49–51 cm. The assemblage consists of *Prunopyle* sp. A., *Hexastylus* spp., *Carpocanarium papillosum*, *Antarctissa robusta*, and *Siphocamppearachnea* group. The first appearance of *Cyrtocapsella robusta* together with *Stylosphaera radios*a occurs between Samples 113-690B-7H-5, 49–51 cm, and 113-690B-7H-6, 49–51 cm. The *Cyrtocapsella robusta* Zone is missing in Hole 690B, due to the occurrence of a hiatus in the late Oligocene. The age of the lower part of the upper Oligocene cannot yet be defined in detail. The last appearance of *Stylosphaera radios*a, together with *Lychnocanoma conica* and the first appearance of *Cycladophora antiqua*, *Eucyrtidium cienkowskii* group, and *Lithomelissa* cf. *ehrenbergi*, occurs above Hiatus N1 between Samples 113-689B-6H-6, 49–51 cm, and 113-689B-7H-1, 49–51 cm. Above Hiatus N1 *Corythospyris fiscella* and *Druppatractus hastatus* group appear for the first time and range up to the sediment interval marked by Hiatus N2A. *Velicucullus altus* does not occur in the *Cycladophora antiqua* Zone of Hole 690B. This indicates that the upper part of the *Cycladophora antiqua* Zone, which is recovered in Hole 689B, is missing. The first appearance of *Cyrtocapsella longithorax*, together with *Velicucullus altus*, *Dendrosprysis stabilis*, and *Corythospyris* sp. A., occurs above Hiatus N2A. The base and top of the *C. longithorax* Zone are marked by Hiatus N2A and N2B. Above Hiatus N2B *C. golli golli*, *C. tetraperata*, *C. golli regipileus*, and *Stauropiphos communis* occur for the first time. The top of the *C. golli regipileus* Zone and the base of the *E. punctatum* Zone cannot be defined accurately because of the occurrence of Hiatus N3. The first occurrences of *Cycladophora humerus*, *Lychnocanoma* sp. B, and *Antarctissa deflandrei* are between Samples 113-690B-5H-6, 49–51 cm, and 113-690B-6H-1, 49–51 cm. The *C. humerus* Zone and the overlying *Actinomma golownini* Zone are separated by Hiatus N4A. The first appearance of *Dendrosprysis megalcephalis* occurs between Samples 113-690B-5H-4, 49–51 cm, and 113-690B-5H-5, 49–51 cm, the last appearance of *D. megalcephalis* and the first appearance of *Cornutella clathrata* between Samples 113-690B-6H-3, 49–51 cm, and 113-690B-6H-4, 49–51 cm. The first appearance of *Cycladophora spongothorax* together with *Collophaerid* sp. B is placed between Samples 113-690B-5H-1, 49–51 cm, and 113-690B-5H-2, 49–51 cm.

TAXONOMY

Order POLCYSTINA Ehrenberg, 1838; emend. Riedel, 1967

Suborder SPUMELLARIA Ehrenberg, 1875

Family COLLOSPHAERIDAE Müller, 1858

Genus COLLOSPHAERA Müller, 1858

Collophaerid sp. A

(Plate 1, Fig. 2)

Description. Spherical shell, smooth surface with few irregularly shaped and spaced large and small pores. Large pores extend outward into tubes.

Measurements based on six specimens from Samples 113-689B-7H-2, 107–109 cm, to 113-689B-6H-3, 58–60 cm. Diameter of the shell 121–150 µm, number of large pores on half-equator 3–4, diameter of the pores 13–26 µm.

Occurrence in Holes 689B and 690B. Middle Miocene.

Collophaerid sp. B
(Plate 1, Fig. 11)

Description. Large spherical shell with numerous irregularly shaped and scattered pores, which extended outward into cylindrical tubes. The ends of the tubes are notched.

Occurrences in Holes 689B and 690B. Late middle Miocene.

Remarks. The species is similar to *Collophaerid* (sp. in Keany, 1979, pl. 1, fig. 4) and similar to *Acrosphaera* sp.—“conical pore” collophaerid (Lazarus, this volume).

Genus *DISOLENIA* Ehrenberg, 1860

Disolenia spp. group
(Plate 1, Figs. 3 A, B)

Description. *Disolenia* spp. includes all collophaerids with external pored tubules. The number of the tubules varies between three and seven.

Occurrences in Holes 689B and 690B. Early to middle Miocene.

Remarks. This species group includes all species of *Disolenia* and *Solesolenia*.

Genus *ACROSPAERA* Haeckel, 1881

Acrosphaera spp.
(Plate 1, Fig. 1)

Occurrences in Holes 689B and 690B. Rare in lower Miocene sediments, more abundant in middle Miocene sediments.

Remarks. This species group includes all species of *Acrosphaera*.

Family ACTINOMMIDAE Haeckel, 1862; emend. Sanfilippo and Riedel, 1980

Genus *ACTINOMMA* Haeckel, 1860b

Actinomma golownini Petrushevskaya
(Plate 1, Fig. 8)

Actinomma golownini Petrushevskaya, 1975, p. 569, pl. 2, fig. 16.

Actinomma tanyacantha Chen, 1975, p. 450, pl. 11, figs. 5, 6.

Description. Cortical shell polygonal to cubical with subcircular pores, primary spines three-bladed, inflated at the connection to the cortical shell. Primary spines connect both medullary shells with the cortical shell. Both medullary shells are spherical, with subcircular small pores.

Occurrences in Holes 689B and 690B. The FAD of *A. golownini* occurs at the base of the *A. golownini* Zone around 13.1 Ma.

Remarks. The polygonal to cubical shapes of *A. golownini* (= *A. tanyacantha* in Chen 1975) have not been described either by Petrushevskaya (1975) or by Chen (1975). There are indications that *A. golownini* evolved from the spherical form *Actinomma* sp. A. *A. golownini* can be distinguished from *Actinomma* sp. A by its polygonal to cubical shape, the larger size of the cortical shell and pores, the larger, and at the connection to the cortical shell, strongly inflated spines.

Actinomma cf. *holtedahli* Björklund
(Plate 1, Figs. 4 A, B)

Actinomma holtedahli Björklund, 1976, p. 1121, pl. 20, figs. 8, 9.

Occurrences in Holes 689B and 690B. Rare in Oligocene and lowermost lower Miocene sediments.

Actinomma medusa (Ehrenberg) Petrushevskaya
(Plate 1, Fig. 7)

Actinomma medusa (Ehrenberg) Petrushevskaya, 1975, p. 568, pl. 2, figs. 6–8.

Actinomma medusa (Ehrenberg) subsp. ss. Petrushevskaya, 1975, p. 568, pl. 2, fig. 10.

Description. Shell robust, including one cortical and two medullary shells. Cortical shell very strongly silicified, with a slightly cubical outline and subcircular pores. Outer medullary shell subcircular with smaller subcircular pores. Outer medullary shell is connected to the cortical shell by four to six bars.

Measurements based on nine species from Samples 113-689B-8H-5, 121–123 cm, to 113-689B-8H-1, 56–58 cm. Diameter of the cortical shell

138–156 μm , of the outer medullary shell 39–52 μm , of the inner medullary shell 13–16 μm , number of pores in diameter of the cortical shell is 9–10.

Occurrences in Holes 689B and 690B. Oligocene and early Miocene, few to common.

Remarks. The species is very variable as also described in Petrushevskaya (1975).

Actinomma sp. A
(Plate 1, Fig. 5)

Description. Robust form composed of one cortical and two medullary shells. All shells are spherical. Cortical shell with subcircular pores of nearly the same size. Outer medullary shell connected to the cortical shell with six stout three-bladed spines.

Occurrences in Holes 689B and 690B. FAD of *Actinomma* sp. A occurs in the lower part of the *Eucyrtidium punctatum* Zone.

Measurements based on 13 specimens from Samples 113-689B-7H-4, 148–150 cm, to 6H-5, 54–56 cm. Length of the spines 31–50 μm , diameter of the cortical shell 81–114 μm , of the outer medullary shell 31–46 μm , of the inner medullary shell 16–18 μm , number of pores on diameter of the cortical shell is 10.

Remarks. This species differs from *A. golownini* in having spherical cortical and medullary shells, a smaller cortical shell diameter, and smaller spines. *Actinomma* sp. A is probably the ancestral form of *A. golownini*. The transition is shown by a gradual growing of the cortical shell and its pores and by changing of the shape of the cortical shell from spherical to polygonal to cubical by the development of strongly inflated spines at the connection to the cortical shell. The size difference of the medullary shells is not very distinct.

Actinomma sp. B
(Plate 1, Figs. 7 A, B)

Description. Very robust form consisting of one cortical and two medullary shells, with several small conical spines. The pores of the cortical shell are subcircular and sometimes hexagonally framed, the pores of the outer medullary shell are subcircular to circular and distinctly smaller.

Measurements based on 14 specimens from Samples 113-689B-8H-5, 145–147 cm, to 8H-1, 56–58 cm. Length of spines 26–40 μm , diameter of cortical shell 110–135 μm , of outer medullary shell 34–57 μm , number of pores on diameter of the cortical shell is 9–10.

Occurrences in Holes 689B and 690B. *Actinomma* sp. B is common to abundant throughout the early and middle Miocene.

Remarks. *Actinomma* sp. B is similar to *Hexacromy whole delicatulum* (Petrushevskaya, 1975, p. 569, pl. 2, fig. 11), but the description in Petrushevskaya is very incomplete and the species is not very well illustrated.

Genus *CENOSPHAERA* Ehrenberg, 1854

Cenosphaera sp. A
(Plate 3, Fig. 12)

Cenosphaera? oceanica Clark and Campbell, Petrushevskaya, 1975, figs. 12 and 13, pl. 31, fig. 5.

Cenosphaera sp. C Lazarus and Pallant, 1988, p. 29, pl. 7, figs. 7 and 8.

Description. Large, spherical, thin-walled shell, easily broken.

Occurrences in Holes 689B and 690B. Oligocene and early Miocene.

Genus *CARPOSPHAERA* Haeckel, 1881

Carposphaera subbotinae (Borisenko) Sanfilippo and Riedel
(Plate 1, Figs. 9A, B)

Carposphaera subbotinae (Borisenko) Sanfilippo and Riedel, 1973, p. 490, pl. 4, fig. 3; pl. 23, figs. 4, 5.

Occurrences in Holes 689B and 690B. In upper lower Miocene and middle Miocene sediments, rare.

Genus *HEXASTYLUS* Haeckel, 1881

Hexastylus spp. Nigrini and Lombari
(Plate 1, Fig. 10)

Hexastylus spp. Nigrini and Lombari, 1984, p. S17, pl. 3, figs. 1 a-c.

Description. Single spherical shell with six spines arising from the cortical shell, which have nearly the same length. Pores circular to subcircular, eight on a half-equator.

Measurements based on nine specimens from Sample 113-689B-9H-6, 71–73 cm. Length of the spines 24–47 μm , diameter of the cortical shell 113–134 μm , number of pores in 100 μm 8–9.

Occurrences in Holes 689B and 690B. Oligocene and early Miocene.

Remarks. The surface of the cortical shell is not as smooth as described by Nigrini and Lombari (1984). The species is similar to *Hexastylus simplex* in Vinassa de Regny, 1900, p. 570, pl. 1, fig. 20, and to *Hexacromy whole sexaculeatum* (Stöhr) shown in Petrushevskaya, 1975, p. 569, pl. 2, figs. 3–5, but has no inner shells.

Genus *HEXACONTIUM* Haeckel, 1887

Hexacontium cf. *enthacanthum* Jörgensen
(Plate 2, Figs. 2 A, B)

Hexacontium enthacanthum Jörgensen, 1900, p. 52, pl. 2, fig. 14, pl. 4, fig. 20; Benson, 1966, p. 149, pl. 3, figs. 13, 14, pl. 4, figs. 1–3; Nigrini and Moore, 1979, p. S45, pl. 5, figs. 1 a,b.

Occurrences in Holes 689B and 690B. Early and middle Miocene, rare.

Hexacontium spp.
(Plate 2, Figs. 1 A, B)

Hexacontium spp. Nigrini and Moore, 1979, p. S19, pl. 3, figs. 2 a, b.

Occurrences in Hole 689B and 690B. Early and middle Miocene, rare.

Genus *DRUPPATRACTUS* Haeckel, 1887

Druppatractus hastatus Blueford group
(Plate 2, Fig. 3)

Druppatractus hastatus Blueford, 1982, p. 206, pl. 6, figs. 3–4; Lazarus and Pallant, 1988, p. 42, pl. 6, figs. 13–15.

Druppatractus sp. Chen, 1975, p. 453, pl. 20, figs. 11, 12.
Stylosphaera spp. Nigrini and Lombari, 1984, p. S31, pl. 4, fig. 4a,b.

Occurrences in Holes 689B and 690B. Oligocene and Miocene.

Genus *STYLATRACTUS* Haeckel, 1887

Stylatractus neptunus Haeckel
(Plate 2, Figs. 8, 9)

Stylatractus neptunus Haeckel, 1887, p. 328, pl. 17, fig. 6; Riedel, 1958, p. 226, pl. 1, fig. 9.

Stylatractus sp. Petrushevskaya, 1967, p. 27, fig. 15, I-IV.

Stylatractus spp., Nigrini and Moore, 1979, p. S55, pl. 7, figs. 1 a, b.

Description. See Nigrini and Moore (1979) for complete description. Measurements based on 10 specimens from Samples 113-689B-8H-2, 120–122 cm, to 113-689B-7H-1, 70–72 cm. Length of the polar spines 33–95 μm and 33–80 μm , length of the cortical shell 107–160 μm , width 93–134 μm , number of pores in 100 μm is 6–8; length of the outer medullary shell 68–86 μm , width 55–76 μm ; length of the inner medullary shell 27–43 μm , width 27–39 μm .

Occurrences in Holes 689B and 690B. Early and middle Miocene.

Remarks. The species occurs in Quaternary sediments (Petrushevskaya and Kozlova, 1972) and is present in modern plankton from the South Atlantic (Nigrini and Moore, 1979) but is also found in Miocene sediments from equatorial Pacific (Blueford, 1982). The species is very similar to *Stylatractus santaeanae*. It differs from *S. santaeanae* by its larger pores on the cortical shell and the shorter at the base fluted spines.

Stylatractus santaeanae (Campbell and Clark)

Petrushevskaya and Kozlova
(Plate 2, Fig. 6)

Stylatractus santaeanae (Campbell and Clark) Petrushevskaya and Kozlova, 1972, p. 520, pl. 11, fig. 10.

Lithatractus santaeanae Campbell and Clark, 1944, p. 19, pl. 2, figs. 20–22.

Amphisphaera santaeanae (Campbell and Clark) Petrushevskaya, 1975, p. 570, pl. 2, fig. 2.

Description. Cortical and outer medullary shells ellipsoidal, inner medullary shell more spherical to subspherical. Shells are joined together by several radial bars. Cortical shell thick-walled, thorny with subcircular pores. Polar spines heavy, long, unequal in length.

Measurements based on five specimens from Samples 113-689B-9H-1, 71–73 cm, to 8H-5, 145–147 cm. Length of the polar spines 71–103 µm and 73–153 µm, length of the cortical shell 110–137 µm, width 89–110 µm, number of pores in 100 µm is 10–11; length of the outer medullary shell 76–81 µm, width 63–74 µm, length of the inner medullary shell 29 µm, width 26 µm.

Occurrences in Holes 689B and 690B. Rare in Oligocene and Miocene sediments.

Remarks. The species differs from *S. neptunus* by its longer and stronger spines and the higher number of pores on the cortical shell. According to Petrushevskaya and Kozlova (1972), *S. santaeanneae* has a thicker-walled third shell than *S. neptunus*.

Genus *STYLOSPHAERA* Ehrenberg, 1847b

Stylosphaera radiosa Ehrenberg
(Plate 2, Figs. 4A, B, C; 7)

Stylosphaera radiosa Ehrenberg, 1854, p. 256; 1875, pl. 24, fig. 5.
? *Druppatractus agostinelli* Carnevale, 1908, p. 20, pl. 3, fig. 10.

Amphisphaera radiosa (Ehrenberg) group Petrushevskaya, 1975, p. 570, pl. 2, figs. 18–20.

Stylosphaera coronata coronata Ehrenberg in Chen, 1975, p. 455, pl. 5, figs. 1, 2.

Occurrences in Holes 689B and 690B. Oligocene.

Remarks. The species shown by Chen (1975) is not *S. coronata coronata*, which is described and illustrated by Sanfilippo and Riedel, 1973, p. 520, pl. 1, figs. 13–17, pl. 25, fig. 4. The species varies in having a more spherical, smaller shell, often bearing two spines (one at each pole).

Stylosphaera dixyphos Ehrenberg
(Plate 2, Fig. 7)

Haliomma dixyphos Ehrenberg, 1844, p. 83; 1854, pl. 22, fig. 31.
Amphisphaera dixyphos (Ehrenberg) Petrushevskaya, 1975, p. 570, pl. 2, fig. 17.

Occurrences in Holes 689B and 690B. Oligocene, rare.

Stylosphaera coronata laevis Ehrenberg group
(Plate 2, Fig. 5)

Stylosphaera laevis Ehrenberg, 1873, p. 259; 1875, pl. 25, fig. 6.

Stylosphaera coronata laevis (Ehrenberg) Sanfilippo and Riedel, 1973, p. 520, pl. 1, fig. 19; pl. 25, figs. 5, 6.

Occurrences in Holes 689B and 690B. Oligocene to middle Miocene.

Remarks. This species group has a great variability.

Stylosphaera sp. A
(Plate 2, Fig. 10)

Description. Cortical shell spherical with small, subcircular, sometimes hexagonally framed pores; surface of the cortical shell rough. Medullary shell spherical, connected with the cortical shell by several radial spines. Cortical shell with two stout cylindrical axial spines, slightly unequal in length.

Measurements based on 16 specimens from Samples 113-689B-7H-2, 107–109 cm, to 113-689B-6H-2, 9–11 cm. Length of the polar spines 30–82 µm and 65–109 µm, diameter of the cortical shell 83–104 µm, of the outer medullary shell 36–42 µm, of the inner medullary shell 18–20 µm. Number of pores on half-equator of the shell is 9–10.

Occurrences in Holes 689B and 690B. Middle Miocene.

Genus *AMPHISTYLUS* Haeckel, 1881

Amphistylus angelinus (Campbell and Clark) Chen
(Plate 2, Figs. 11 A, B, C)

Amphistylus angelinus (Campbell and Clark) Chen, 1975, p. 453, pl. 21, figs. 3, 4.

Stylosphaera angelinus Campbell and Clark, 1944, p. 12, pl. 1, figs. 14–20.

Axoprunum angelinum (Campbell and Clark) Kling, 1973, p. 634, pl. 6, fig. 18.

? *Stylatractus universus* Hays, Nigrini and Lombardi, 1984, p. S29, pl. 4, fig. 3.

Occurrences in Holes 689B and 690B. Early and middle Miocene.

Genus *STAUROXIPHOS* Haeckel, 1887

Stauroxiphos communis Carnevale
(Plate 2, Fig. 12)

Stauroxiphos communis Carnevale, 1908, p. 15, pl. 2, fig. 9.

Lithatractus timmsi Campbell and Clark, 1944, p. 18, pl. 2, figs. 18–19.

Druppatractus nanus Blueford, 1982, p. 204, pl. 7, figs. 3a–4.

Stylatractid sp. E Lazarus and Pallant, 1987, p. 45, pl. 6, figs. 21, 22, 28.

Occurrences in Holes 689B and 690B. Late early Miocene and middle Miocene.

Family *SPONGURIDAE* Haeckel, 1862; emend. Petrushevskaya, 1975

Genus *SPONGOCORE* Haeckel, 1887

Spongocore spp.
(Plate 3, Fig. 1)

Spongocore group Mullineaux and Westberg-Smith, 1986, p. 65, pl. 1, fig. 13; Lazarus and Pallant, 1988, p. 34, pl. 8, figs. 1, 2.

Occurrences in Holes 689B and 690B. Oligocene and Miocene.

Family *PHACODISCIDAE* Haeckel, 1881

Genus *HELIODISCUS* Haeckel, 1862; emend. Nigrini, 1967

Heliodiscus sp. A
(Plate 3, Figs. 2, 3)

Heliodiscus sp. Björklund, 1976, p. 1124, pl. 14, figs. 13, 14.

Occurrences in Holes 689B and 690B. Middle Miocene.

Family *COCCODISCIDAE* Haeckel 1862; emend. Sanfilippo and Riedel, 1980

Subfamily *ARTISCINAE* Haeckel, 1881; emend. Riedel, 1967

Genus *DIDYMOCYRTIS* Haeckel, 1860b

Didymocytis sp.
(Plate 3, Fig. 4)

Description. Cortical shell rather thick-walled, ellipsoid with subcircular, hexagonally framed pores. At each pole arises a subcylindrical spongy column. Two medullary shells, spherical, connected with the cortical shell by radial bars.

Measurements based on five specimens from Samples 113-689B-6H-3, 58–60 cm. Length of the cortical shell 112–139 µm, breadth of the cortical shell 86–106 µm, outer medullary shell diameter 39–49 µm, inner medullary shell diameter 20–23 µm, number of pores along the length of the cortical shell, 13, along the breadth, 9.

Occurrences in Holes 689B and 690B. The species occurs in a short interval of the middle portion of the middle Miocene.

Remarks. *Didymocytis* sp. is similar to *Cannartus*(?) sp. aff. *laticonus* Riedel in Petrushevskaya, 1975, p. 577, pl. 7, figs. 5–7; Sanfilippo et al., 1973, p. 216, pl. 1, figs. 4–6. *Didymocytis* sp. has no equatorial constriction and protuberances, the cortical shell has no tuberculate surface, and the spongy polar columns are relatively narrow. Sanfilippo et al. (1973) reported Mediterranean specimens of *C. laticonus* different from those of the tropical Pacific. The Mediterranean specimens have more robust and sometimes nontuberculate cortical shells. Sanfilippo et al. (1973) interpreted these differences as a different stage in the evolutionary lineage. The Antarctic species *Didymocytis* sp. might represent the adaptation of tropical specimens of *C. laticonus* to the cold-water regime in the Antarctic Ocean at a warmer time period in the middle Miocene when tropical forms probably immigrated to the Southern Ocean.

Family *SPONGODISCIDAE* Haeckel, 1862; emend. Riedel, 1967

Genus *SPONGODISCUS* Ehrenberg, 1854a

Spongotrochus craticulatus (Stöhr) Petrushevskaya
(Plate 3, Fig. 7)

Spongotrochus craticulatus Stöhr, 1880, p. 118, pl. 6, fig. 12.

Spongodiscus craticulus (Stöhr) Petrushevskaya, 1975, p. 574, pl. 5, figs. 9, 10.

Occurrences in Holes 689B and 690B. Miocene.

Genus *STYLODICTYA* Ehrenberg 1847a; emend. Kozlova in Petrushevskaya and Kozlova, 1972

Styłodictya aculeata Jörgensen
(Plate 3, Fig. 9)

Styłodictya aculeata Jörgensen, 1905, p. 119, pl. 10, fig. 41; Petrushevskaya, 1967, p. 35, pl. 17, figs. 1-3; Petrushevskaya and Kozlova, 1972, p. 526, pl. 18, fig. 6; Nigrini and Lombari, 1985, p. S69, pl. 10, figs. 1 a, b.

Occurrences in Holes 689B and 690B. Latest Oligocene and early Miocene.

Styłodictya validispina Jörgensen
(Plate 3, Fig. 10)

Styłodictya validispina Jörgensen, 1905, p. 119, pl. 10, fig. 40; Petrushevskaya, 1967, p. 33, fig. 17, IV-V; Nigrini and Moore, 1979, p. S103, pl. 13, figs. 5a, b; Nigrini and Lombari, 1985, p. S71, pl. 10, fig. 2.

Occurrences in Holes 689B and 690B. Early and middle Miocene.

Genus *CIRCODISCUS* Kozlova in Petrushevskaya and Kozlova, 1972

Circodiscus ellipticus (Stöhr) group Petrushevskaya
(Plate 3, Fig. 8)

Circodiscus ellipticus (Stöhr) group Petrushevskaya, 1975, p. 575, pl. 6, figs. 1-6.

Trematodiscus ellipticus Stöhr, 1880, p. 108, pl. 4, fig. 16.

?*Perichlamidium irregulare* Vinassa de Regny, 1900, pl. 2, fig. 7.

?*Ommatodiscus circularis* Carnevale, 1908, pl. 4, fig. 9; Dumitrica, 1968, pl. 1, fig. 2.

?*Porodiscus vinassai* Principi, 1909, p. 12, pl. 1, fig. 32.

Occurrences in Holes 689B and 690B. Early middle Miocene.

Genus *SPONGOPYLE* Dreyer, 1889

Spongopyle osculosa Dreyer
(Plate 3, Fig. 11)

Spongopyle osculosa Dreyer, 1889, p. 42, pl. 11, figs. 99, 100; Riedel, 1958, p. 226, pl. 1, fig. 12; Nigrini and Moore 1979, p. S115, pl. 15, fig. 1; Nigrini and Lombari, 1984, p. S77, pl. 11, figs. 1 a, b.

Spongodiscus(?) osculosus (Dreyer), Petrushevskaya, 1967, p. 42, figs. 20-22.

Occurrences in Holes 689B and 690B. Miocene.

Genus *SPONGOTROCHUS* Haeckel, 1860

Spongotrochus glacialis Popofsky group

Spongotrochus glacialis Popofsky, 1908, p. 228, pl. 26, fig. 8, pl. 27, fig. 1, pl. 28, fig. 2; Riedel, 1958, p. 227, pl. 2, figs. 1, 2.

Spongotrochus glacialis Popofsky group Petrushevskaya, 1975, p. 575, pl. 5, fig. 8, pl. 35, figs. 1-6 (with synonymy); Nigrini and Moore, 1979, p. S117, pl. 15, figs. 2a-d.; Nigrini and Lombari, 1985, p. S79, pl. 11, fig. 2.

Occurrences in Holes 689B and 690B. Miocene.

? *Spongotrochus* spp.
(Plate 3, Figs. 17A, B)

Occurrences in Holes 689B and 690B. Late Oligocene to early Miocene.

Remarks. This species group includes all species of the genus ?*Spongotrochus* that occur in the upper Oligocene and lower Miocene sequences except *S. glacialis*.

Family PYLONIIDAE Haeckel, 1881

Genus *PHORTICJUM* Haeckel, 1881

Phorticum polycladum Tan and Tchang
(Plate 3, Fig. 5)

Phorticum polycladum Tan and Tchang, 1976, p. 267, fig. 39 a, b.

Occurrences in Holes 689B and 690B. Present in middle Miocene sediments.

Genus *TETRAPYLE* Müller, 1858

Tetrapyle octacantha Müller
(Plate 3, Fig. 6)

Tetrapyle octacantha Müller, 1858, p. 33, pl. 2, figs. 12, 13, pl. 3, figs. 1-12; Nigrini and Lombari, 1984, p. S87, pl. 12, figs. 3 a,b.

Occurrences in Holes 689B and 690B. Present in lower Miocene sediments.

Genus *PRUNOPYLE* Dreyer, 1889

Prunopyle hayesi Chen group
(Plate 3, Fig. 14)

Prunopyle hayesi Chen, 1975, p. 454, pl. 9, figs. 3-5.

Ommatodiscus haekeli Stöhr group, Petrushevskaya, 1975, p. 572, pl. 3, figs. 12-16; pl. 32, figs. 1-7.

Occurrences in Holes 689B and 690B. Oligocene and Miocene.

Prunopyle tetrapila Hays group
(Plate 3, Fig. 13)

Prunopyle tetrapila Hays, 1965, p. 172, pl. 2, fig. 5.

Occurrences in Holes 689B and 690B. Oligocene and Miocene.

Remarks. This species group has a high variability.

Prunopyle titan Campbell and Clark
(Plate 3, Fig. 16)

Prunopyle titan Campbell and Clark, 1944, p. 20, pl. 3, figs. 1-3; Hays, 1965, p. 173, pl. 2, fig. 4; Weaver, 1976, p. 578, fig. 6.

Occurrences in Holes 689B and 690B. The species occurs throughout the Miocene with different abundances.

Remarks. The size of *P. titan* is strongly variable. Campbell and Clark (1944) report only a single measurement for the shell in their description, but the figured specimens also are smaller.

?*Prunopyle* sp. A
(Plate 3, Fig. 15)

Description. Similar to *P. hayesi*. Shell spherical, consisting of radiating spines and densely spiral shell. Pylome very small, difficult to see.

Measurements based on 10 specimens from Sample 113-689B-8H-4, 144-146 cm. Cortical shell diameter 205-329 µm.

Occurrences in Holes 689B and 690B. Late Oligocene to early middle Miocene.

Prunopyle sp. B group
(Plate 4, Figs. 3 A, B)

Remarks. This group is similar to *P. titan* group, but it differs in being smaller and rounder at the end opposite the pylome.

Measurements based on 17 specimens from Samples 113-689B-8H-5, 145-147 cm, to 6H-5, 144-146 cm. Cortical shell length 130-148 µm, cortical shell breadth 83-96 µm, number of pores of the cortical shell is 14-16 in 100 µm.

Occurrences in Holes 689B and 690B. Late Oligocene and throughout the early and middle Miocene, common.

Prunopyle sp. C
(Plate 4, Fig. 6)

Description. Cortical shell ellipsoidal with small subcircular pores, arranged in radial rows. Surface slightly spongy. Medullary shell spherical. Pylome circular, surrounded by several conical spines.

Measurements based on five specimens from Samples 113-689B-7H-5, 86-88 cm. Cortical shell length 200-204 µm, breadth 165-166 µm; outer medullary shell diameter 65-79 µm; number of pores on the cortical shell is 11-12 in 100 µm.

Occurrences in Holes 689B and 690B. Oligocene and early Miocene.

Prunopyle sp. D
(Plate 4, Figs. 1 A, B)

Description. Cortical shell ellipsoidal, flatly rounded at the poles, surface slightly spongy, pores subcircular, medullary shell spherical to subspherical. Pylome circular, small, surrounded by short small spines.

Measurements based on six specimens from Samples 113-689B-8H-5, 145–147 cm, to 7H-6, 117–119 cm. Cortical shell length 148–174 µm, breadth 96–130 µm, outer medullary shell diameter 52–57 µm, number of pores on the cortical shell is 14–16 in 100 µm, width of the pylome 39–50 µm.

Occurrences in Holes 689B and 690B. Early and middle Miocene.

Family LITHELIIDAE Haeckel, 1862
Genus *LARCOPYLE* Dreyer, 1889

Larcopyle bütschlii Dreyer
(Plate 4, Fig. 4)

Larcopyle bütschlii Dreyer, 1889, p. 124, pl. 10, fig. 70, Nigrini and Lombari 1985, p. S89, pl. 13, figs. 1 a, b.

Occurrences in Holes 689B and 690B. Late Oligocene and Miocene.

Genus *LITHOCARPIUM* Stöhr, 1880
Lithocarpium polyacantha Campbell and Clark group,
Petrushevskaya
(Plate 4, Fig. 2)

Larnacantha polyacantha Campbell and Clark, 1944, p. 30, pl. 5, figs. 4–7.

Lithocarpium polyacantha (Campbell and Clark) group, Petrushevskaya, 1975, p. 572, pl. 3, figs. 6–8 (only).

Occurrences in Holes 689B and 690B. Early and middle Miocene.

Genus *LITHELIUS* Haeckel, 1862
Lithelius nautiloides group Popofsky
(Plate 4, Fig. 5)

Lithelius nautiloides Popofsky, 1908, p. 230, pl. 27, fig. 4 (only); Nigrini and Lombari, 1984, p. S97, pl. 14, figs. 2a, b.

Occurrences in Holes 689B and 690B. Present in lower and middle Miocene sediments.

Remarks. This species group also includes the species *Lithelius* sp., Nigrini and Lombari, 1984, p. S99, pl. 14, figs. 3a–c.

Family THOLONIDA Haeckel, 1887
Tholoniid sp. A
(Plate 4, Fig. 7A, B)

Amphitholus(?) sp. A Lazarus and Pallant, 1988, p. 56, pl. 8, figs. 4, 10.

Description. Cortical shell with six cupolas, pores subcircular. Outer and inner medullary shell ellipsoidal. All shells are connected by radial beams.

Measurements based on four specimens from Sample 113-689B-7H-5, 86–88 cm. Cortical shell length 148 µm, breadth 120 µm, pore number in 100 µm is 18; outer medullary shell length 109 µm, breadth 99 µm; inner medullary shell length 23 µm, breadth 13 µm. Between cortical and outer medullary shell and outer and inner medullary shell radial beams form seven different located chambers.

Occurrences in Holes 689B and 690B. Middle Miocene.

Tholoniid sp. B
(Plate 4, Fig. 8)

Description. Cortical shell ellipsoidal with four cupolas, pores circular to subcircular, outer and inner medullary shell ellipsoidal. All shells are connected by radial beams.

Measurements based on four specimens from Samples 113-689B-9H-3, 71–73 cm, to 8H-3, 120–122 cm. Cortical shell length 140–156 µm, breadth 117–143 µm; outer medullary shell length 81–96 µm, breadth 49–75 µm; inner medullary shell length 23–42 µm, breadth 16–29 µm; number of pores on the cortical shell is 8 in 100 µm.

Occurrences in Holes 689B and 690B. Oligocene and early Miocene.

Suborder NASSELLARIA Ehrenberg, 1875
Family PLAGONIIDAE Haeckel, 1881; emend. Riedel, 1967b
Genus *ANTARCTISSA* Petrushevskaya

Antarctissa robusta Petrushevskaya
(Plate 4, Fig. 9)

Antarctissa robusta Petrushevskaya, 1975, p. 591, pl. 11, figs. 21, 22, 24.

Antarctissa capitata Petrushevskaya, 1975, p. 591, pl. 11, fig. 24.

?*Antarctissa equiceps* (Campbell and Clark) group, Petrushevskaya, 1975, p. 591, pl. 11, figs. 23, 25.

Antarctissa antedenticulata Chen, 1975, p. 456, pl. 18, figs. 1, 2.

Occurrences in Holes 689B and 690B. Oligocene and Miocene.

Antarctissa deflandrei (Petrushevskaya) Lazarus
(Plate 4, Figs. 10 A, B)

Antarctissa deflandrei (Petrushevskaya) Lazarus (this volume), pl. 3, figs. 18–19.

Botryopera deflandrei Petrushevskaya, 1975, p. 592, pl. 11, figs. 30–31.

Antarctissa conradae Chen, 1975, p. 457, pl. 17, figs. 1–5.

Occurrences in Holes 689B and 690B. Middle to late Miocene.

Remarks. There are indications that *A. deflandrei* evolved gradually from *A. robusta* in the middle Miocene. Because of the gradual transition, it is necessary to define the limit between the two forms for using the first appearance of *A. deflandrei* as a stratigraphic marker (as proposed by Chen, 1975). But the high abundance of *A. deflandrei* is characteristic of the *A. deflandrei* Zone in the late middle Miocene.

Genus *CERATOCYRTIS* Bütschli, 1882

Ceratocyrtis mashae Björklund
(Plate 4, Figs. 15, A, B, C)

Ceratocyrtis mashae, Björklund, 1976, p. 1125, pl. 17, figs. 1–8.

Description. Small cephalis and large thorax. The small pored cephalis is partially sunken into the thorax; the pores of the thorax are large and irregular.

Measurements based on 10 specimens from Samples 113-689B-9H-3, 71–73 cm, to 7H-1, 70–72 cm. Length of cephalis 21–39 µm, of thorax 68–117 µm, width of cephalis 23–39 µm, of thorax 91–117 µm, number of pores in 100 µm 7–8.

Occurrences in Holes 689B and 690B. Oligocene to early Miocene.

Ceratocyrtis cf. cucularis Ehrenberg
(Plate 4, Fig. 11)

Ceratocyrtis cucularis Ehrenberg group, Dzinoridze et al. 1978, pl. 26, fig. 12, pl. 41, figs. 14–16.

Description. This form is similar to *C. mashae*, but the small cephalis is more separated from the thorax. The pores of the thorax are smaller, and the cephalis has short apical horns.

Measurements based on 10 specimens from Samples 113-698B-8H-2, 57–59 cm, to 113-689B-7H-2, 70–72 cm. Length of cephalis 18–26 µm, of thorax 70–117 µm, width of cephalis 88–143 µm, number of pores in 100 µm is 7–10.

Occurrences in Holes 689B and 690B. Early to middle Miocene.

Ceratocyrtis stigi (Björklund) Nigrini and Lombari
(Plate 4, Fig. 12)

Ceratocyrtis stigi (Björklund) Nigrini and Lombari, 1984, p. N 13, pl. 15, fig. 7.

Lithomelissa stigi Björklund, 1976, p. 1125, pl. 15, figs. 12–17.

Lithomelissa sp. C Chen, 1975, p. 458, pl. 11, figs. 4, 5.

Lithomelissa sp. Björklund, 1976, pl. 15, figs. 9–11.

Ceratocyrtis panicula Petrushevskaya, in Petrushevskaya and Kozlova, 1979, p. 115, fig. 289.

Occurrences in Holes 689B and 690B. Oligocene and Miocene.

Ceratocyrtis sp. A
(Plate 4, Fig. 14)

Description. Large robust form, with small cephalis and large thorax, heavily silicified; pores of the thorax large, irregular, and often hexagonally framed.

Measurements based on five specimens from Samples 113-689B-7H-7, 21–23 cm, to 113-689B-7H-6, 70–72 cm. Length of cephalis 26–31 µm, of thorax 120–143 µm, width of cephalis 39 µm, of thorax 156–182 µm, number of pores 4–5 in 100 µm.

Occurrences in Holes 689B and 690B. *Ceratocyrtis* sp. A was only found in a short interval in the early Miocene of Hole 689B.

Remarks. This species can be separated from *C. mashae* and *C. cucularis* by its large size, heavily silicified shell, and often hexagonally framed pores.

Genus *LITHOMELISSA* Ehrenberg

Lithomelissa cf. *ehrenbergi* Bütschli sensu Chen
(Plate 4, Fig. 13)

Lithomelissa sp. A aff. *L. ehrenbergi* Bütschli, Chen 1975, p. 458, pl. 11, figs. 1, 2.

Description. Compare Chen (1975).

Measurements based on 19 specimens from Samples 113-689B-8H-2, 57-59 cm, to 113-689B-7H-5, 86-88 cm. Length of cephalis 31-42 µm, of thorax 44-83 µm, width of cephalis 34-39 µm, of thorax 52-65 µm, number of pores on the thorax 14-16 in 100 µm.

Occurrences in Holes 689B and 690B. Early to middle Miocene.

Remarks. *L. cf. ehrenbergi* is similar to *L. robusta* and can be distinguished from it in having a smaller thorax and higher pore number.

Lithomelissa robusta Chen
(Plate 5, Figs. 2A, B)

Lithomelissa robusta Chen, 1975, p. 457, pl. 9, figs. 1, 2.

Description. Thick-walled shell. Cephalis spherical, bearing a three-bladed apical spine about the same or half of the length of the cephalis. Pores of the cephalis circular to subcircular. Thorax subcylindrical, in the upper part sometimes bearing three three-bladed wings. Pores of the thorax subcircular and regular; mouth open.

Measurements based on 12 specimens from Samples 113-689B-9H-6, 71-73 cm, to 113-689B-8H-4, 144-146 cm. Length of the cephalis 32-42 µm, of thorax 47-103 µm, width of the cephalis 42-52 µm, of the thorax 65-94 µm, number of pores on the thorax is 8 in 100 µm.

Occurrences in Holes 689B and 690B. Oligocene.

Remarks. Not all specimens have distinctly developed wings.

Lithomelissa tricornis Chen
(Plate 5, Fig. 3)

Lithomelissa tricornis Chen, 1975, p. 458, pl. 8, figs. 6, 7.

Occurrences in Holes 689B and 690B. Present in Oligocene sediments.

Tripilidium (?) *clavipes*
(Plate 5, Fig. 1)

Tripilidium (?) *clavipes advena* Clark and Campbell, 1945, p. 34, pl. 7, figs. 31-33.

Description. Cephalis spherical, bearing a strong apical spine, often thorny. Cephalis appears to have two chambers because of the apical spine in the cephalic wall. Cephalis with small irregular pores, thorax with larger irregular pores.

Measurements based on eight specimens from Samples 113-689B-8H-5, 145-147 cm, to 113-689B-8H-1, 144-146 cm. Length of cephalis 42-52 µm, of thorax 52-82 µm, width of cephalis 57-68 µm, of thorax 90-125 µm, number of pores on the thorax is 12-15 in 100 µm.

Occurrences in Holes 689B and 690B. Oligocene to early Miocene.

Family TRISSOCYCLIDAE Haeckel, 1881; emend. Goll, 1968
= *Acanthodesmiidae* Haeckel, 1862 in Riedel, 1971

Genus *CORTHOSPYRIS* Haeckel 1881; emend. Goll, 1976

Corythospyris fiscella Goll
(Plate 5, Figs. 4A, B; 7)

Corythospyris fiscella Goll, 1978, p. 178, pl. 5, figs. 1-21.

Description. Small robust shell with circular to subcircular pores; sagittal ring more subcircular. Pores adjacent to the sagittal ring are sometimes larger and elliptical in outline. Apical horn is short, basal feet, if they are developed, are short and thorned at the end.

Measurements are based on seven specimens from Samples 113-689B-9H-2, 71-73 cm, to 113-689B-8H-3, 86-88 cm. Width 68-78 µm, height 43-57 µm, number of pores 8-10 in 100 µm.

Occurrences in Holes 689B and 690B. Oligocene and early Miocene.

Corythospyris sp. A
(Plate 5, Figs. 6 A, B)

Description. Similar to the previous form. Robust shell with smaller more circular to subcircular pores, basal feet are mostly developed and

often longer than in *Corythospyris fiscella*. In some specimens the basal feet are connected by a distal latticed wall.

Measurements based on 30 specimens from Samples 113-689B-8H-3, 56-58 cm, to 7H-3, 145-147 cm. Width 78-114 µm, height 52-78 µm, number of pores 10-12 in 100 µm.

Occurrences in Holes 689B and 690B. Early Miocene.

Remarks. The species differs from *Corythospyris fiscella* in having a larger shell, higher pore numbers, and more pronounced basal feet. Because of the gradual development of these parameters, *Corythospyris* sp. A probably evolved from *Corythospyris fiscella*.

Trissocyclid sp. A
(Plate 5, Figs. 5A, B, C)

Description. Heavily constructed shell, sagittal ring D-shaped, pores are circular to subcircular, pores adjacent to the sagittal ring often tend to be larger and elliptical in outline. Three strong basal feet, sometimes connected with a distal latticed wall.

Measurements based on 20 specimens from Samples 113-689B-7H-6, 117-119 cm, to 113-689B-6H-5, 144-146 cm. Width 96-120 µm, height 65-99 µm, length of the feet 26-30 µm, number of pores is 10-14 in 100 µm.

Occurrences in Holes 689B and 690B. Early Miocene.

Remarks. *Trissocyclid* sp. A is similar to *Triceraspyris coronatus* (Weaver, 1976, p. 580, pl. 2, figs. 4-5, pl. 6, figs. 8-9), which occurs in Pliocene sediments.

Genus *DENDROSPYRIS* Haeckel 1881; emend. Goll, 1968

Dendrospyris stabilis Goll
(Plate 5, Figs. 8 A, B)

Dendrospyris stabilis Goll, 1968, p. 1422-1423, pl. 173, figs. 16-18.

Occurrences in Holes 689B and 690B. Early Miocene.

Dendrospyris rhodospyroides (Petrushhevskaya) n. comb.
(Plate 5, Figs. 9 A, B)

Desmospyris rhodospyroides Petrushhevskaya, 1975, p. 593, pl. 10, figs. 27-29, 31, 32.

Dendrospyris haysi Chen, 1975, p. 455, pl. 15, figs. 3-5.

Occurrences in Holes 689B and 690B. Early and middle Miocene.

Remarks. This species can be distinguished from *D. stabilis* by the larger size of the shell and larger pores. The gradual growth of shell and pores might indicate that *D. rhodospyroides* evolved from *D. stabilis*, which was also proposed by Chen (1975).

Dendrospyris megalcephalis Chen
(Plate 5, Fig. 15)

Dendrospyris megalcephalis Chen 1975, p. 455, pl. 14, figs. 3-5.

Occurrences in Holes 689B and 690B. The species occurs only in a short interval in the late middle Miocene.

Family CARPOCANIIDAE Haeckel 1887; emend. Riedel, 1967

Genus *CARPOCANISTRUM* Haeckel

Carpocanistrum spp.
(Plate 5, Fig. 13)

Carpocanistrum spp. Riedel and Sanfilippo, 1971, p. 1596, pl. 1G, figs. 8-13, 14, 15, pl. 2F, figs. 5-6, pl. 3D, figs. 1, 2, 6, 7, 8, 9; Nigrini and Moore, 1979, p. N23, pl. 21, figs. 1 a-c, Nigrini and Lombardi, 1984, N81-82, pl. 21, figs. 1 a, b.

Carpocanistrum group A, Westberg-Smith and Riedel, 1984, p. 493-494, pl. 5, figs. 11 A, B.

Carpocanistrum group beta Westberg-Smith and Riedel, 1984, p. 494, pl. 5, fig. 12.

Occurrences in Holes 689B and 690B. Oligocene and Miocene.

Carpocanarium papillosum (Ehrenberg) Nigrini and Moore
(Plate 5, Fig. 14)

Carpocanarium papillosum (Ehr.) Nigrini and Moore, 1979, N27, pl. 21, fig. 3 (with synonymy).

Occurrences in Holes 689B and 690B. Oligocene and Miocene.

Family THEOPERIDAE

Haeckel, 1881; emend. Riedel, 1967

Genus *CORNUTELLA* Ehrenberg, 1838; emend. Nigrini, 1967*Cornutella profunda* Ehrenberg*Cornutella clathrata* beta *profunda* Ehrenberg, 1858, pl. 35b, fig. 21; Bailey, 1856, p. 2, pl. 1, fig. 23.*Cornutella profunda* Ehrenberg, 1858, p. 31; Riedel, 1958, p. 232, pl. 3, figs. 1, 2.*Cornutella hexagona* Haeckel, 1887, p. 1180, pl. 54, fig. 9.**Occurrences in Holes 689B and 690B.** Present in Oligocene and Miocene sediments.*Cornutella clathrata* Ehrenberg

(Plate 8, Fig. 8)

Cornutella clathrata Ehrenberg, 1838, p. 129; 1844, p. 77; 1847, p. 42, 1854, pl. 22, figs. 39 a-c, 1854, p. 1183.*Cornutella clathrata* alpha Ehrenberg 1858, p. 31.*Cornutella curvata* Haeckel 1887, p. 1183.**Description.** As for *Cornutella profunda*. The species is characterized by its curved shell.**Occurrences in Holes 689B and 690B.** *C. clathrata* appears first at the base of the *A. deflandrei* Zone in the late middle Miocene.**Remarks.** Ehrenberg (1858) referred *Cornutella clathrata alpha* to *C. clathrata* and *C. clathrata* beta to *C. profunda* (in Foreman and Riedel, 1972).Genus *CYCLAMPTERIUM* Haeckel, 1887*Cyclampterium milowi* Riedel and Sanfilippo
(Plate 7, Fig. 8)*Cyclampterium milowi* Riedel and Sanfilippo, 1971, p. 1593, pl. 3B, fig. 3; pl. 7, figs. 8-9; Sanfilippo and Riedel, in Sanfilippo et al., 1973, p. 220, pl. 4, figs. 12-14; Riedel and Sanfilippo, 1978, p. 67, pl. 4, fig. 14.*Cyclampterium(?) longiventer* Chen, 1975, p. 459, pl. 10, fig. 7.*Thysocyrts* sp. Petrushevskaya, 1975, p. 580, pl. 8, fig. 10.**Occurrences in Holes 689B and 690B.** Middle Miocene.Genus *CYRTOCAPSELLA* Haeckel, 1887*Cyrtocapsella cornuta* (Haeckel) Sanfilippo and Riedel
(Plate 6, Figs. 2 A, B)*Cyrtocapsa (Cyrtocapsella) cornuta* Haeckel, 1887, p. 1513, pl. 78.*Cyrtocapsella cornuta* Sanfilippo and Riedel, 1970, p. 453, pl. 1, figs. 19-20; Nigrini and Lombari, 1985, p. N101, pl. 23, fig. 1.**Occurrences in Holes 689B and 690B.** Late early to early middle Miocene.*Cyrtocapsella longithorax* (Petrushevskaya) n. comb.

(Plate 5, Figs. 12A, B)

Theocorys longithorax Petrushevskaya, 1975, p. 580, pl. 8, figs. 17, 18, pl. 22, fig. 2.*Cyrtocapsella isopera* Chen, 1975, p. 460, pl. 11, figs. 7-9, Weaver, 1976, p. 581, pl. 3, figs. 5-6, pl. 9, figs. 4, 6.**Occurrences in Holes 689B and 690B.** Early to middle Miocene.*Cyrtocapsella tetrapera* Haeckel

(Plate 6, Figs. 1 A, B)

Cyrtocapsa (Cyrtocapsella) tetrapera Haeckel, 1887, p. 1512, pl. 78, fig. 5.*Cyrtocapsella tetrapera* Sanfilippo and Riedel, 1970, p. 453, pl. 1, figs. 1-3; Nigrini and Lombari, 1984, p. N109-110, pl. 23, fig. 5.**Occurrences in Holes 689B and 690B.** Early to middle Miocene.*Cyrtocapsella robusta* n. sp.

(Plate 5, Figs. 10, 11)

Description. Cephalis spherical and small with circular pores, bearing one short apical horn. Thorax campanulate with longitudinally aligned circular pores of nearly uniform size. Abdomen cylindrical or

inverted conical and inflated. The pores of the abdomen are circular to subcircular and have nearly the same size as the pores of the thorax.

Measurements based on 15 specimens from Samples 113-689B-9H-3, 71-73 cm, 113-689B-8H-6, 71-73 cm. Diameter of cephalis 18-21 µm, length of thorax 42-53 µm, of abdomen 55-68 µm; width of thorax 63-66 µm, of abdomen 53-75 µm, number of pores in 100 µm of longitudinal rows is 13-14.

Occurrences in Holes 689B and 690B. Late Oligocene.**Remarks.** The species can be separated from *Cyrtocapsella longithorax* by its larger and fewer pores. Petrushevskaya (1975) did not distinguish between the Miocene form of *Theocorys longithorax* and the Oligocene form.*Cyrtocapsella robusta* is probably the ancestor form of *C. longithorax*.**Etymology.** "robusta," robust.**Holotype.** Sample 113-689B-9H-1, 71-73 cm, pl. 5, fig. 11; deposited in the Nordseemuseum of the Alfred-Wegener Institute, Bremerhaven.Genus *CYRTOPERA* Haeckel, 1881*Cyrtopera laguncula* Haeckel*Cyrtopera laguncula* Haeckel, 1887, p. 1451, pl. 75, fig. 10; Benson, 1966, p. 510-513, pl. 35, figs. 3, 4; Chen, 1975, p. 460, pl. 18, fig. 9. *Cyrtocapsa* sp. Riedel, 1958, p. 244, pl. 4, fig. 11.**Occurrences in Holes 689B and 690B.** In Miocene sediments, rare.Genus *DICTYOPHIMUS* Ehrenberg, 1847a*Dictyophimus gracilipes* Bailey
(Plate 7, Fig. 10)*Dictyophimus gracilipes* Bailey, 1856, p. 4, pl. 1, fig. 8; Petrushevskaya, 1967, p. 65, figs. 38, 39.*Pseudodictyophimus gracilipes* (Bailey) Björklund, 1976, p. 1124, pl. 9, figs. 1-5; pl. 11, figs. 6, 7.**Occurrences in Holes 689B and 690B.** Early and middle Miocene.*Dictyophimus cf. platycephalus* Haeckel
(Plate 7, Fig. 11)*Dictyophimus playcephalus* Haeckel 1887, p. 1198, pl. 60, figs. 4, 5; Petrushevskaya, 1967, p. 71, fig. 42, I-III.*Pseudodictyophimus* sp. aff. *P. gracilipes* (Bailey) Björklund, 1976, p. 1124, pl. 16, figs. 1-5.**Occurrences in Holes 689B and 690B.** Early and middle Miocene.Genus *EUCYRTIDIUM* Ehrenberg, 1847a*Eucyrtidium calvertense* Martin group
(Plate 6, Figs. 4, 5A, B, C)*Eucyrtidium calvertense* Martin, 1904, p. 450, pl. 130, fig. 5.**Description.** Multisegmented stichocyrtid with four to seven segments. Small spherical to subspherical cephalis and small conical thorax. Abdomen inflated, inverted, conical. Circular to subcircular pores arranged in longitudinal, sometimes furrowed rows. Three to four pores in one row of one segment.**Occurrences in Holes 689B and 690B.** Middle Miocene.**Remarks.** The species has a high variability.*Eucyrtidium cienkowskii* Haeckel group, Sanfilippo et al.
(Plate 6, Figs. 3A, B, C, D)*Eucyrtidium cienkowskii* Haeckel, 1887, p. 1493, pl. 80, fig. 9.*Eucyrtidium cienkowskii* Haeckel group Sanfilippo et al. 1973, p. 221, pl. 5, figs. 7-11.**Occurrences in Holes 689B and 690B.** Early to middle Miocene.*Eucyrtidium punctatum* Ehrenberg
(Plate 6, Fig. 6)*Lithocampe punctata* Ehrenberg, 1844, p. 84.*Eucyrtidium punctatum* (Ehrenberg) Ehrenberg, 1857, p. 43; 1854, pl. 22, fig. 24.*Eucyrtidium punctatum* Ehrenberg group, Sanfilippo et al. 1973, p. 221, pl. 5, figs. 15-16.**Occurrences in Holes 689B and 690B.** Early middle Miocene.

Genus *LYCHNOCANOMA* Haeckel, 1887

Lychnocanoma conica (Clark and Campbell) n. comb.
(Plate 6, Fig. 8; Pl. 7, Figs. 1 A, B)

Lychnocanium conicum Clark and Campbell, 1942, p. 71, pl. 9, fig. 38.
Lychnocanella conica Petrushevskaya, 1975, p. 583, pl. 12, figs. 2, 11-15.

Lychnocanoma sphaerothorax Weaver, 1976, p. 581, pl. 5, figs. 4, 5.

Description. Similar to *Lychnocanoma* sp. A, but smaller in size with a larger cephalis in comparison to the thorax, which is more separated. Cephalis with scattered small circular pores, bearing a conical apical horn of approximately the same length as the cephalis. Thorax with hexagonally framed circular to subcircular pores arranged in longitudinal rows. Three short stout three-bladed feet, slightly divergent.

Occurrences in Holes 689B and 690B. Late Oligocene to early Miocene.

Remarks. This species can be distinguished from *Lychnocanoma* sp. A by its smaller size, its larger and more separated cephalis, the longer and pronounced feet, the smoother surface of the shell, and the longitudinal rows of pores.

Lychnocanoma sp. A
(Plate 6, Fig. 7)

Description. Cephalis small, hemispherical, bearing a conical apical horn. Thorax truncate spherical with hexagonally framed subcircular to circular pores. Three very short feet.

Occurrences in Holes 689B and 690B. Late Oligocene.

Lychnocanoma sp. B
(Plate 7, Figs. 2 A, B)

Description. Cephalis spherical, scattered with small circular pores, bearing a conical apical horn one and a half times the length of the cephalis. Thorax hemispherical to conical with circular to subcircular, sometimes hexagonally framed pores, arranged in longitudinal rows. Three strongly marked feet, which are distinctly longer than the feet of the previous described forms.

Occurrences in Holes 689B and 690B. Middle middle Miocene.

Remarks. *Lychnocanoma* sp. B is similar to *Lychnocanoma grande rugosum*, which occurs in upper Miocene and lower Pliocene sediments.

Genus *GONDWANARIA* Petrushevskaya, 1975

Gondwanaria deflandrei Petrushevskaya
(Plate 7, Fig. 7)

Gondwanaria deflandrei Petrushevskaya, 1975, p. 584, pl. 9, figs. 8, 9.

Occurrences in Holes 689B and 690B. The species occurs only in a short interval of the late early Miocene.

Remarks. The species is not very well illustrated by Petrushevskaya (1975).

Gondwanaria japonica (Nakaseko) Petrushevskaya group
(Plate 7, Figs. 3 A, B)

Sethocyrtis japonica Nakaseko, 1963, p. 176, pl. 1, figs. 6, 10; Nakaseko and Sugano, 1973, pl. 4, fig. 2.

Gondwanaria japonica (Nakaseko) group Petrushevskaya, 1975, p. 584, pl. 8, fig. 15, pl. 9, figs. 2-7, pl. 12, fig. 1.

Occurrences in Holes 689B and 690B. Early to middle Miocene *G. japonica* also occurs in lower Miocene sediments from the Norwegian Sea according to Björklund (1976).

Gondwanaria sp. A
(Plate 7, Fig. 6)

Description. Cephalis small, spherical to subspherical, with scattered small circular to subcircular pores, bearing one conical apical horn of nearly the length of the thorax. The cephalis is usually separated from the thorax by a neck. Thorax is conical with circular to subcircular pores and bears two wings. The shell has no subdivision between thorax and abdomen but the thorax is slightly constricted.

Occurrences in Holes 689B and 690B. Middle Miocene.

Remarks. The species is very similar to the species called *G. dogieli* forma "C" shown in Dzinoridze et al. (1978) but is different from *G.*

dogieli described in Petrushevskaya and Kozlova (1972) and Petrushevskaya (1975). The species also is similar to *Lipmanella xiphophorum* sensu Petrushevskaya and Kozlova (1972) as illustrated by Björklund (1976).

Genus *ARTOPHORMIS* Haeckel, 1881

Artophormis gracilis Riedel
(Plate 7, Fig. 5)

Artophormis gracilis Riedel, 1959, p. 300, pl. 2, figs. 12, 13; Sanfilippo et al., 1973, pl. 4, fig. 4.

Occurrences in Holes 689B and 690B. *A. gracilis* was only found in Hole 689B in a short interval in the early Miocene.

Artophormis gracilis does not occur in upper Oligocene sequences of Holes 689B and 690B.

Genus *Calocyclus* Ehrenberg, 1847b

Calocyclus cf. *semipolita* Clark and Campbell
(Plate 7, Fig. 4)

Calocyclus semipolita Clark and Campbell, 1942, p. 83, pl. 8, figs. 12, 14, 17-19, 21-23.

Theocotyle robusta Petrushevskaya, 1975, p. 580, pl. 8, fig. 9, pl. 22, fig. 1.

Occurrences in Holes 689B and 690B. Early Miocene.

Remarks. *Calocyclus* cf. *semipolita* differs in its distribution from *C. semipolita*, which is an Eocene form.

Genus *Saccospyris* Haeckel, 1907

Saccospyris antarctica Petrushevskaya

Saccospyris antarctica Petrushevskaya, 1975, p. 589, pl. 13, figs. 19, 20. *Cannabotryid* group Westberg-Smith and Riedel, 1984, p. 494, pl. 6, fig. 6.

Occurrences in Holes 689B and 690B. Early Miocene.

Genus *CORYTHOMELISSA* Campbell, 1951

Corythomelissa horrida Petrushevskaya
(Plate 7, Fig. 9)

Corythomelissa horrida Petrushevskaya, 1975, p. 590, pl. 11, figs. 14, 15, pl. 21, fig. 9.

Occurrences in Holes 689B and 690B. Lower middle Miocene sediments.

Genus *CYCLADOPHORA* Ehrenberg, 1847

Cycladophora conica Lombari and Lazarus
(Plate 7, Fig. 12)

Cycladophora conica Lombari and Lazarus, 1988, p. 105, pl. 3, figs. 1-16 (with synonymy).

Occurrences in Holes 689B and 690B. Oligocene to Miocene.

Cycladophora golli golli (Chen) Lombari and Lazarus
(Plate 8, Figs. 1 A, B)

Cycladophora golli golli (Chen) Lombari and Lazarus, 1988, p. 124, pl. 11, figs. 3, 4.

Lophocyrtis golli Chen, 1975, p. 461, pl. 12, figs. 4, 5; Weaver, 1976, p. 581, pl. 4, figs. 9, 10.

Occurrences in Holes 689B and 690B. Early to middle Miocene.

Cycladophora golli regipileus (Chen) Lombari and Lazarus
(Plate 8, Figs. 2 A, B)

Cycladophora golli regipileus (Chen) Lombari and Lazarus, 1988, p. 124, pl. 11, figs. 6, 8, 9.

Lophocyrtis regipileus Chen, 1975, p. 461, pl. 12, figs. 6, 7, Weaver, 1976, p. 581, pl. 4, figs. 6-8.

Occurrences in Holes 689B and 690B. Late early Miocene to middle Miocene, *C. golli regipileus* occurs later than *C. golli golli*.

Cycladophora humerus (Petrushevskaya) Lombari and Lazarus
(Plate 8, Figs. 3 A, B)

Cycladophora humerus (Petrushevskaya) Lombari and Lazarus, 1988,
p. 123, pl. 9, figs. 1–6.

Clathrocyclas humerus Petrushevskaya, 1975, p. 586, pl. 15, figs. 22,
23; pl. 43, figs. 1, 2.

Occurrences in Holes 689B and 690B. Middle middle Miocene.

Cycladophora spongothorax (Chen) Lombari and Lazarus
(Plate 8, Fig. 10)

Cycladophora spongothorax (Chen) Lombari and Lazarus, 1988, p. 122,
pl. 8, figs. 1–6.

Theocalyptra bicornis (Popofsky) *spongothorax* Chen, 1975, p. 462, pl.
12, figs. 1–3.

Occurrences in Holes 689B and 690B. Late middle Miocene to late
Miocene.

Cycladophora antiqua n. sp.
(Plate 7, Figs. 13A, B)

Description. Cephalis small, hemispherical, with scattered small circular to subcircular pores, bearing two stout three-bladed apical horns one and a half times as long as the cephalis. Upper thorax conical with subspherical pores. Lower thorax wider and convex, with larger hexagonally framed subcircular pores arranged in horizontal rows. Abdomen long and distinct, wider than the lower thorax, with pores of nearly the same size as of the lower thorax, distal pores sometimes irregular and larger. Upper and lower thorax and abdomen are each separated from one another by an internal ring.

Measurements based on 10 specimens from Samples 113-689B-8H-3, 56–58 cm, to 113-689B-7H-5, 143–145 cm. Length of cephalis 16–18 μm , width 18–21 μm ; length of thorax 84–92 μm , width 79–100 μm ; length of abdomen 32–52 μm , width 126–152 μm ; length of apical horns 18 μm ; number of pores on the thorax and on the abdomen is 10–12 in 100 μm of horizontal rows.

Remarks. *Cycladophora antiqua* can be distinguished from *Cycladophora humerus* by its longer and wider abdomen and its smaller cephalis, and from *Cycladophora golli golli* by its campanulate shape of the shell and the wide divergent abdomen.

Occurrences in Holes 689B and 690B. Early Miocene.

Etymology. "antiqua," old.

Holotype. Sample 113-689B-8H-1, 120–122 cm (pl. 7, fig. 13 a), de-
posited in the Nordseemuseum of the Alfred-Wegener Institute, Bremer-
haven.

Family ARTOSTROBIIDAE Riedel 1967; emend. Foreman, 1973
Genus *PHORMOSTICHOARTUS* Campbell 1951; emend. Nigrini
1977

Phormostichoartus corbula (Harting) Nigrini
(Plate 8, Fig. 7)

Phormostichoartus corbula (Harting) Nigrini, 1977, p. 252, pl. 1, fig.
10 (with synonymy); Nigrini and Lombari, 1984, N179, pl. 31, figs.
4a, b.

Occurrences in Holes 689B and 690B. Late middle Miocene (*Antar-
tissa deflandrei* Zone).

Genus *SIPHOCAMPE* Haeckel, 1881; emend. Nigrini, 1977

Siphocampe arachnea (Ehrenberg) Nigrini group
(Plate 8, Figs. 4 A, B)

Lithocampe lineata Ehrenberg, 1838, p. 130.

Siphocampe arachnea (Ehrenberg) group, Nigrini, 1977, p. 255, pl. 3,
figs. 7, 8.

Occurrences in Holes 689B and 690B. Oligocene and Miocene.

Genus *VELICUCULLUS* Riedel and Campbell, 1952

Velicucullus cf. oddgurneri Björklund
(Plate 8, Fig. 6)

Velicucullus oddgurneri Björklund, 1976, p. 1126, pl. 19, figs. 6–9.
Lampromitra coronata Keany, 1979, p. 56, pl. 4, fig. 10, pl. 5, fig. 14.

Occurrences in Holes 689B and 690B. Late early Miocene.

Remarks. The distribution of *V. cf. oddgurneri* is different from *V. oddgurneri*, which occurs in the late Oligocene and *Lampromitra coro-
nata*, which is described from lower Pliocene sediments (Keany, 1979).

Velicucullus altus n. sp.
(Plate 8, Figs. 5A, B, C)

Description. The genus is characterized by the velum on the under-
side of its thorax. Small hemispherical cephalis with small circular pores.
Cephalis and thorax are separated only by a moderate constriction. Up-
per thorax large, broad conical shaped with large, subcircular, and ir-
regularly arranged pores. The lower thorax is flat and spongy.

Measurements based on 10 specimens from Samples 113-689B-8H-3,
56–58 cm, to 113-689B-8H-1, 120–122 cm. Diameter of velum 46 μm ,
diameter of outer rim of thorax of approximately 200 μm ; height of
cephalis 23–26 μm , width 26–33 μm ; height of thorax 167–215 μm ,
width of thorax (upper part) 100–133 μm , width of thorax (lower part)
200–217 μm ; number of pores on the thorax is 7–9 in 100 μm .

Remarks. *Velicucullus altus* can be distinguished from *V. cf. odd-
gurneri* by its robust shell, its broad and conical thorax, and its thorax,
which is not as flatly expanded as that of *V. cf. oddgurneri*.

Occurrences in Holes 689B and 690B. Early early Miocene.

Etymology. "altus," high.

Holotype. Sample 113-689B-8H-2, 86–88 cm (pl. 8, fig. 5 A), depos-
ited in the Nordseemuseum of the Alfred-Wegener Institute, Bremerha-
ven.

Genus STICHOPHORMIS Haeckel, 1881

Stichophormis sp. Chen
(Plate 8, Fig. 9)

Stichophormis sp. Chen 1975, p. 462, pl. 13, fig. 8.

Occurrences in Holes 689B and 690B. Lower part of the *E. puncta-
tum* Zone, in the middle Miocene.

Remarks. The species occurs only in a short interval.

ACKNOWLEDGMENTS

I am grateful to W. R. Riedel, C. Nigrini, A. Sanfilippo, and
S. A. Kling for taxonomic discussion. D. Lazarus is thanked for
samples, discussion, and taxonomic notes. I wish to thank R.
Gersonde and V. Spieß for contributing stratigraphic data. Ute
Bock and Inge Klappstein are thanked for laboratory and technical
assistance.

This is Alfred-Wegener Institute Contribution No. 231.

REFERENCES

- Abelmann, A., 1989. Freeze-drying simplifies the preparation of micro-
fossils. *Micropaleontology*, 34:371.
- , in press. Early to Mid-Miocene radiolarian stratigraphy of
the Kerguelen Plateau. *In Schlich, R., Wise, S. W., Jr., et al., Proc.
ODP Sci. Results*, 120: College Station, TX (Ocean Drilling Pro-
gram).
- Bailey, J. W., 1856. Notice of microscopic forms found in the soundings
of the sea of Kamtschatka—with a plate. *Am. J. Sci. Arts*, 2:1–6.
- Barker, P. F., and Kennett, J. P., et al., 1988. *Proc. ODP Sci. Results*,
113: College Station, TX (Ocean Drilling Program).
- Benson, R. N., 1966. Recent Radiolaria from the Gulf of California
[Ph.D. diss.] Univ. Minnesota, Minneapolis.
- Berggren, W. A., Kent, D. V., and Van Couvering, J. A., 1985. The Ne-
ogene geochronology and chronostratigraphy. *In Snelling, N. J. (Ed.),
The Chronology of the Geological Record*. Geol. Soc. London Mem.,
10:211–260.
- Björklund, K. R., 1976. Radiolaria from the Norwegian Sea, Leg 38 of
the Deep Sea Drilling Project. *In Talwani, M., Udistsev, G., et al.
Init. Repts. DSDP*, 38: Washington (U.S. Govt. Printing Office),
1101–1168.
- Blueford, J. R., 1982. Miocene actinomimid Radiolaria from the equato-
rial Pacific. *Micropaleontology*, 28:189–213.
- Borisenko, N. L., 1960. The radiolarians of the lower and middle Eo-
cene of Western Kubanj. *Trans. All Union Sci. Res. Inst. Oil Gas*, 4:
219–232.

- Bütschli, O., 1882. Beiträge zur Kenntnis der Radiolarienskelette, insbesondere der der Cyrtida. *Z. Wiss. Zool.*, 36:485-540.
- Campbell, A. S., 1951. New genera and subgenera of Radiolaria. *J. Paleontol.*, 25:527-530.
- Campbell, A. S., and Clark, B. L., 1944. Miocene radiolarian fauna from southern California. *Spec. Pap. Geol. Soc. Am.*, 51:1-77.
- Carnevale, P., 1908. Radiolarie e sillicoflagellati di Bergonzano (Reggio Emilia). *Veneto Sci. Lett. Arti Mem.*, 28:1-46.
- Chen, H., 1974. Some new Tertiary radiolarians from deep-sea sediments. *Micropaleontology*, 20:480-492.
- _____, 1975. Antarctic Radiolaria. In Hayes, D. E., Frakes, L. A., et al. *Init. Repts. DSDP* 28: Washington (U.S. Govt. Printing Office), 437-514.
- Clark, B. L., and Campbell, A. S., 1942. Eocene radiolarian faunas from the Mt. Diablo area, California. *Spec. Pap. Geol. Soc. Am.*, 39:1-112.
- _____, 1945. Radiolaria from the Kreyhagen Formation, near Los Banos, California. *Geol. Soc. Am. Mem.*, 10:1-66.
- Dreyer, F., 1889. Morphologische Radiolarienstudien. I. Die Pylombildungen in vergleichend-anatomischer und entwicklungsgeschichtlicher Beziehung bei Radiolarien und Protisten überhaupt nebst System und Beschreibung neuer und der bis jetzt bekannten pylomatissen Spumellarien. *Jena. Z. Med. Naturwiss.*, 23:1-138.
- Dumitrica, P., 1968. Consideratii micropaleontologice aspura orizontului argilos ou radiolari din tortonianul regiunii carpatic. *Studii si cercetari de geologie-geografie, ser. geol.*, Bucarestii, 13:227-241.
- Dzinoridze, R. N., Jouse, A. P., Koroleva-Golikova, G. S., Kozlova, G. E., Nagaeva, G. S., Petrushevskaya, M. G., and Strelnikova, N. L., 1978. Diatom and radiolarian Cenozoic stratigraphy, Norwegian Basin, DSDP Leg 38. In Talwani, M., Udrinsev, G., et al., Suppl. to Vols. 38, 39, 40 and 41. *Init. Repts. DSDP*: Washington (U.S. Govt. Printing Office), 289-428.
- Ehrenberg, C. G., 1838. Über die Bildung der Kreidefelsen und des Kreidemergels durch unsichtbare Organismen. *Abh. Kgl. Akad. Wiss. Berlin*:59-147.
- _____, 1844. Über zwei neue Lager von Gebirgsmassen aus Infusorien als Meeres-Absatz in Nord-Amerika und eine Vergleichung derselben mit den organischen Kreidegebilden in Europa und Afrika. *Kgl. Preuss. Akad. Wiss. Berlin*:57-97.
- _____, 1847a. Über eine halibolithische, von Herrn Schomburgk entdeckte, vorherrschend aus mikroskopischen Polycystinen gebildete Gebirgsmasse von Barbados. *Monatsber. Kgl. Preuss. Akad. Wiss. Berlin*:382-385.
- _____, 1847b. Über die mikroskopischen kieselschaligen Polycystinen als mächtige Gebirgsmasse von Barbados und über das Verhältnis der aus mehr als 300 neuen Arten bestehenden ganz eigentümlichen Formengruppe jener Felsmasse zu den jetzt lebenden Tieren und zur Kreidebildung. Eine neue Anregung zur Erforschung des Erdenlebens. *Monatsber. Kgl. Preuss. Akad. Wiss. Berlin*:40-60.
- _____, 1854a. Die systematische Charakteristik der neuen mikroskopischen Organismen des tiefen atlantischen Ozeans. *Monatsber. Kgl. Preuss. Akad. Wiss. Berlin*:236-250.
- _____, 1854b. *Mikrogeologie*, 27:1-374, ATLAS, 1-31, 40 pls., Fortsetzung (1856), 1-88, Leipzig (Voss).
- _____, 1858. Kurze Charakteristik der 9 neuen Genera und der 105 neuen Species des ägäischen Meeres und des Tiefgrundes des Mittelmeeres. *Monatsber. Kgl. Preuss. Akad. Wiss. Berlin*: 10-40.
- _____, 1860. Über den Tiefgrund des stillen Ozeans zwischen Kalifornien und den Sandwich-Inseln aus bis 15600' Tiefe nach Leutnant Brooke. *Monatsber. Kgl. Preuss. Akad. Wiss. Berlin*: 819-833.
- _____, 1872. Mikrogeologische Studien über das kleinste Leben der Meeres-Tiefgründe aller Zonen und dessen geologischen Einfluß *Monatsber. Kgl. Preuss. Akad. Wiss. Berlin*: 131-399.
- _____, 1873. Größere Felsproben des Polycystinen-Mergels von Barbados mit weiteren Erläuterungen. *Ber. Kgl. Preuss. Akad. Wiss. Berlin*: 1-131.
- _____, 1875. Fortsetzung der mikrogeologischen Studien als Gesamtübersicht der mikroskopischen Paläontologie gleichartig analysierter Gebirgsarten der Erde, mit spezieller Rücksicht auf den Polycystinen Mergel von Barbados. *Monatsber. Kgl. Preuss. Akad. Wiss. Berlin*: 1-225.
- Foreman, H. P., 1973. Radiolaria of Leg 10 with systematics and ranges for the families Amphipyndacidae, Artostrobidae, and Theoperidae. In Worzel, J. L., Bryant, W., et al. *Init. Repts. DSDP*, 10: Washington (U.S. Govt. Printing Office), 407-474.
- Foreman, H. P., and Riedel, W. R., 1972. Catalogue of polycystine Radiolaria. *Am. Mus. Nat. Hist., Spec. Publ. Ser. 1, Vol. 1*, New York.
- Goll, R. M., 1968. Classification and phylogeny of Cenozoic Trissocyclidae (Radiolaria) in the Pacific and Caribbean basins part I. *J. Paleontol.*, 42:1409-1432.
- _____, 1969. Classification and phylogeny of Cenozoic Trissocyclidae (Radiolaria) in the Pacific and Caribbean basins, part II. *J. Paleontol.*, 43:322-339.
- _____, 1976. Morphological intergradation between modern population of *Lophospyris* and *Phormospyris* (Trissocyclidae, Radiolaria). *Micropaleontology*, 22:379-418.
- _____, 1978. Five trissocyclid Radiolaria from Site 38. In Talwani, M., Udrinsev, G., et al., Suppl. to Vols. 38, 39, 40, and 41. *Init. Repts. DSDP*: Washington (U.S. Govt. Printing Office), 177-191.
- Haeckel, E., 1860a. Über neue, lebende Radiolarien des Mittelmeeres und die dazu gehörigen Abbildungen. *Monatsber. Kgl. Preuss. Akad. Wiss. Berlin*: 794-817.
- _____, 1860b. Fernere Abbildungen und Diagnosen neuer Gattungen und Arten von lebenden Radiolarien des Mittelmeeres. *Monatsber. Kgl. Preuss. Akad. Wiss. Berlin*: 835-845.
- _____, 1862. *Die Radiolarien (Rhizopoda Radiaria)* Reimer, Berlin: 1-572.
- _____, 1881. Entwurf eines Radiolarien-Systems auf Grund von Studien der Challenger-Radiolarien. *Jena. Z. Naturwiss.*, 15:418-472.
- _____, 1887. Report on the Radiolaria collected by H.M.S. Challenger during the years 1873-1876. *Rept. Sci. Results H.M.S. Challenger 1873-1876, Zoology*, 18, 2 parts.
- Haecker, V., 1907. Altertümliche Sphaerellarien und Cyrtellarien aus grossen Meerestiefen. *Archiv für Protistenkunde*, 10.
- Hays, J. D., 1965. Radiolaria and late Tertiary and Quaternary history of Antarctic Seas. In Llano, G. A. (Ed.), *Biology of Antarctic Seas II*, Am. Geophys. Union Antarct. R. Ser., 5:125-184.
- Hays, J. D., and Opdyke, N. D., 1967. Antarctic Radiolaria, magnetic reversals and climatic change. *Science*, 158:1001-1011.
- Jørgensen, E., 1900. Protophyten und Protozoen in Plankton der Norwegischen Westküste. *Bergens Mus. Arbok. Naturvitensk. Rekke*: 51-95.
- _____, 1905. The protist plankton and the diatoms in bottom samples. *Bergens Museums Skr.*, 1:49-151.
- Keany, J., 1979. Early Pliocene radiolarian taxonomy and biostratigraphy in the Antarctic region. *Micropaleontology*, 25:50-74.
- Kling, S. A., 1973. Radiolaria from the eastern North Pacific, Deep Sea Drilling Project, Leg 18. In Kulm, L. D., von Huene, R., et al. *Init. Repts. DSDP*, 18: Washington (U.S. Govt. Printing Office), 155-182.
- Lazarus, D., and Pallant, A., 1988. Oligocene and Neogene Radiolaria from the Labrador Sea, ODP Leg 105. In Arthur, M. A., Srivastava, S. P., et al., *Proc. ODP Sci. Results*, 105: College Station, TX (Ocean Drilling Program).
- Loeblich, A. R., and Tappan, H., 1961. Remarks on the systematics of the Sarcomina (Protozoa), renamed homonyms and new and validated genera. *Proc. Biol. Soc. Washington*, 74:213-234.
- Lombari, G., and Lazarus, D., 1988. Neogene cycladophorid radiolarians from North Atlantic, Antarctic, and North Pacific deep-sea sediments. *Micropaleontology*, 35:97-135.
- Martin, G. C., 1904. *Radiolaria*. Maryland Geological Survey (Miocene), Baltimore, Johns Hopkins Press: 447-459.
- Moore, T. C., Jr., 1971. Radiolaria. In Tracey, J. L., Jr., et al., *Init. Repts. DSDP*, 8: Washington (U.S. Govt. Printing Office), 727-775.
- _____, 1973. Method of randomly distributing grains for microscopic examination. *J. Sediment. Petrol.*, 43:904-906.
- Müller, J., 1858. Über die Thalassicollen, Polycystinen und Acanthometren des Mittelmeeres. *Abh. Kgl. Preuss. Akad. Wiss. Berlin*: 1-62.
- Mullineaux, L. S., and Westberg-Smith, M. J., 1986. Radiolarians as paleoceanographic indicators in the Miocene Monterey Formation, Upper Newport Bay, California. *Micropaleontology*, 32:48-70.
- Nakaseko, K., 1963. Neogene Cyrtoidae (Radiolaria) from the Isozaki Formation in Ibaraki Prefecture, Japan. *Osaka Univ. Sci. Repts.*, 12:165-198.
- Nakaseko, K., and Sugano, K., 1973. Neogene radiolarian zonation in Japan. *Geol. Soc. Japan Mem.*, 8:23-34.
- Nigrini, C., 1967. Radiolaria in pelagic sediments from the Indian and Atlantic Oceans. *Bull. Scripps Inst. Oceanogr.*, 11:1-25.
- _____, 1970. Radiolarian in the North Pacific and their application to a study of Quaternary sediments in core V20-130. *Geol. Soc. Am. Mem.*, 126:139-175.

- _____, 1977. Tropical Cenozoic Artostrobiidae (Radiolaria). *Micro-paleontology*, 23:241-269.
- Nigrini, C., and Lombardi, G., 1984. A guide to Miocene Radiolaria. *Cushman Found. Foram. Res. Spec. Publ.*, 22.
- Nigrini, C., and Moore, T. C., Jr., 1979. A guide to modern Radiolaria. *Cushman Found. Foraminiferal Res., Spec. Publ.*, 16.
- Petrushevskaya, M. G., 1967. Radiolarians of order Spumellaria and Nassellaria of the Antarctic Region. In Andriiashev, A. P., and Ushakov, P. V. (Eds.), *Biological Report of the Soviet Antarctic Expedition 1955-1958*, Jerusalem (Israel Progr. Sci. Trans.) 3:2-186.
- _____, 1975. Cenozoic radiolarians of the Antarctic, Leg 29, Deep Sea Drilling Project. In Kennett, J. P., Houtz, R. E., et al., *Init. Repts. DSDP*, 29: Washington (U.S. Govt. Printing Office), 541-676.
- Petrushevskaya, M. G., and Kozlova, G. E., 1972. Radiolaria: Leg 14, Deep Sea Drilling Project. In Hayes, D. E., Pimm, A. C., et al., *Init. Repts. DSDP*, 14: Washington (U.S. Govt. Printing Office), 495-648.
- Popofsky, A., 1908. Die Radiolarien der Antarktis (mit Ausnahme der Tripyleen). *Deutsche Südpolar-Expedition 1901-1903*, 10(3):183-303.
- _____, 1913. Die Nassellarien des Warmwassergebietes. *Deutsche Südpolar-Expedition 1901-1903*, Report 14(1), (Zool. v. 6): 217-416.
- Principi, P., 1909. Contributo allo studio dei Radiolari Miocenici Italiani. *Bull. Soc. Geol. It.*, 28:1-22.
- Riedel, W. R., 1958. Radiolaria in Antarctic sediments. *Repts. B.A.N.Z. Antarct. Res. Exped.*, B-6(10):218-254.
- _____, 1959. Oligocene and lower Miocene Radiolaria in tropical Pacific sediments. *Micropaleontology*, 5:285-302.
- _____, 1967a. Subclass Radiolaria. In Harland, W. B., et al. (Eds.), *The Fossil Record*. Geol. Soc. London:291-298.
- _____, 1967b. Some new families of Radiolaria. *Proceed. Geol. Soc. London*, 1640:148-149.
- _____, 1971. Systematic classification of Polycystine Radiolaria. In Funnell, B. M., and Riedel, W. R. (Eds.), *Micropaleontology of Oceans* (Cambridge Univ. Press), 649-661.
- Riedel, W. R., and Campbell, A. S., 1952. A new Eocene radiolarian genus. *J. Paleontol.*, 26:667-669.
- Riedel, W. R., and Sanfilippo, A., 1970. Radiolaria, Leg 4, Deep Sea Drilling Project. In Bader, R. G., Gerard, R. D., et al. *Init. Repts. DSDP*, 4: Washington (U.S. Govt. Printing Office), 503-575.
- _____, 1971. Cenozoic Radiolaria from the western tropical Pacific, Leg 7. In Winterer, E. L., Riedel, W. R., et al. *Init. Repts. DSDP*, 7, Pt. 2: Washington (U.S. Govt. Printing Office), 1529-1672.
- Sanfilippo, A., Burckle, L. H., Martini, E., and Riedel, W. R., 1973. Radiolarians, diatoms, silicoflagellates, and calcareous nannofossils in the Mediterranean Neogene. *Micropaleontology*, 19:209-234.
- Sanfilippo, A., and Riedel, W. R., 1973. Cenozoic Radiolaria (exclusive of Theoperids, Artostrobiids, and Amphipyndacids) from the Gulf of Mexico, Deep Sea Drilling Project Leg 10. In Worzel, J. L., Bryant, W., et al., *Init. Repts. DSDP*, 10: Washington (U.S. Govt. Printing Office), 457-611.
- _____, 1980. A revised generic and suprageneric classification of the Artiscins (Radiolaria). *J. Paleontol.*, 54:1008-1011.
- Sanfilippo, A., Westberg-Smith, M. J., and Riedel, W. R., 1985. Cenozoic Radiolaria. In Bolli, H. M., Saunders, J. B., and Perch-Nielsen, K. (Eds.), *Plankton Stratigraphy*: Cambridge (Cambridge Univ. Press), 631-712.
- Schröder, O., 1914. Die nordischen Nassellarien. *Nord. Plankton*, 7:67-146.
- Stöhr, E., 1880. Radiolarienfauna der Tripoli von Grotte, Provinz Girgenti in Sizilien. *Paleontographica*, 26:69-124.
- Strelkov, A. A., and Reshetnjak, V. V., 1971. Kolonialnie radiolarii Spumellaria mirovogo okeana. In Radiolarii mirovogo okeana po materialam sovetskikh ekspeditsii, Issledovaniya, Fauna Morei, Lenigrad, Nauka, 9:295-369.
- Tan, Zhiyuan, and Tchang, Tso-Run, 1976. Studies on the Radiolaria of the East China Sea II. Spumellaria, Nassellaria, Phaeodaria, Sticholonchea. *Stud. Mar. Sinica*, 11:217-310.
- Tauxe, L., Petersen, N. P., and LaBreque, J. L., 1984. Magnetostratigraphy of Leg 73 sediments. In Hsü, K. L., LaBreque, J. L., et al., *Init. Repts. DSDP*, 73: Washington (U.S. Govt. Printing Office), 609-621.
- Vinassa de Regny, P. E., 1900. Radiolari Miocenici Italiani. *Reale Accad. Sci. Inst. Bologna Mem.*, 5:565-595.
- Weaver, F. M., 1973. Pliocene paleoclimatic and paleoglacial history of East Antarctica recorded in deep-sea piston cores. *Florida State Univ. Sed. Res. Lab. Contr.*, 36:1-142.
- _____, 1976. Antarctic Radiolaria from the southeast Pacific Basin, DSDP Leg 35. In Hollister, C. D., Craddock, C., et al. *Init. Repts. DSDP*, 35: Washington (U.S. Govt. Printing Office), 569-603.
- _____, 1983. Cenozoic radiolarians from the southwest Atlantic, Falkland Plateau Region, Deep Sea Drilling Project Leg 71. In Ludwig, W. J., Krasheninnikov, V. A., et al. *Init. Repts. DSDP*, 71: Washington (U.S. Govt. Printing Office), 667-686.
- Westberg-Smith, M. J., and Riedel, W. R., 1984. Radiolarians from the Western Margin of the Rockall Plateau: Deep Sea Drilling Project Leg 81. In Roberts, D. G., Schnitker, D., et al. *Init. Repts. DSDP*, 81: Washington (U.S. Govt. Printing Office), 479-502.

Date of initial receipt: 20 March 1989

Date of acceptance: 11 October 1989

Ms 113B-200

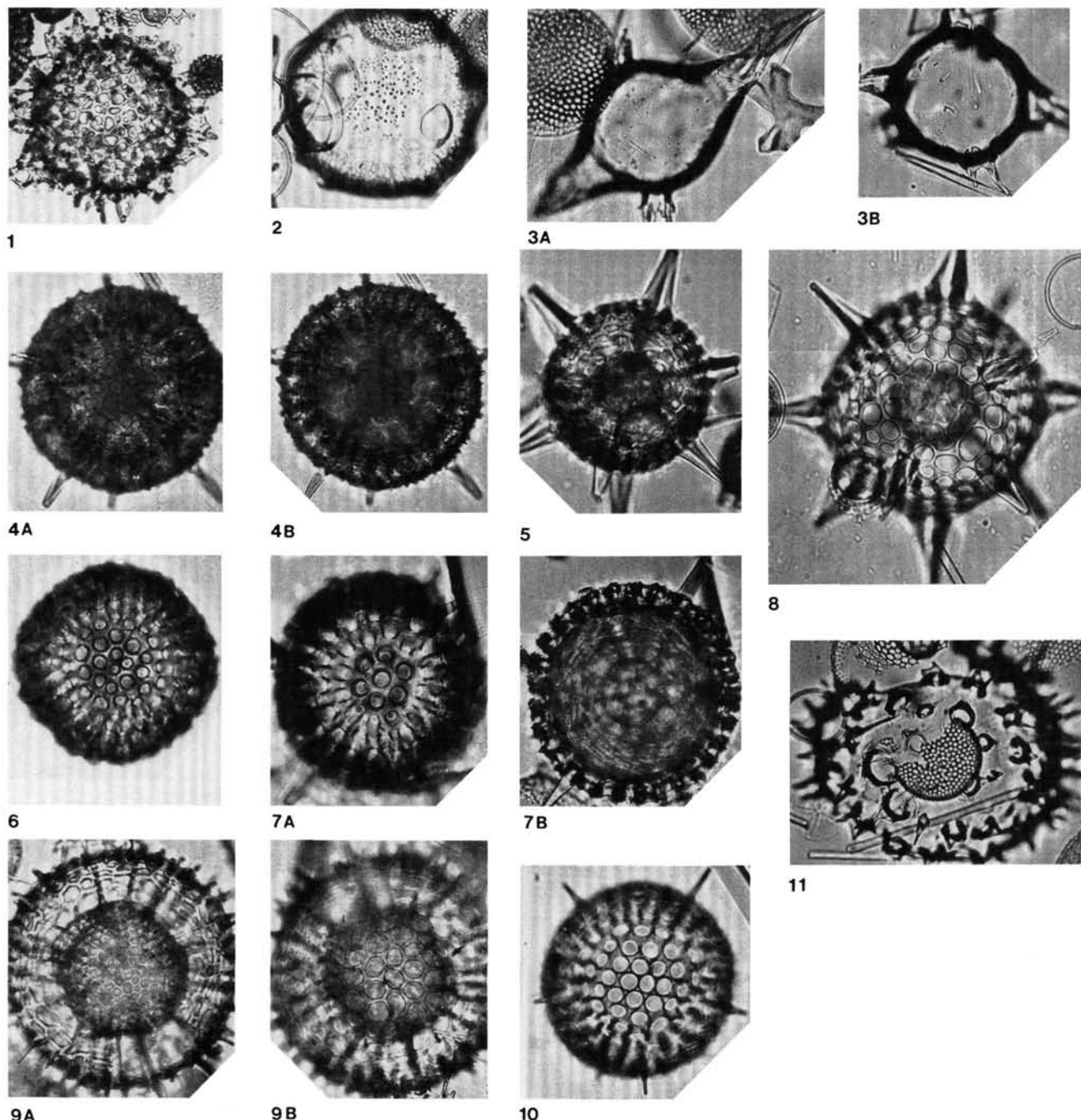


Plate 1. 1. *Acrosphaera* spp., $\times 109$, Sample 113-689B-7H-6, 60–62 cm. 2. *Collospaenid* sp. A, $\times 228$, Sample 113-689B-6H-7, 32–34 cm. 3. (A) *Disolenia* spp., $\times 260$, Sample 113-689B-8H-2, 57–59 cm; (B), $\times 260$, Sample 113-689B-8H-2, 57–59 cm. 4. (A, B) *Actinomma holtedahli*, $\times 224$, Sample 113-689B-9H-3, 71–73 cm. 5. *Actinomma* sp. A, $\times 224$, Sample 113-689B-7H-5, 71–73 cm. 6. *Actinomma medusa*, $\times 224$, Sample 113-689B-9H-3, 71–73 cm. 7. (A, B) *Actinomma* sp. B group, $\times 224$, Sample 113-689B-8H-3, 86–88 cm. 8. *Actinomma golownini*, $\times 224$, Sample 113-689B-6H-2, 133–135 cm. 9. (A, B) *Carposphaera subbotinae*, $\times 177$, Sample 113-689B-7H-6, 145–147 cm. 10. *Hexastylus* spp., $\times 224$, Sample 113-689B-8H-6, 71–73 cm. 11. *Collospaenid* sp. B, $\times 185$, Sample 113-689B-6H-1, 84–86 cm.

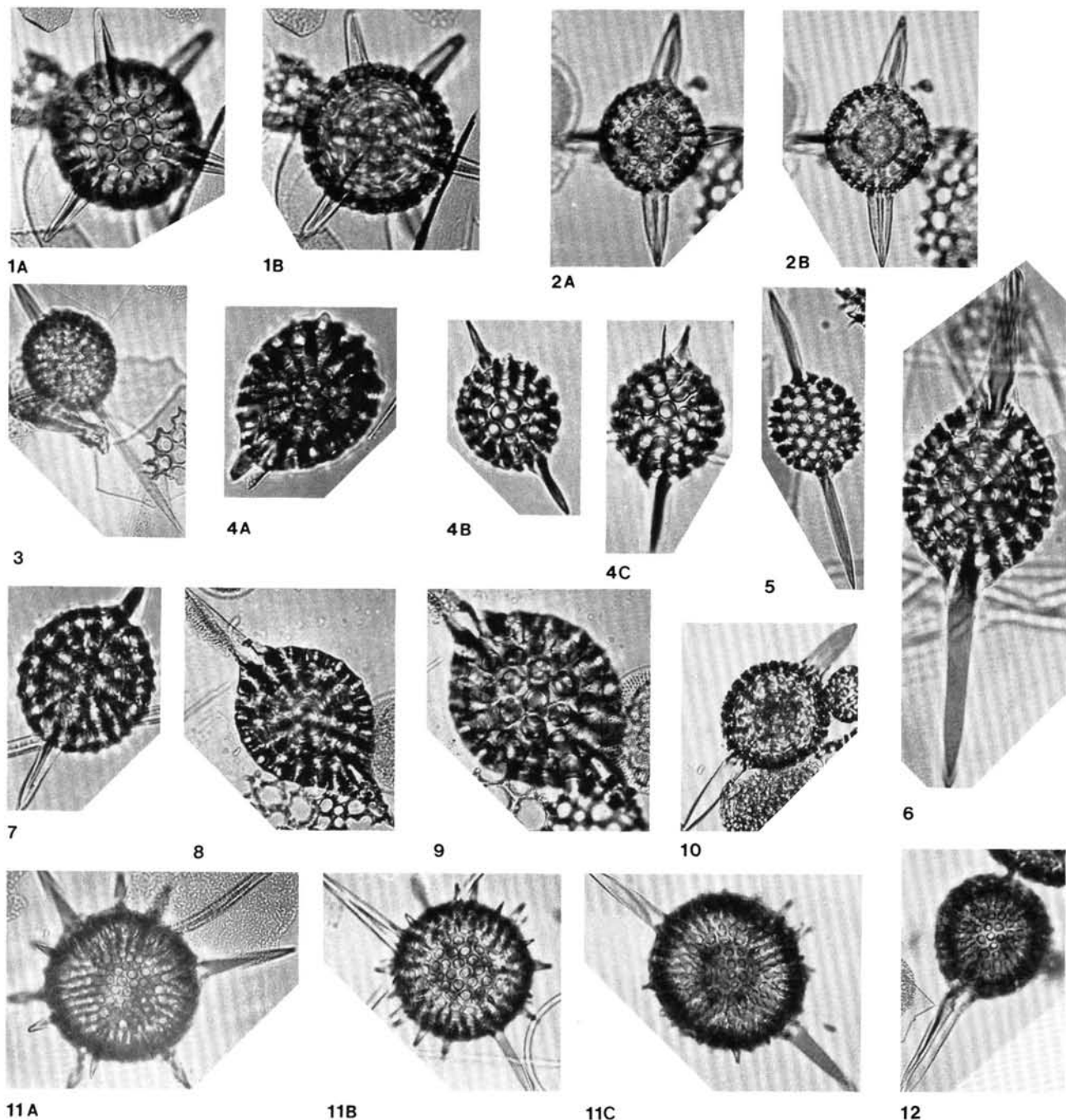


Plate 2. 1. (A, B) *Hexacontium* spp., $\times 220$, Sample 113-689B-8H-3, 56–58 cm. 2. (A, B) *Hexacontium* cf. *enthaecanthum*, $\times 220$, Sample 113-689B-8H-3, 56–58 cm. 3. *Druppactractus hastatus* group, $\times 220$, Sample 113-689B-8H-3, 86–88 cm. 4. (A, B, C) *Stylosphaera radiosa* $\times 220$, Sample 113-689B-9H-2, 71–73 cm. 5. *Stylosphaera coronata laevis* group, $\times 220$, Sample 113-689B-9H-3, 71–73 cm. 6. *Stylatractus santaeanae*, $\times 220$, Sample 113-689B-9H-1, 71–73 cm. 7. *Stylosphaera dixyphos*, $\times 220$, Sample 113-689B-9H-3, 71–73 cm. 8. *Stylatractus neptunus*, $\times 220$, Sample 113-689B-6H-5, 144–146 cm. 9. *Stylatractus neptunus*, $\times 220$, Sample 113-689B-8H-5, 55–57 cm. 10. *Stylosphaera* sp. A, $\times 220$, Sample 113-689B-7H-3, 145–147 cm. 11. (A) *Amphistylus angelinus*, $\times 220$, Sample 113-689B-8H-3, 86–88 cm; (B), $\times 220$, Sample 113-689B-9H-1, 71–73 cm; (C), $\times 220$, Sample 113-689B-7H-6, 60–62 cm. 12. *Stauroxiphos communis* $\times 220$, Sample 113-689B-7H-6, 89–91 cm.

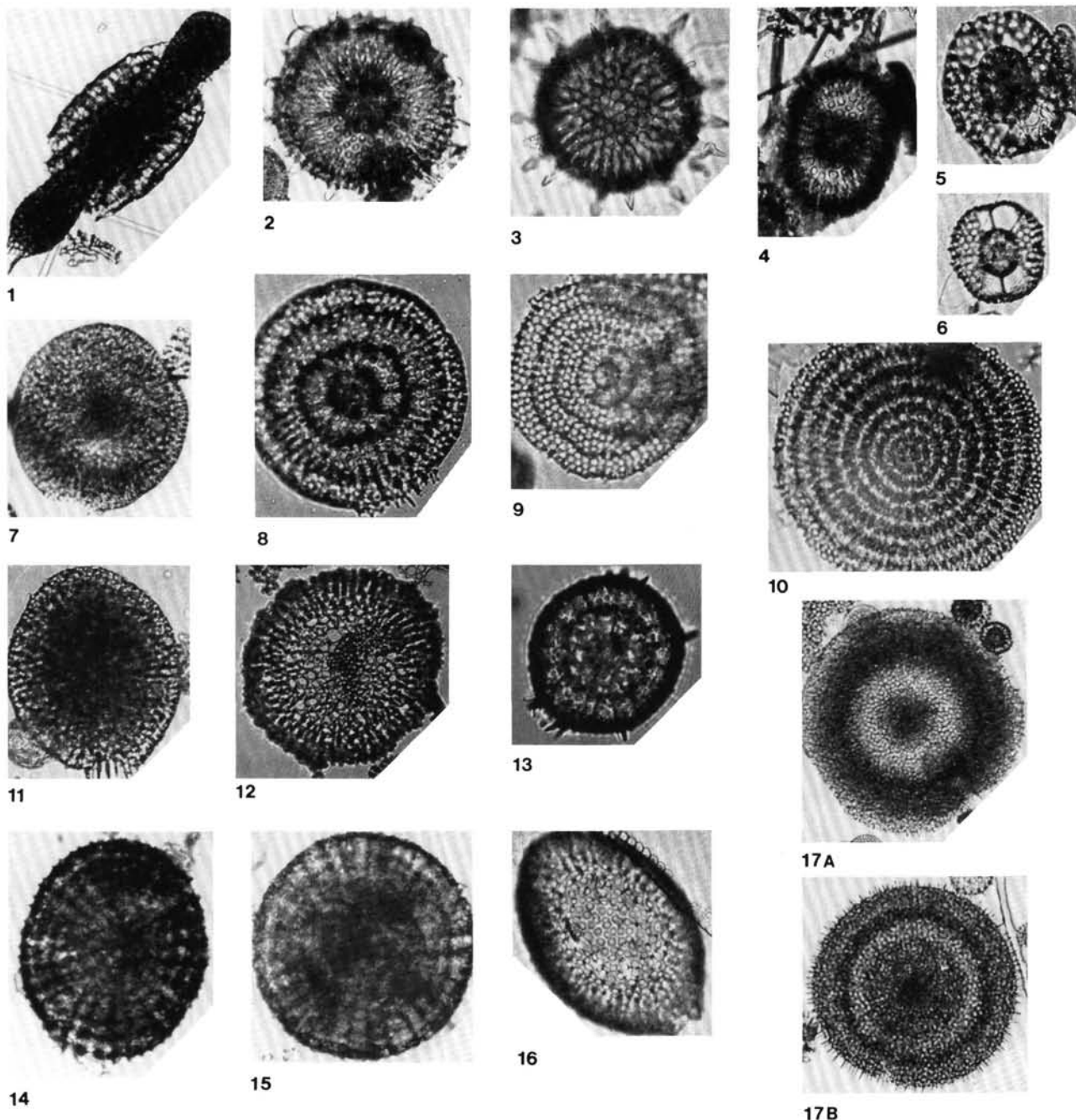


Plate 3. 1. *Spongocore* spp., $\times 220$, Sample 113-689B-9H-1, 71–73 cm. 2. *Heliodiscus* sp. A, $\times 220$, Sample 113-689B-8H-3, 65–67 cm. 3. *Heliodiscus* sp. A, $\times 220$, Sample 113-689B-8H-3, 56–58 cm. 4. *Didimocyrts* sp., $\times 220$, Sample 113-689B-6H-3, 91–93 cm. 5. *Phorticium polycladum*, $\times 220$, Sample 113-689B-6H-4, 56–58 cm. 6. *Tetrapyle octacantha*, $\times 220$, Sample 113-689B-8H-1, 144–146 cm. 7. *Spongodiscus craticulatus*, $\times 133$, Sample 113-689B-8H-3, 120–122 cm. 8. *Circodiscus ellipticus*, $\times 220$, Sample 113-689B-8H-2, 120–122 cm. 9. *Stylodictya aculeata*, $\times 220$, Sample 113-689B-8H-5, 86–88 cm. 10. *Stylodictya validispina* $\times 220$, Sample 113-689B-8H-1, 56–58 cm. 11. *Spongopyle osculosa*, $\times 220$, Sample 113-689B-7H-5, 55–57 cm. 12. *Cenosphara* sp. A, $\times 67$, Sample 113-689B-9H-2, 71–73 cm. 13. *Prunopyle tetrapila*, $\times 220$, Sample 113-689B-7H-6, 60–62 cm. 14. *Prunopyle hayesi* group, $\times 133$, Sample 113-689B-8H-3, 120–122 cm. 15. *Prunopyle* sp. A, $\times 107$, Sample 113-689B-7H-6, 86–88 cm; (B) $\times 67$, Sample 113-689B-8H-5, 86–88 cm.

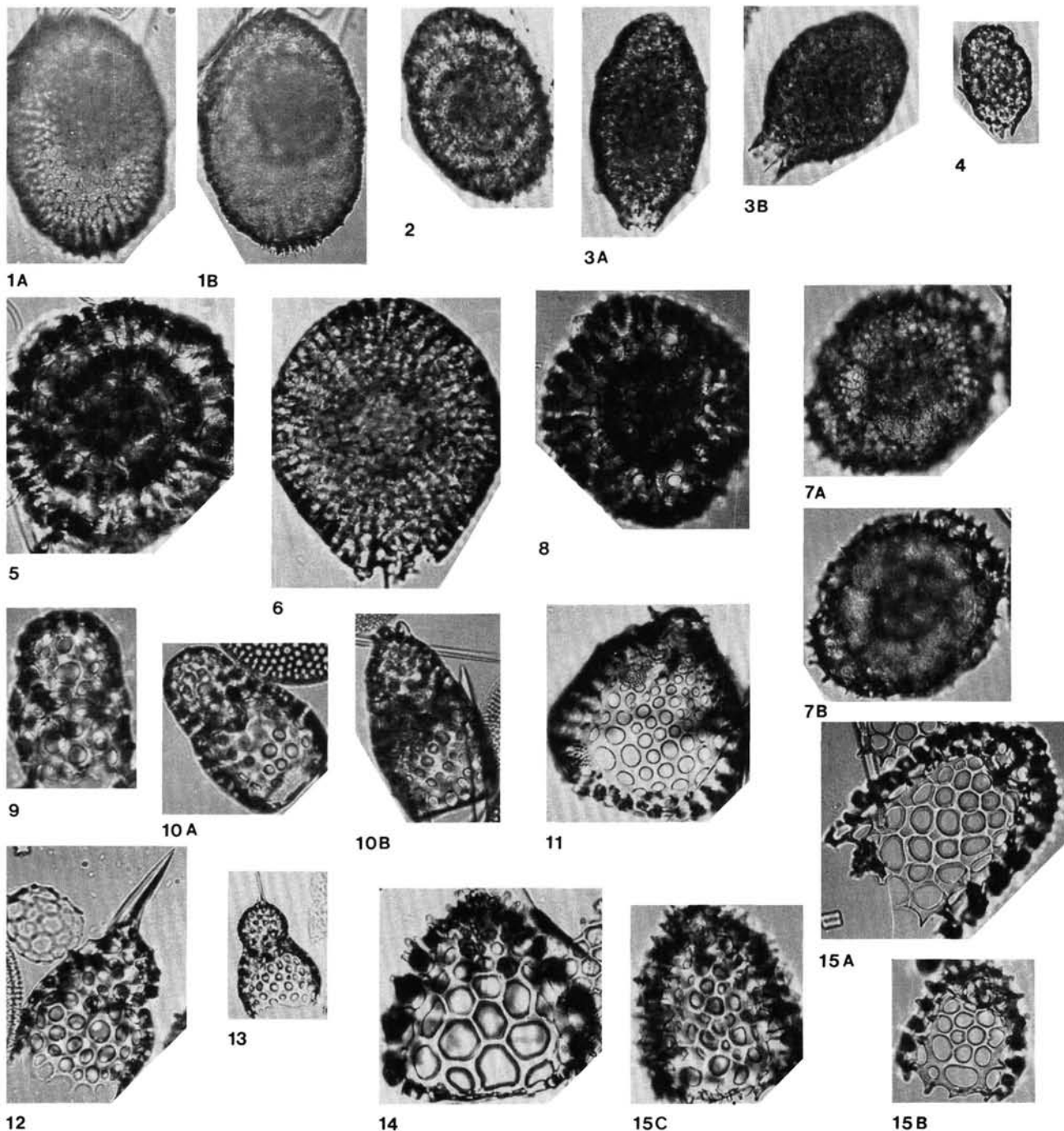


Plate 4. 1. (A, B) *Prunopyle* sp. D, $\times 224$, Sample 113-689B-8H-3, 86–88 cm. 2. *Lithocarpium polyacantha* group, $\times 224$, Sample 113-689B-7H-6, 117–119 cm. 3. (A, B) *Prunopyle* sp. B group, $\times 224$, Sample 113-689B-7H-6, 60–62 cm. 4. *Larcopyle bütschlii*, $\times 224$, Sample 113-689B-7H-3, 144–147 cm. 5. *Lithelius* sp. cf. *nautiloides*, $\times 224$, Sample 113-689B-7H-2, 65–67 cm. 6. *Prunopyle* sp. C, $\times 224$, Sample 113-689B-7H-5, 86–88 cm. 7. (A, B) *Tholoniid* sp. A, $\times 224$, Sample 113-689B-7H-5, 86–88 cm. 8. *Tholoniid* sp. B, $\times 224$, Sample 113-689B-9H-3, 71–73 cm. 9. *Antarctissa robusta*, $\times 277$, Sample 113-689B-8H-5, 86–88 cm. 10. (A) *Antarctissa deflandrei*, $\times 282$, Sample 113-689B-5H-2, 49–51 cm; (B), $\times 282$, Sample 113-689B-6H-2, 32–34 cm. 11. *Ceratocyrtis* cf. *cucullaris*, $\times 224$, Sample 113-689B-7H-7, 21–23 cm. 12. *Ceratocyrtis stigi*, $\times 224$, Sample 113-689B-8H-2, 120–122 cm. 13. *Lithomelissa* cf. *ehrenbergi*, $\times 224$, Sample 113-689B-8H-1, 144–146 cm. 14. *Ceratocyrtis* sp. A, $\times 177$, Sample 113-689B-7H-7, 21–23 cm. 15. (A, B) *Ceratocyrtis mashae*, $\times 224$, Sample 113-689B-9H-3, 71–73 cm; (C), $\times 224$, Sample 113-689B-8H-1, 144–146 cm.

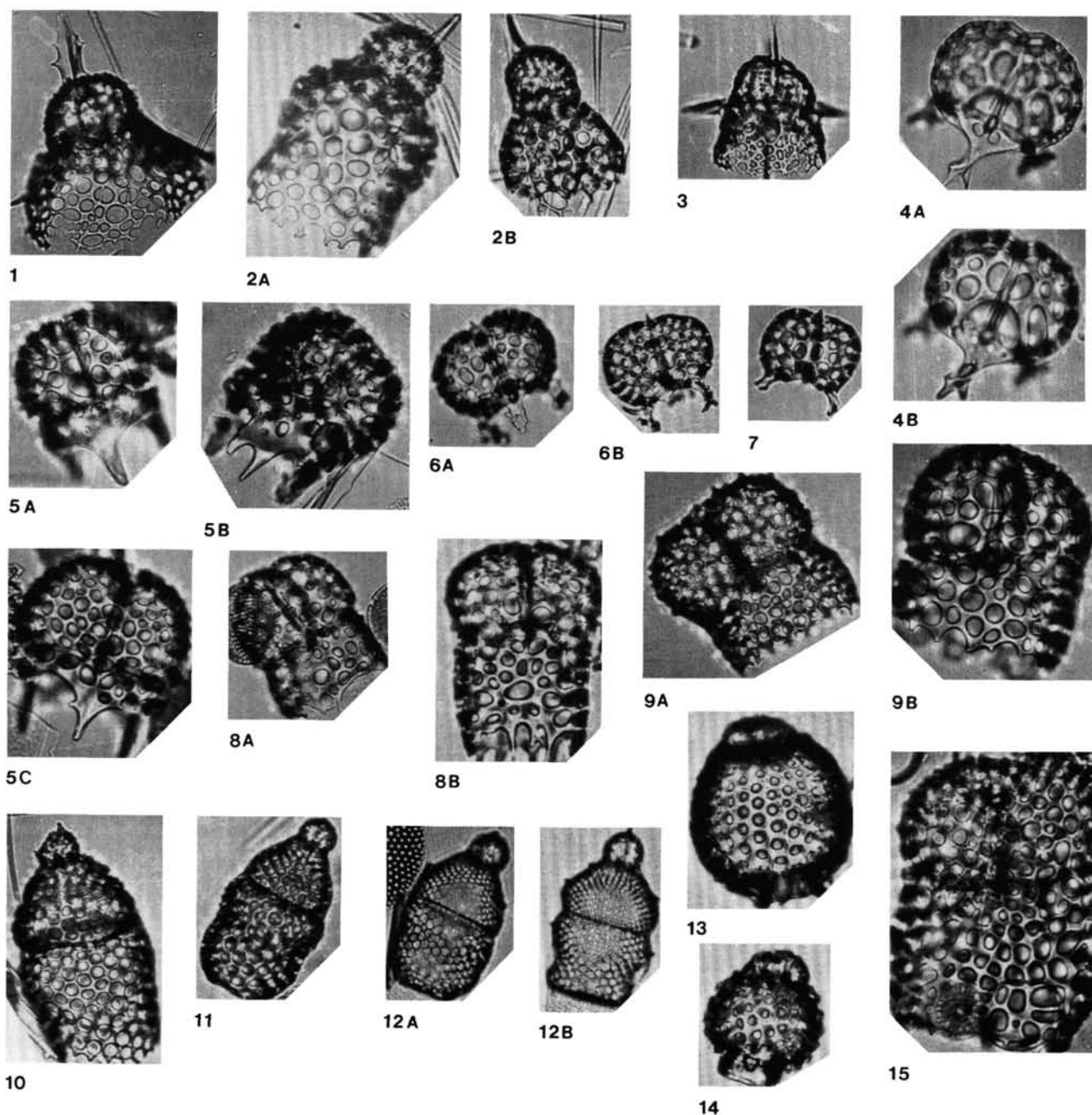


Plate 5. 1. *Tripilidium clavipes*, $\times 220$, Sample 113-689B-8H-2, 57-59 cm. 2. (A) *Lithomelissa robusta*, $\times 273$, Sample 113-689B-8H-4, 144-146 cm, (B) $\times 220$, Sample 113-689B-9H-6, 71-73 cm. 3. *Lithomelissa tricornis*, $\times 220$, Sample 113-689B-9H-1, 71-73 cm. 4. (A, B) *Corythospyris fiscella*, $\times 348$, Sample 113-689B-8H-4, 86-88 cm. 5. (A, B) *Trissocyklid* sp. A, $\times 220$, Sample 113-689B-7H-6, 89-91 cm; (C), $\times 220$, Sample 113-689B-7H-5, 120-122 cm. 6. (A) *Corythospyris* sp. A, $\times 220$, Sample 113-689B-8H-1, 120-122 cm; (B), $\times 220$, Sample 113-689B-7H-6, 89-91 cm; 7. *Corythospyris fiscella*, $\times 220$, Sample 113-689B-8H-6, 71-73 cm. 8. (A) *Dendrospyris stabilis*, $\times 220$, Sample 113-689B-7H-6, $\times 282$, Sample 113-689B-7H-5, 86-88 cm. 9. (A) *Dendrospyris rhodospyrodes*, $\times 220$, Sample 113-689B-7H-5, 55-57 cm; (B), $\times 220$, Sample 113-689B-7H-5, 86-88 cm. 10. *Cyrtocapsella robusta*(?), $\times 220$, Sample 113-689B-9H-1, 71-73 cm. 11. *Cyrtocapsella robusta* n. sp., $\times 220$, Sample 113-689B-9H-1, 71-73 cm. 12. (A) *Cyrtocapsella longithorax*, $\times 220$, Sample 113-689B-8H-2, 86-88 cm; (B), $\times 220$, Sample 113-689B-8H-2, 57-59 cm. 13. *Caropcanistrum* spp., $\times 220$, Sample 113-689B-7H-4, 148-150 cm. 14. *Carpocanarium papillosum*, $\times 220$, Sample 113-689B-9H-2, 71-73 cm. 15. *Dendrospyris megalcephalis*, $\times 220$, Sample 113-689B-6H-2, 133-135 cm.

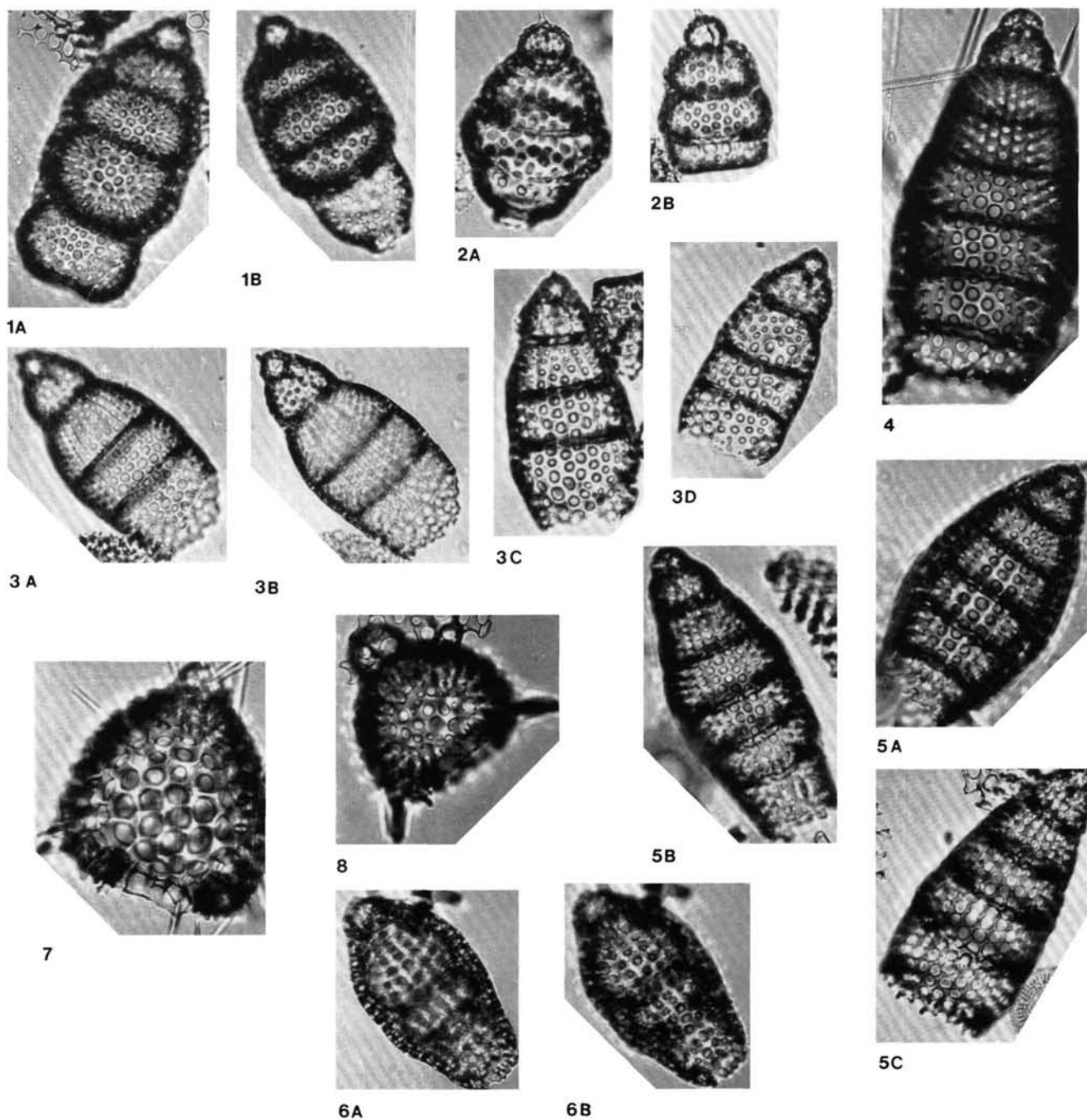


Plate 6. 1. (A) *Cyrtocapsella tetraptera*, $\times 220$, Sample 113-689B-7H-5, 143–145 cm; (B), $\times 220$, Sample 113-689B-7H-6, 89–91 cm. 2. (A) *Cyrtocapsella cornuta*, $\times 220$, Sample 113-689B-7H-5, 86–88 cm; (B), $\times 220$, Sample 113-689B-7H-6, 117–119 cm. 3. (A, B) *Eucyrtidium cienkowskii* group $\times 220$, Sample 113-689B-7H-5, 143–145 cm; (C, D), $\times 220$, Sample 113-689B-7H-4, 148–150 cm. 4. *Eucyrtidium calvertense* group(?), $\times 220$, Sample 113-689B-6H-3, 58–60 cm. 5. (A, B) *Eucyrtidium calvertense* group, $\times 220$, Sample 113-689B-7H-1, 70–72 cm; (C), $\times 220$, Sample 113-689B-7H-2, 107–109 cm. 6. (A, B) *Eucyrtidium punctatum*, $\times 220$, Sample 113-689B-7H-3, 145–147 cm. 7. *Lychnocanoma* sp. A, $\times 220$, Sample 113-689B-9H-6, 71–73 cm. 8. *Lychnocanoma conica*, $\times 220$, Sample 113-689B-9H-3, 71–73 cm.

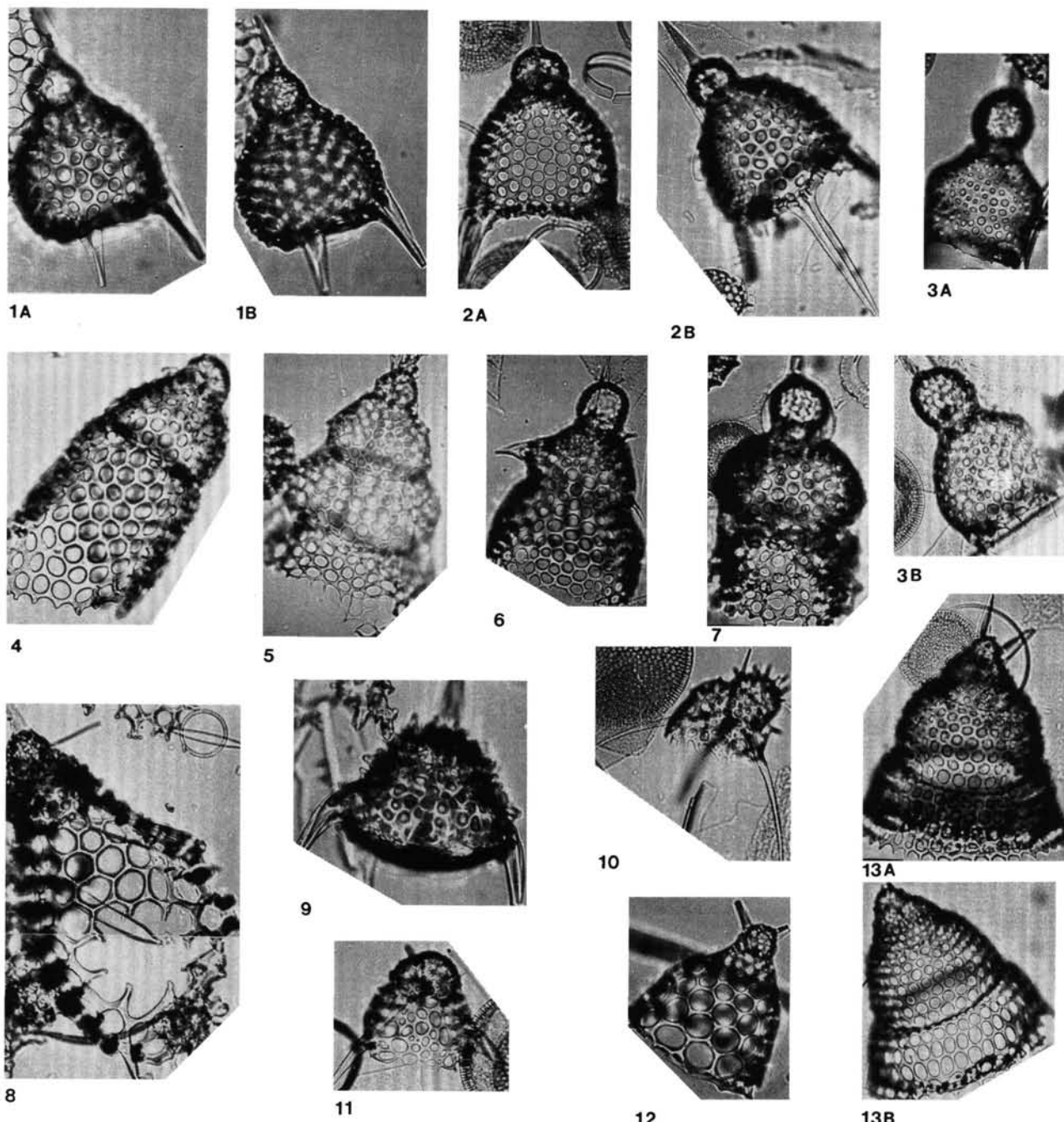


Plate 7. 1. (A, B) *Lychnocanoma conica*, $\times 217$, Sample 113-689B-9H-2, 71–73 cm. 2. (A) *Lychnocanoma* sp. B, $\times 217$, Sample 113-689B-6H-6, 84–86 cm; (B), $\times 217$, Sample 113-689B-6H-5, 70–72 cm. 3. (A) *Gondwanaria japonica* group, $\times 217$, Sample 113-689B-7H-6, 89–91 cm; (B), $\times 217$, Sample 113-689B-8H-2, 57–59 cm. 4. *Calocyclus cf. semipolita*, $\times 217$, Sample 113-689B-7H-6, 60–62 cm. 5. *Artophormis gracilis*, $\times 217$, Sample 113-689B-8H-4, 86–88 cm. 6. *Gondwanaria* sp. A, $\times 217$, Sample 113-689B-8H-2, 57–59 cm. 7. *Gondwanaria deflandrei*, $\times 217$, Sample 113-689B-7H-2, 70–72 cm. 8. *Cyclampterium milowi*, $\times 171$, Sample 113-689B-7H-3, 56–58 cm. 9. *Corythomelissa horrida*, $\times 217$, Sample 113-689B-8H-2, 120–122 cm. 10. *Dictyophimus gracilipes*, $\times 217$, Sample 113-689B-8H-2, 57–59 cm. 11. *Dictyophimus cf. platycephalus*, $\times 217$, Sample 113-689B-8H-1, 144–146 cm. 12. *Cycladophora conica*, $\times 217$, Sample 113-689B-8H-6, 71–73 cm. 13. (A) *Cycladophora antigua* n. sp., $\times 217$, Sample 113-689B-8H-1, 120–122 cm; (B), $\times 217$, Sample 113-689B-8H-1, 144–146 cm.

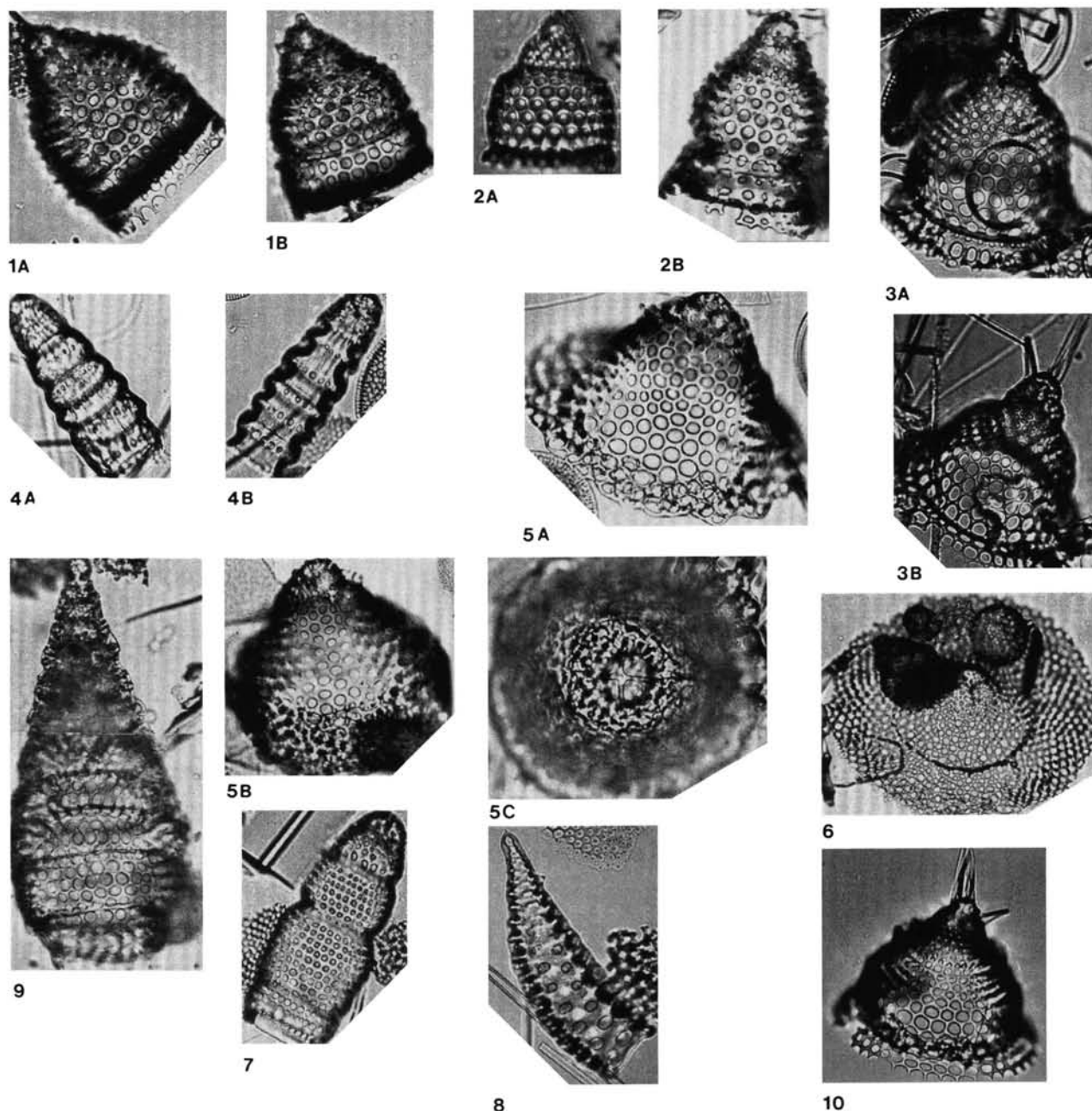


Plate 8. 1. (A) *Cycladophora golli golli*, $\times 224$, Sample 113-689B-7H-5, 120–122 cm; (B), $\times 224$, Sample 113-689B-7H-4, 120–122 cm. 2. (A) *Cycladophora golli regipileus*, $\times 224$, Sample 113-690B-6H-3, 49–51 cm; (B), $\times 224$, Sample 113-689B-7H-5, 55–57 cm. 3. (A) *Cycladophora humerus*, $\times 224$, Sample 113-689B-6H-7, 32–34 cm; (B), $\times 224$, Sample 113-689B-6H-3, 91–93 cm. 4. (A) *Siphocampe arachnea* group, $\times 224$, Sample 113-689B-9H-1, 71–73 cm; (B), $\times 224$, Sample 113-689B-8H-1, 88–90 cm. 5. (A, B) *Velicucullus altus* n. sp., $\times 224$, Sample 113-689B-8H-2, 86–88 cm; (C), $\times 224$, Sample 113-689B-8H-2, 57–59 cm. 6. *Velicucullus cf. oddgurneri*, $\times 109$, Sample 113-689B-7H-6, 117–119 cm. 7. *Phormostichoartus corbula*, $\times 224$, Sample 113-689B-6H-2, 83–85 cm. 8. *Cornutella clathrata*, $\times 224$, Sample 113-689B-6H-2, 83–85 cm. 9. *Stichophoromis* sp., $\times 224$, Sample 113-689B-5H-6, 145–147 cm. 10. *Cycladophora spongorthorax*, $\times 185$, Sample 113-689B-5H-6, 145–147.